Review

Physical and Chemical Properties of Carbon Nanotubes in view of Mechanistic Neuroscience Investigations. Some Outlook from Condensed Matter, Materials Science and Physical Chemistry.

Stefano A. Mezzasalma [1,2] 0000-0002-2968-7497, Lucia Grassi [3] and Mario Grassi [3]*

[1]   Ruđer Bošković Institute, Materials Physics Division, Bijenička cesta 54, 10000 Zagreb, Croatia; Stefano.Mezzasalma@irb.hr

[2]   Lund Institute for advanced Neutron and X-ray Science (LINXS), Lund University, IDEON Building, Delta 5, Scheelevägen 19, 223 70 Lund, Sweden

[3]   Department of Engineering and Architecture, Trieste University, via Valerio 6, I-34127 Trieste, Italy

*   Correspondence: mario.grassi@dia.units.it

Abstract: The open border between non-living and living matter, suggested by increasingly emerging fields of nanoscience interfaced to biological systems, requires a detailed knowledge of nanomaterials properties. An account of the wide spectrum of phenomena, belonging to physical chemistry of interfaces, materials science, solid state physics at the nanoscale and bioelectrochemistry, thus is acquainted for a comprehensive application of carbon nanotubes interphased with neuron cells. This review points out a number of conceptual tools to further address the ongoing advances in coupling neuronal networks with (carbon) nanotube meshworks, and to deepen the basic issues that govern a biological cell or tissue interacting with a nanomaterial. Emphasis is given here to the properties and roles of carbon nanotube systems at relevant spatiotemporal scales of individual molecules, junctions and molecular layers, as well as to the point of view of a condensed matter or materials scientist. Carbon nanotube interactions with blood-brain barrier, drug delivery, biocompatibility and functionalization issues are also regarded.

Keywords: carbon nanotubes; neuronal cells; charge transport; percolation; nanobiotechnology; drug delivery

Contents

1. Introduction

1.1. General Remarks

Literature on carbon nanotubes is immense, both in terms of fundamental features and prospective applications. With such a level of differentiation and specialization, however, it may be tough for the interested researcher who does not work in fields complementary to her/his expertise to have such a broad spectrum of phenomenologies at hand. This may be probably the case of the biologist or neuroscientist approaching complex issues in nanophysics and nanochemistry, who discovers in carbon nanotubes (and alike systems) a great resource to deepen and innovate the study of living matter, up to foster the advances in molecular medicine, surgery and pharmaceutics we all hope for. The present review thus wishes to draw a synoptic picture of carbon nanotube properties that may have potential impact to life sciences, especially neurosciences, and which are often treated separately. Through a specific context, i.e. the interaction between neurons and carbon nanotubes (NCN), a wide spectrum of phenomenologies, from condensed matter physics to drug delivery, will be explored in the hope of redesigning and stimulating a more quantitative framework for a cross-disciplinary research. In addition to a comprehensive overview of various aspects here concerned, the reader will perhaps be more stimulated to formulate questions than answers, to look for more pieces to be added than to extract. However, this is precisely one of this review's main objectives: to hint insights and a number of tools for a broader and more detailed *mechanistic* analysis which, then, normally represents the starting point for an effective approach to more complex issues (like e.g. the dynamical organization of cellular networks, morphological problems, etc.).

1.2. Phenomenological Considerations

The nervous system is built up by nervous tissues, formed in turn by nerve cells (neurons and neuroglial cells). Structure and function of neurons are basically the same in all animal species, i.e. they comprise a soma (cell body), axon and dendrites (neurites), receive and elaborate nerve signals (action potentials) that are then transmitted to other neurons [1]. Functional recovery of neurons and

neuroregeneration (i.e. repair and restoration of neurons destroyed in neurodegenerative disorders) need axonal regrowth and enhancing the ability of neurons to transmit nerve signals (e.g. by means of functional synapses). This may be either obtained intrinsically or extrinsically, i.e. by endowing neuron cells with a higher growth capability or embedding them into a stimulating environment [2]. With the advent of nanomaterials as carbon nanotubes, there appeared the intriguing prospect of regulating neuronal phenomena via the design of new cellular environment at the nanometer scale, and it was discovered that carbon-derived nanostructures can own a role in neuro-regeneration and neurite outgrowth. An initial groundbreaking observation, more than twenty years ago, was that neurons seeded on carbon nanotube substrates were not only surviving but growing and enhancing their axonal processes [3].

Since then, a number of interactions or coupling mechanisms in neuron/carbon nanotube (NCN) interphases[1] were reported to establish in various systems (see e.g. [4–6]). Nowadays carbon nanotubes are believed to mimic the neural-tissue nanotopography (Fig. 1) and/or conductivity, and are regarded as a promising one-dimensional nanomaterials class in neuroengineering approaches to managing neurological disorders [7,8]. From a mechanistic-molecular point of view, however, this research
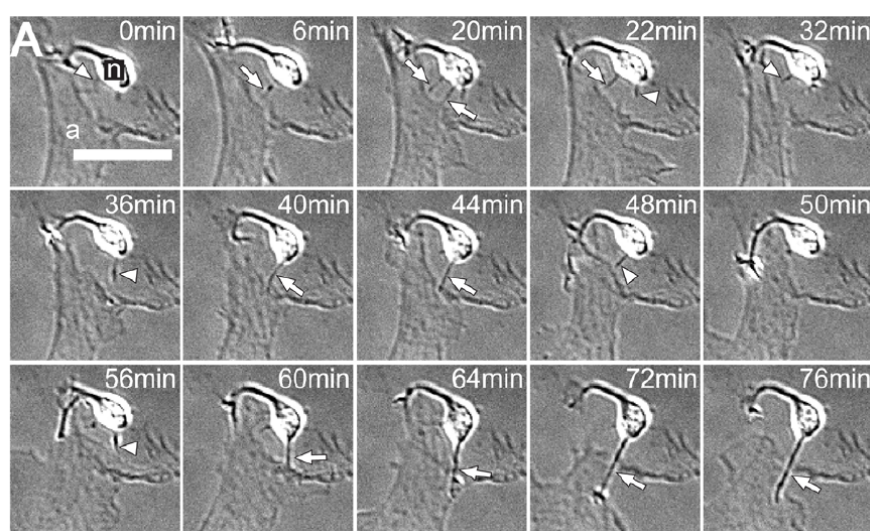

Figure 1. Formation of tunneling-nanotube structures between neurons (*n*) and astrocytes (*a*). Shown from a scratch time (A) are a number of frames depicting their formation (arrows). Neurons display tubular extensions before tunneling and after their breakage (arrowheads). Tunneling structures spread depolarization signals and set up an electrical coupling between astrocytes and neurons (adapted from ref. [9]). Scale bar = 20 μm.

certainly needs to receive more attention. A quantitative knowledge of these mechanisms may not only open up applications in biomedicine and nanobiotechnology, but will shed further light on the complex domain where physics and chemistry meet biology at the nanoscale. In an established phenomenology, which can now be deemed as prototypical (see e.g. [4,10]), hippocampal cells were grown in-vitro on carbon nanotube films,[2] which were stably deposited on glass substrates, and their biological activity was studied by means of electrophysiology experiments. By statistically comparing such responses with those originating from identical cells, but cultured on glass substrates alone (unperturbed 'control' cultures), the activity of neurons interplaying with nanotubes turned out to be notably improved. The couple of quantities, both measured in individual cells and whose behavior best summarizes

---

[1] The word 'interphase' is overall preferred in the following to 'interface', as the latter more suits hard particles whose charge distribution is strictly confined in two dimensions. The presence of soft living matter may better comply here with a three-dimensional phase description.

[2] Or 'meshworks', 'mats', layers.

this achievement, were the frequency of spontaneous activity and the afterdepolarization (potential) of a biological membrane. In the first case, where each neuron reflected the activity of neighbour cells, the response gives indications on the overall network performance. This frequency counts how many action potentials or post-synaptic currents are recorded in unit time, and can be detected by current or voltage clamp techniques. In the second case, where cells were (pharmacologically) isolated from the network, the influence of the neighboring meshwork could better emerge and be characterized. Specifically, in investigating on how the coupling with nanotubes might alter the control polarization state, a membrane afterdepolarization process, further exciting the neuronal activity, was brought to light as well. Cultured neurons on carbon nanotubes then were reported to almost double the probability of synapse development, with a remarkable connectivity increment bringing to a steep increase of neuronal postsynaptic currents [11–13]. Today it seems also to be established that NCN interactions influence neurons at single-cell levels, enhancing (GABAergic/Glutamatergic) synaptogenesis and heterogeneous short-term synaptic plasticity [5,14].

Confirmations of a positive feedback between nanoparticles and cell activity can be extensively found in the bio-inspired literature, where pristine or functionalized nanotubes were also used as signal recording systems (microtransducers) for the electrical activity of neuronal networks in-vitro [15], as micro fiber-shaped neural probes [16], neuromorphic devices (e.g. synaptic network thin-film transistors) [17], in electrochemical sensing of neurological drugs and neurotransmitters [18–20], in nanobioelectronic and biosensor applications [21,22], also in combination with charge-coatings [23], metal-sputtered graphene hybrid sheets [24], metallocene-based compounds [25], fibers [26], collagen [27], redox and conducting polymers [28]. Carbon nanotubes, also in combination with conducting polymers were also suggested to form superior molecular materials for improving neural electrodes, bioactivity recording and stimulation (both extracellular/intracellular) [29,30], owing particularly to their long-term behavior [31], low impedance and high charge-storage capacity [32]. Obviously, carbon nanomaterials as carbon nanotubes or graphene do not represent the only promising materials class. For instance, in-vivo interactions of cnidaria Hydra vulgaris with semiconducting (CdSe/CdS) quantum nanorods can produce too an elicited tentacle-writhing response, governed by Ca^{2+} ions [33]. It was ascribed to unique shape-tunable electrical features of quantum nanorods, each carrying a large dipole moment and near-field perturbing the membrane conductance, with consequent firing of action potentials (see Fig. 2).
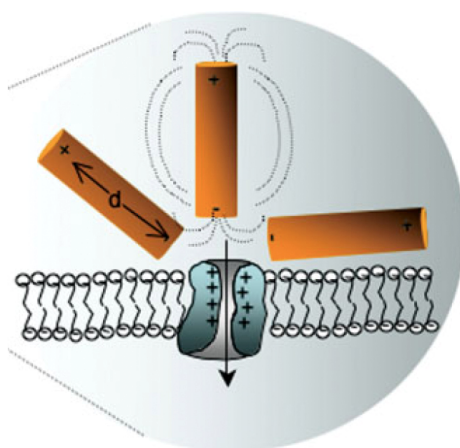
Figure 2. Scheme of membrane conductance change by means of dipole moment effects of nanorods (here $d \sim$ dozens of nm).

Another interesting materials class is given by the piezoelectric Boron Nitride Nanotubes (BNNs). They were incubated with neuronal (PC12) cells upon ultrasounds (i.e mechanical stress), and the consequent polarization of nanotubes (length $= 200 - 600$ nm, diameter ≈ 50 nm) delivered electrical stimulus to the cells (sprouting 30% more than in control states after a 9-days exposure) [34]. To identify

some crucial points of this research, some queries may be usefully formulated from a quantitative point of view. What are the mechanistic reading keys for understanding the activity of carbon nanotubes on neurons, like the excitation and propagation of signals, ionic conductivity changes, and intercellular signaling via synaptic transmission ? Which forms of non-living matter are able to elicit similar effects, and on what basis ? Then, how does the biological response vary with molecular or meshwork physical/chemical parameters ? Said differently, which physico-mathematical variables may reproducibly affect it, and what are their fundamental equations ? Lastly, may nanomaterials such as carbon nanotubes be deemed as foreign 'accessories' of a neuronal cell or do they rather stand for active 'prolongations' of it ? Answering these points in detail requires a deep knowledge of biomaterials properties from the point of view of disciplines such as inorganic and organic physical chemistry, biophysics, materials science, polymer physics, hard and soft condensed matter. Clearly, beyond experimental issues are their theoretical counterparts, either involving classical or
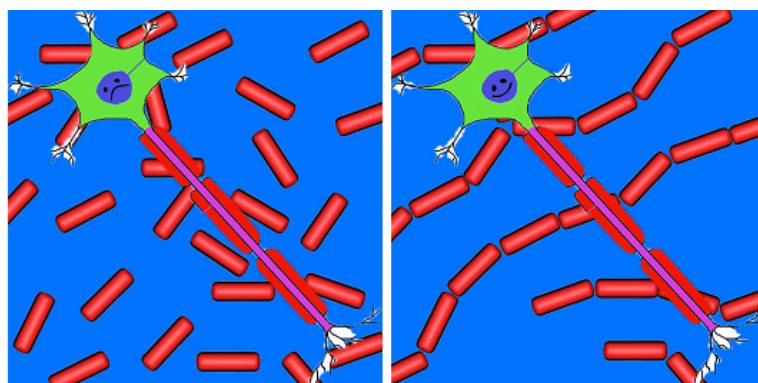

Figure 3. Pictorial illustration of a cell sensitive to network connectivity onto a substrate. Random and separated nanorod monolayer (left), structured and connected nanorod network (right).

quantum-semiclassical aspects, and aiming at first-principles NCN descriptions. The next paragraphs thus will face the potential impact that several physical and chemical features may have on this broad bio-based work, hopefully convincing the audience of how this framework may be further extraordinarily rich, and yet in need of more exact analysis and cross-disciplinary ideas.

2. Molecular Chirality, Adhesion and Cell Mechanics

Cell adhesion is very important in tissue growth, organization and morphogenesis. As an example, neuronal differentiation is affected by the amount and subcellular distribution of integrin clusters (i.e. regulating adhesion). Any material employed in electrophysiology experiments should be biocompatible, adhering enough to cells and triggering the delivery of electrical stimuli to get or modulate the biological activity. Nanomaterials toxicity has been scrutinized for several years (see e.g. [35–43] and references therein). Toxicology response in-vitro is usually reduced by decreasing the metal content upon chemical purification or by ad hoc-surface functionalization, somehow loosening the cell/nanotube contact and sometimes inducing neuronal differentiation [39,44]. Functionalized multi-walled carbon nanotubes were found nontoxic e.g. to PC-12 (pheochromocytoma) neuron cells [45]. Carboxylation, in particular, proved to be effective to prevent microvascular brain cells from an increase of endothelial permeability [46], while dual covalent/noncovalent single-walled functionalization routes were useful to get multifunctional tools for cellular delivery [47]. In all generality, results indicate that carbon nanotubes, whether they are single-walled, multi-walled, assembled into composite bioscaffolds or with nanofibers, may be used as substrates to support neurite outgrowth and synaptic function [48–53], branching and intricate connections between neurites, dendrites and astrocytes [43], to improve recovery and promote excitability of dissociated neonatal neurons (see Fig. 4) [54], to enhance neurotrophin release [55], stem cell neurogenesis and differentiation [56–59], surface wettability and cell adhesion at early stages [60], may be used as a

new type of actin altering agent [61] and, in the form of a highly conductive few-walled matrix, to boost neural maturation mechanisms [62]. A main downside of their usage as inherent medication in
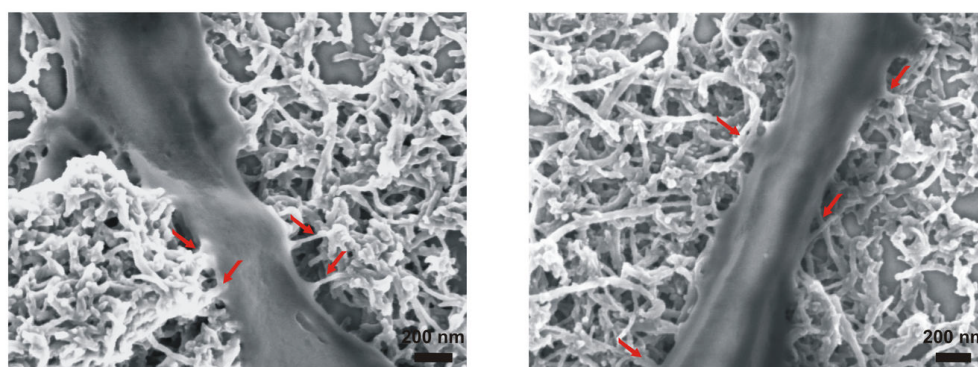

Figure 4. SEM images of neurites from neurons isolated from the neonatal rat spinal cord and grown on a multi-walled carbon nanotube layer. Numerous tight contacts (red arrows) establish between nanotubes and neuronal membranes (adapted from ref. [54]).

neurology diseases especially resides in the competing effects of brain degradation and excretion, to be tailored with care according to the targeted in-vivo application [63]. More details on carbon nanotube toxicity versus biocompatibility are supplied in Section 8.

Among the features regulating cellular recognition, activation and adhesion (such as wettability, topographic structures, surface chemistry), chirality is known to cover a particular role. Many biological processes are very sensitive to molecular chirality, the study of chiral interactions between cells and substrates having already been advanced for some time [64]. Surface chirality is supposed to be recognized by cells through their high chiral selectivity to certain biomolecules and biopolymers [65]. Single-walled nanotubes with lower chiral indices seem to develop a significant adhesion to lipid bilayers and make use of different time-evolving processes to ease internalization in the membrane (see Fig. 4) [66]. Ammonium-functionalized multi-walled nanotubes were observed to be internalised in both phagocytic and non-phagocytic cells on the basis of two mechanisms. Individually, via membrane wrapping or direct membrane translocation, in clusters, within vesicular compartments [67]. Cell adhesion is also enhanced by applying electrical fields larger than ~ 1 V/cm, taking into account that it gets fully depleted at ~ 5 V/cm [68]. In NCN, while ad-hoc functionalizations of nanotubes may improve the compatibility of carbon nanotubes with chiral molecules [69], the extraordinary properties they display are deeply affected by their 'helicity',[3] which stands for a terse summary of molecular diameter, torsion and wrapping [70,71]. Among the three main families of (single-walled) nanotubes, armchair (n, n), zig-zag $(n, 0)$ and "chiral", only the third possesses non-superimposable mirror images (left- and right-handed helical stereoisomers [72]). Changing the nanotube helicity can modify some stereospecific cell interaction and, for example, the electrical behavior. To which quantitative extent such two responses, for neuronal adhesion and electrical activity, could be separated or standing for an unique effect represents an open question that is interesting on its own right.

On the other hand, adhesion of filaments to soft living matter is not only governed by biology and chemical treatments, but mechanics and geometric patterning too. A variational criterion for the total energy functional can be therefore set and solved for the most significant quantities met in the mechanics of interfaces, as bending rigidity, curvature, surface tension, and various contact potentials [73]. The roughness of nanotube surfaces then may certainly have an impact on the neuron-nanotube adhesion [74,75] and on the electrochemical time/frequency response [26]. From the biological point

---

[3]   Often and improperly called 'chirality'. This and other similar words, like 'chiral vector' or 'chiral index', in carbon nanotube chemistry are not strictly connected with the exact chirality definition of stereochemistry.

of view, the effect of curvature might also be studied by means of Hodgkin-Huxley's equation, and any related model relying on the 'ionic hypothesis' [76]. The specific metric tensor form, as it comes from Laplace's operator in a curvilinear coordinate frame, may alter accordingly the electrokinetic process. Obviously, there is no compelling reason for a continuous extension of a model, from a flat to a curved space, to continue to hold. Moreover, Hodgkin-Huxley's models were questioned over the years to be not universal [77].
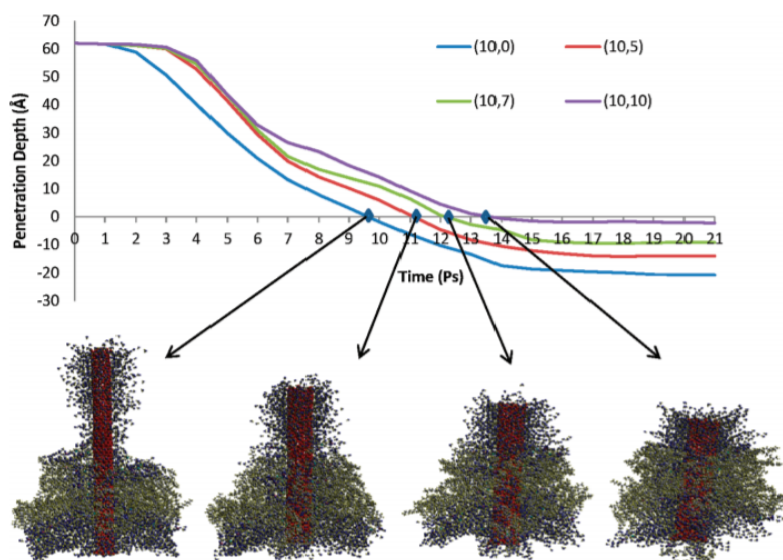

Figure 5. Molecular dynamics calculations of the axial coordinate of the bottommost carbon atom in nanotubes with different chiralities (adapted from ref. [66]).

Lastly, mechanical effects in biological membranes are anything but negligible. Further experiments on neuronal cells could elucidate the roles played by curvature and deformation. The former, for example, was established to be important for the propagation of action potentials from ventricular myocytes (in extended cardiac tissues) [78] and for a prolonged access duration in intracellular recording [79]. Signal velocity and duration turned out to be respectively inhibited and enhanced by increasing the wave path curvature [80]. In addition, non-linear current-voltage characteristics are found in cellular structures under an applied load ($> 5\mu$N, $v = 2$ V) [81]. There are ion channels known to be stretch-activated [82], while an electromechanical transduction mechanism was put forward in some types of cells [83], where membrane stretch and curvature strain modify the ion channel transmission. Afterdepolarization potentials, on the basis of cell specificity and morphology, then would affect the curvature strain, as it is explained by a sort of ferroelectric coupling, still related to molecular chirality. Carbon nanotube meshwork and neural network can also be conceived as two membranes mutually adhering to each other, one biological liquid-like, one other solid-like, provided that the substrate material reasonably allows for this description (as it holds e.g. for a graphene sheet [84]). Note that, when molecular units on the substrate penetrate inside a cell, a mechanical interaction state will be established with microtubules, neurofilaments and filamentous-actin molecules, overlapping a wealthy of time-dependent interactions among bundles of biological filaments [9,85–89] and giving rise in general to a three-fold interphase, such as membrane/liquid solution/carbon nanotube,[4] each displaying their own characteristic spatiotemporal scales.

In summary, influences of chirality, adhesion and cell mechanics are still to be scrutinized. Particularly, chiral properties of nanotubes, and/or other molecules with given stereochemistry, may be conceived as 'chirality carriers'. Changing adhesive and mechanical features can affect the signal transmission

---

[4]   Ignoring the distinction into extracellular and cytoplasmic intracellular solutions.

and interactions among the involved phases. An example may be coupling neurons and nanotubes over the length scale pointed out by some curvature value, either belonging to the biological interphase or some ad-hoc substrate surface.

3. Dispersion, Deposition, Deformation of Carbon Nanotubes

The starting materials processing and the final biological response may be tough to be related with accuracy, a reason lying in the carbon nanotube dispersion and deposition routes. First of all, significant batch-to-batch variations in length, width and number of walls may occur amongst distinct nanotube preparations, as it is tough to control all the parameters [90]. Then, the substrate morphology can be rather diversified, according to the implied interaction strength. For example, single tubes may give rise to equilibrium structures that are locally isotropic, or locally anisotropic but globally isotropic, forming equilibrium isotropic bundle networks or out-of-equilibrium fractal distributions. The deposition process may therefore yield an heterogeneous stress distribution at the nanotube/substrate interface, with possible local perturbations to the cellular coupling.

Deforming a metallic nanotube may also induce, reversibly, electrical conductivity changes [91], as it perturbs the electron band structure on the basis of the chiral vector state [92]. In addition, carbon nanotubes can behave as electromechanical actuators (Fig. 6) [93]. This coupling is rather different
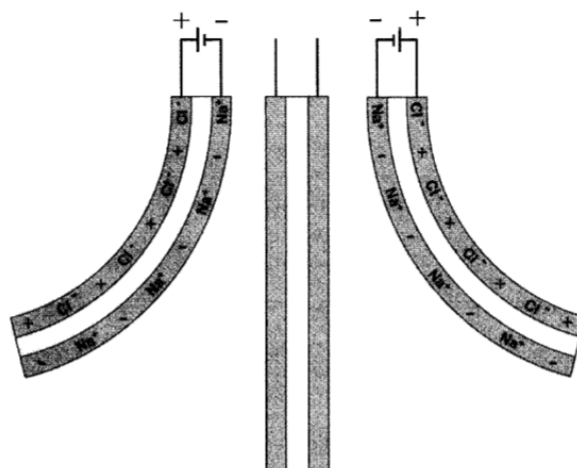
Figure 6. Scheme of a cantilever actuator based on two single-walled nanotube strips (shaded) and operated in aqueous Na^+Cl^-. Ions depicted in nanotube sheets stand for double layer ions at the nanotube bundle surfaces, compensated by the injected charges. When a voltage is applied, the actuator displaces to the left or right (adapted from ref. [93]).

from that encountered in conventional piezoelectric materials, and is ascribed to phonon frequency shifts upon charge injection [94]. In NCN experiments, where nanotubes adhere to the substrate, such an effect may be compromised. Notwithstanding, as electromechanical processes form a relevant part of cell functioning (see also e.g. 'ferroelectricity' and 'flexoelectric' phenomena), it looks promising for designing some new work.

It is worthwhile to remember that a number of neuroscientists conjectured the occurrence of mechanical perturbations traveling along axonal fibers [95,96]. In brief, nerve fibers and cells would swell when action potentials are fired. This insight was supported by several phenomenologies, like dislocations, mechanical and temperature responses, which turn out to be in-phase with the spiked potentials. Temperature, particularly, would undergo an initial increase followed by a cooling, suggesting a mechanism of pulse generation accompanied by an in-phase isentropic transformation. The experimental signature of this occurrence was ascribed to turbidity, fluorescence and birifrangence changes [97], none of them however being contemplated by any basic or modified Hodgkin-Huxley's electrophysiological model. We will get back to such thermodynamic aspects again. Finally, a

non-thermal mechanism of weak microwave field impact on a nerve fiber was proposed to occur in the frequency range $(0.03 - 0.3)$ THz [98,99]. Pronounced resonances, related to ultrasonic membrane vibrations, would establish upon interaction with electromagnetic radiation, and it would be interested to test the role that carbon nanotubes may take in the general context of THz excitation in biological membranes (see e.g. a Frölich-like condensation recently conjectured in lysozyme protein crystals [100]).

Stepping back to materials processing, the relations among structural properties and stress states in thin films, evaporated under high-vacuum conditions, is an old issue of surface and vacuum sciences. Film morphology is controlled traditionally by changing substrate temperature, deposition rate, and the concentrations of residual gases and impurities. Alongside, mechanical stresses are affected by capillary stresses, domain walls, and adjoining particle forces [101]. To get precise relations among processing, nanostructure and the final biological response, it will first be opportune to identify the nanotube features that may be reasonably regarded as invariant, from their as-prepared synthesis (by arc discharge, chemical vapor deposition, template methods and laser ablation of graphite, among others, at different processing conditions such as pressure, temperature, chemical environment) [102] to the film formation, and then proceed with characterizing the meshworks sent to neurophysiology experiments.

The study of the liquid dispersion, which nanotubes are suspended in and substrates are covered by, also deserves some attention, as another objective is working with homogeneous mats. This is a challenging task, sometimes remedied by clothing nanotubes with conducting polymers [103]. Dispersions of carbon nanotubes can be approached by rod-like solution thermodynamics [104] and were suggested being analogous to polymer solutions [105], though application of well-established prompting interesting yet non-trivial analogies with macromolecular theories (of stiff filaments) seems to be far immediate [106]. The high anisotropy and aspect ratio, in fact, impact their diffusive behavior without compromising their motion in a crowded medium. Single-walled molecules (of length $\approx 3 - 15$ nm, diameter $\approx 0.7 - 1.2$ nm) displayed a movement analogous to reptation [de Gennes] in concentrated gels [107], while nanotubes long (0.5–1) μm with diameters (1˜5) nm diffused rather efficiently within the brain extracellular space, pointing out more or less directly the relevance of quantities typically met in the study of polymer solutions and gels, as viscosity coefficients and particle-matrix interactions [108]. Jointly to strong intertube van der Waals's attraction forces [109] that follow from nanometer-sized diameters at mesoscopic length scales, suspensions of rods show a variety of interaction phenomena, specific to anisotropic particles [110,111]. In tissue cultures like bronchial epithelial and fibroblast cell lines, hydrophobicity turns out to be the main factor affecting aggregation of as-prepared and purified multi-walled carbon nanotubes, while ionic strength would mainly control the dispersability of carboxylated tube molecules, with augmented negative surface charge [112]. Along this line, an interesting analysis would be on the relation between nanotube number density of functional surface groups and the dispersability[5] of carbon nanotubes in a number of dispersants. Reactions like 1,3-dipolar cycloaddition [113] (see Fig. 29) or the organic covalent 4-methoxyphenyl substitution [44] may provide with a suitable framework to express fundamental quantities, e.g. Flory's and Huggins's parameter, as a function of the mean chemical functionalisation per tube. An effective dispersion study can be conducted by rheology experiments, quite familiar in colloid science, on viscoelastic properties at different solid fractions in both steady and dynamic-oscillatory modes. We mean here measurements of shear stress and viscosity at variable shear rates [114] and, when more molecular details are necessary, of complex viscosity, storage and loss moduli against the controlled-strain frequency [115]. Preparing samples of reproducible and variable homogeneity may clearly benefit from techniques such as electrophoretic deposition, regarded to be one of the most promising [116]. Other remarks may come from the contact, total or partial, of nanotubes with

---

[5]   Not seldom confused with the solubility concept.

(extracellular and cytoplasm) electrolyte solutions, as set by the experiments in-vitro. Adsorption phenomena can exploited in fact to change the mechanical features of adsorbants, as it happens for example when oxygen is adsorbed onto graphene, modifying its bending rigidity and possibly its adhesion properties [117]. Charging a metal electrode creates a surface stress that is linearly scaling with charge density, tensile or compressive states being predicted respectively for negative or positive charging. Dispersant reagents adsorbed on the nanotube surface can also modify its cellular interplay, especially by means of oxidative stress [118].

Finally, to face a discussion of issues in the surface and interface science of clean and adsorbate-covered nanotube systems [119] falls outside the aims of this review. Adsorbate-induced processes at solid-gas or solid-electrolyte interfaces are traditional subjects of thermodynamics (see Guggenheim's and Gibbs's approaches [120]), yet the measurements of interfacial quantities continue to pose challenging issues. A feasible proposal would be carrying out a mechanical mat description in three main circumstances, after its deposition on the glass substrate, when it is in contact with the extracellular solution alone, and just before the electrophysiology experiments, in contact with the biological phase as well.

To recapitulate, the work described in this section addresses possible modifications that nanotube films undergo upon the processing of materials and sample preparations. The type of carbon nanotube suspension (e.g. individual or cluster molecules) and their surface group functionalizations (e.g. with large or small molecular weights) are expected to play an important role to set the dominant mechanisms affecting cellular uptakes. Furthermore, nothing could rule out beforehand a NCN interaction of mechanical nature, resulting into a coupling of the ion channel charge injection with an electromechanical perturbation of the carbon phase.

4. Percolation, Mass Concentration and Geometrical Effects

Substrates in NCN experiments were densely covered by carbon nanotubes [4,5,10,121–124]. With increasing concentration of the initial dispersions, mats get thicker and thicker, their mean height starting to exceed the mean nanotube diameter from some density threshold onwards. Unless to work far below this value, an account of film thickness effects should be therefore in order. A second observation on the films normally used in NCN interphases is to consider them (well) above the so-called electrical 'percolation point' (see Fig. 7) [125,126]. This threshold generally
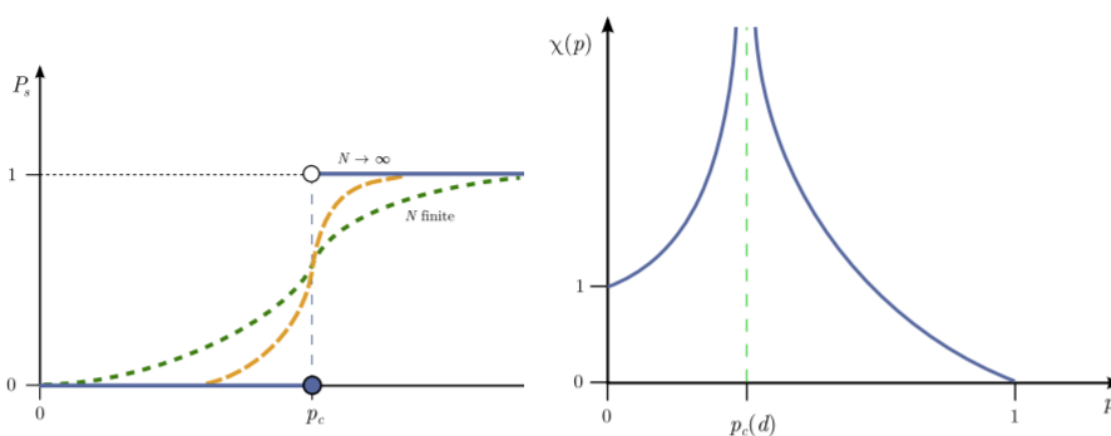
Figure 7. Scheme of relevant quantities in a percolation process. On the left, generic plot of percolation probability (P_s) as a function of site occupancy (p) and system size (N). On the right, mean cluster size (χ) versus p (adapted from ref. [127]).

denotes the concentration value that, for a given lattice symmetry and occupancy mechanism (site or bond percolation, for instance), identifies the minimum loading of material needed to generate the first connected path, or 'infinite' cluster, spanning a representative volume element. In any

medium coalescing into a continuous network, electrical percolation is in essence a geometric phenomenon. Otherwise, one should regard the prevailing transport processes (e.g. electron tunneling). Junction resistance, between electrical units, is of a certain importance as well. If it is much larger than the resistance of conducting units, as expected in a nanotube layer, then working above the percolation threshold equally entails an aleatory distribution of energy barriers for charge transfer. In electrophysiology experiments, however, carbon nanotubes can form interfaces with cellular liquids and interphases with biological matter, both producing different effects on the electrical and dielectric properties. In general, while contact resistivity at the interface certainly decreases the electrical conductivity, a high interfacial resistivity inhibits tunneling between adjacent units, leading to low-loss percolative networks [128]. At any rate, the roles of bathing electrolyte solution and neuronal membrane on the charge transmission should be inquired. This will be mainly discussed in the next sections, devoted to electron and electrochemical processes. In the following, the expected percolation phenomena will geometrically be examined.

Basic concepts of percolation theory are highly general and applicable to numerous physical situations, both static and dynamic [127,129], either in a scalar or vector formulation. They are fruitful to model any mechanism of electrical conduction (ionic, for instance [130]), network connectivity (rheological [131], elastic [132]) and to be widened to eventually take multiphasic media (as carbon nanotubes-polymer composites [133]) into account. This would be the case, for example, of a macromolecular compound or a filler, physically covering the substrates or chemically linked to carbon molecules. Clearly, every time a percolation threshold may play some role, to determine it can prevent the experimenters from material wastes. Reducing the nanotube density could improve biocompatibility, also related to a substrate concentration threshold for apoptosis [134].

In the present case, an 'electrotonic' hypothesis was introduced to explain the afterdepolarization process in cell membranes cultured on nanotube mats [4], where it was put forward that tight contacts among nanotubes and cell membranes are electrically shortcutting proximal and distal neuronal compartments. This insight can be formulated, yet heuristically, when films and bundles of nanotubes pinching the neuronal membrane are dense enough. Neurons, in that case, would convey a fraction of electrostatic energy of biological origin to be reutilised by the cell, coupling soma to dendritic trees by triggering , a voltage perturbation backpropagating action potentials with electrogenesis of Ca^{2+} ions into dendrites [135]. The electrical current evoked consequently would then propagate to the soma, depolarizing the membrane and initiating multiple action potentials. Remind that dendrites express different species of voltage-gated ion channels, many of which being variably distributed along the membrane [136]. Backpropagation is governed, along with dendritic excitability, by ion channels (namely, Na^+, Ca^{2+}, K^+) and their interplay [137]. It is a neuroregenerative regulator implied in synaptic feedback and fine-tuning phenomena, in the release of Ca^{2+}–dependent messengers, in single-cell excitability and spike-time-dependent plasticity. Neurons firing high-frequency action potentials upon NCN interactions seem to be more inclined to back-propagate (e.g. [13,138] and references therein). On this basis, an investigation of the network in light of percolation theory would be promising for a complementary understanding of what is behind NCN interactions.

First of all, one cannot say in advance that the film percolation point necessarily coincides with some electrotonic threshold (if any). We should not forget that, apart from cellular liquids, the system as a whole is basically binary and potentially interdependent [139], with three-fold connectivity paths (neuron-neuron, nanotube-nanotube and neuron-nanotube). While electrical phenomena in such domains proceed at different time scales (conduction velocity of action potentials [76], $|v_a| \approx (1 - 100)$ m s^{-1}, Fermi's velocity of electron conduction [140], $|v_F| \sim 10^6$ m s^{-1}), neuronal dynamics is believed to show correlations over multiple time scales, even in response to stationary or fluctuating signals [141]. In a single neuron, highly cooperative transitions between small numbers of ion channels are able to elicit an action potential [142]. Now it is still to be established whether some further scale, specific to the neuron/nanotube interaction, may or may not arise and require a connected (or percolating) network. Neurons could sensitively respond, in a restricted or the entire concentration

range, to any variation in the amount of nanomaterials interphased with them both intracellularly and extracellularly, where spike and signal amplitudes range respectively within tens of mV and from a few tens to few hundreds of μV [143,144].

Let us introduce to this end two ideal limits, a nanorod-like (conductivity) and a neuron-like (connectivity) regimes, respectively (Fig. 8) It may be that, to attain a significant NCN coupling,

$$\phi_N \longleftarrow \phi' < \phi < \phi'' \longrightarrow \phi_{cnt}$$

$$\text{neuron–like} \qquad\qquad \text{nanorod–like}$$

Figure 8. Sketch of neuron-like (ϕ_N) and nanorod-like (ϕ_{cnt}) limiting regimes. Solid fraction values (ϕ) are of nanotube molecules (bold wavy lines). All schemes in this paper are not to scale.

a dense film is required, forming an electrical network at or slightly above its percolation point. Otherwise, in the second limit, the interacting carbon molecules would more resemble the further elements of a sort of electrically reinforced neuron cell. In it interesting, at this point, to remind that connectedness and conductivity do not represent the same quantity. Dead ends of a percolation cluster only contribute to geometrical connectivity, but do not carry electrical current (or heat, for instance). This implies, near the threshold, that the connectivity rise is quite steep while the one for electrical conductivity is smoother. There is another critical point in a rod network, still to be recalled in this discussion, near which the mean cluster size can remain finite. It is the 'rigidity percolation threshold', describing the transition from a flexible to a rigid state. In a two-dimensional random network of infinitely rigid rods, and connected by free joints, it stands basically for a first-order phase transition [145]. This critical behavior is more relevant to the elastic theory of a disordered material, however, it may serve us to suggest an intermediate connectivity state, lying between nanorod-like and neuron-like regimes. In summary it is studying this 'binary percolation', and not a bare percolation of nanotubes, which may finally elucidate (or disprove) the validity of the former electrotonic hypothesis. About how to get such thresholds, the most realistic approaches are undoubtedly experimental. Substrates should be formed at variable densities, then be characterized to check up if percolation is or is not reached throughout the mat, and be finally addressed to the electrophysiology experiments for deducing the amount of nanotubes at which the biological response is first elicited. To this purpose, various measurements can be generally available, such as dc conductance, complex dielectric constant, magnetoresistance, noise power [146]. The electrical conductivity of carbon nanotube-loaded electrospun scaffolds, based on thermoplastic urethane and interfaced with rat mesenchymal stem cells, was showed to follow a percolation model with threshold ≈ 2.5 wt.% of multi-walled molecules,

suggesting tunneling and conduction mechanisms both to develop below and above the threshold [58]. Theoretically speaking, the most general framework which working in would be the (continuum) percolation of rods. A deeper inspection of cluster and pair connectedness concepts led to a formalism that, on taking advantage of the liquid state theory, benefited with precision and predictability [147]. A result that deserves to be recalled is the expression for the critical density of a dispersion of rods which, in three [two] dimensions, turns out to be proportional to the reciprocal of the mean 'excluded volume' ['excluded area'] about one particle, say [148]:

$$\rho_c(r, L) \; \propto \; \overline{V}_{\text{ex}}^{-1} \qquad [\rho_c(L) \; \propto \; \overline{A}_{\text{ex}}^{-1}] \tag{1}$$

r and L denoting respectively the rod radius and length. It is noteworthy that for sticks, in the 'slender rod' limit (infinite aspect ratio, $a \equiv L/r \to \infty$) and at lowest density orders, the proportionality law becomes an equality.

Notwithstanding, excluded volumes (and areas) are not dimensional invariants, but depend on the rod orientation, or randomness ($g = \overline{\sin \gamma}$, with γ being the angle about the axes of rods). Orientational state and aspect ratio determine the percolating cluster, at a critical volume fraction ($\phi_c = \rho_c V_{\text{rod}}$) that is either expected to decrease with increasing a [149] or g. For a network of single-walled tubes with $a \approx 10^3$, it turns out $O(\phi_c) \approx 10^{-3}$ [150]. The joint variation of a and g can let the critical fraction of a rod system span a wide range of values [151], this strong sensitivity of ϕ_c being expected in a nanotube network as well. With bundles, generally possessing a smaller aspect ratio than individual rods', thresholds should generally increase. Another relation which is not universal is that for the attraction strength and percolation volume fraction. An example just comes from an aqueous dispersion of carbon nanotubes stabilized with surfactant (i.e. the anionic sodium dodecyl sulfate). Unlike the excluded volume rule, where $\overline{V}_{\text{ex}}$ should decrease with particle alignment, an increase of intertube attraction turned out to lower the threshold (see Fig. 9) [152]. This effect was ascribed to be a consequence of
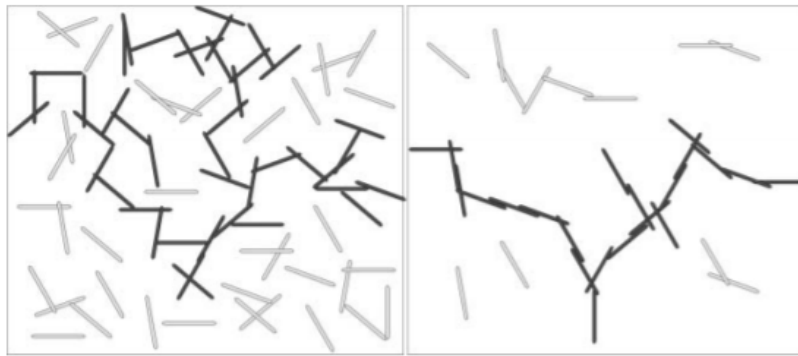

Figure 9. Sketch of percolating nanotube networks, with dark rods forming continuous conductive paths through the sample. On the left, with weak interactions and/or small aspect ratio, the network may be regarded as random. On the right, stronger attractive forces and/or larger aspect ratios make the nanotubes align and lower the percolation threshold (adapted from ref. [152]). More generally, however, the sense of threshold change depends on the particle connectedness, dimensionality and the proximity to criticality [153].

depletion forces, yielding a counterexample that shows the previous equation to be incomplete. To remedy this, one may work in proximity to the critical temperature and, in particular, at the distance where any particle pair can be actually considered as 'connected' [153].

These predictions were confirmed for a number of systems and variables, such as fibers with high aspect ratio, as a function of waviness (see Fig. 10) and 'core softness', quantifying the particle interpenetration [154,155]. For carbon nanotubes in polymeric and colloid media, the critical volume fraction turns out to be highly influenced by the intertube attraction and the amount of longer rods, but is slightly increasing with (a finite) bending flexibility or tortuosity [156]. Length of metal nanowires
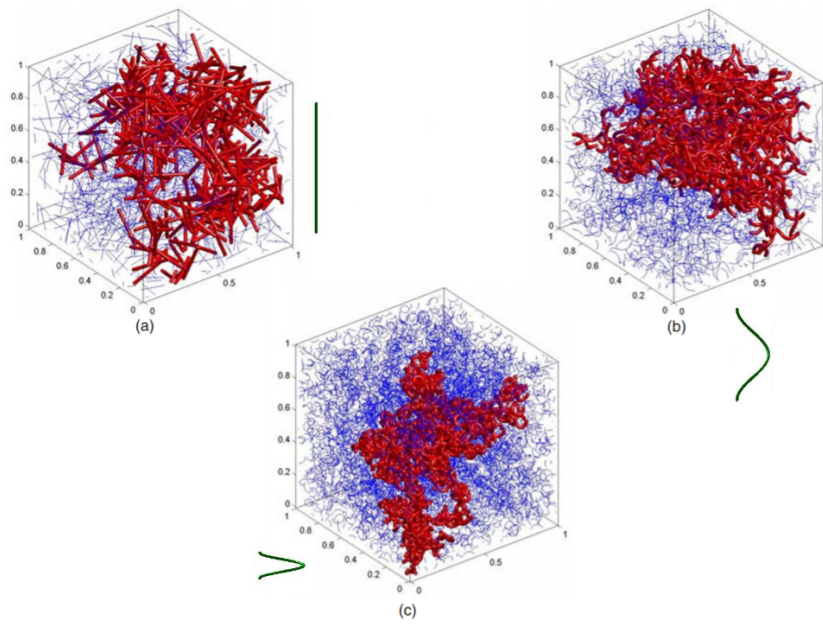
Figure 10. Percolation point with fibers of constant length and aspect ratio ($L = 0.2$, $a = 10$) at increasing waviness. Threshold is inversely proportional to the excluded volume times a constant that increases with waviness (adapted from ref. [155]).

affect as well the electrical conductance and mechanical stress of their percolating networks [157]. It is instructive noting that, from a geometric analysis of piles of frictional straight cylinders, the coordination number z vs a increases limitedly (in $z \approx 6 - 10$) and quite insensitively to friction [158]. In cases like that, the 'random contact model' affords a useful estimation:

$$z/\phi \;=\; \overline{V}_{\mathrm{ex}}/V_{\mathrm{rod}} \;\propto\; \phi_c^{-1} \tag{2}$$

Recall that the electrical conductivity of a composite material is usually lower with wavy than straight tubes [159], while polydispersing the nanotube length should lower the percolation threshold, as longer rods are weighed more than those shorter [156].

We expect a useful applicability of such concepts to the NCN coupling context too, and to benefit from them for a correct data extrapolation. Nonetheless, a couple of remarks are in order. A first is on the space dimensionality that, to be strict with theoretical predictions, may neither be regarded two nor three. A strong dependence on the ratio between nanotube thickness and size may therefore take place. Other sources of non-negligible finite-size or spurious corrections are surely coming up from processing history and sample preparation. There is also a surface contribution to percolation, but it should return a scaling correction as well. When bulk and surface percolate simultaneously, the influence of surface sites becomes negligible with increasing distance of the surface ports (e.g. electrodes) [160]. Last but not least, evaluating a volume or surface fraction (ratio of occupied to unoccupied sites) in such nanometric coverages may bring to further uncertainties that matter a lot in a statistical error analysis.

Another point deserving attention is the geometric characteristics of carbon nanotubes, as nanoparticle geometry can affect cell differentiation [161] and the interaction with biological systems on its own right [162]. Single carbon nanotube molecules are (quasi) one-dimensional, their aspect ratios can be as large as $\log a \approx (4 - 5)$, and may develop a fractal morphology under strong enough out-of-equilibrium conditions. The local structures they give rise are geometrically 'lighter' and thus less invasive than other nanorods, a feature that should not be overlooked in a biological interphase [163]. Besides, the percolation threshold of a fractal aggregate is much lower than in a three-dimensional particle distribution, globally decreasing the loading of the carbon phase along membranes. That remembered,

the main geometric quantities of nanotubes remain the diameter and length, each being characterized by the necessary statistical moments (e.g. expectation value and variance, if statistics is Gaussian). Their change would modify at once various mat properties but, again, it cannot be said that no further effect, specific to geometry, shape and nanostructure, will come into play. As in any process having a strong stochastic nature, nanostructural fluctuations should themselves be examined along the substrate, where meshwork length scales affect the correlation lengths for the nanotube-mediated biological events.

But percolation phenomena are not limited to nanotube meshworks alone. Abrupt connectivity transitions, in response to overall electrical stimuli, were also detected in neuronal networks. The formation of giant percolating clusters was described by a scaling law for the size versus synaptic strength, the critical exponent of which being independent of culture details. It turned out that an analysis of percolation points allows to assign a measure of connectivity to hippocampal and cortical neuron cultures [164]. A critical state also emerged from monitoring a simulated neural network growth process at a constant density of cells [165]. Such suggestions may further enforce the conviction to inquiry the 'criticality-continuity' duality in the NCN coupling. A well-posed framework would be resorting to an overall unique medium, and defining a common volume fraction for a binary (percolation) mechanism. Though we cannot know yet about the feasibility of such an objective, it may be instructive to exemplify it through the percolation scheme classically occurring in a substitutional alloy [166].

In conclusion, a full analysis of connectivity phenomena in light of classical percolation theory would be mandatory to look into NCN interactions. Studying the interplay of geometry, concentration effects and cluster statistics will be promising to better clarify the role of network complexity, and what perturbations at the level of neuronal phase may suffice to get a significant response.

5. Thermal Conduction of Nanotubes and Thermodynamics of Cells

Thermal response of membrane capacitance seems to exhibit intriguing effects, such as membranal dimensional changes and thermally mediated displacement currents [167]. In principle, thermodynamic and heat transport properties (for a general review see e.g. [168]) might be of secondary importance here, as physiological work conditions needed by neuronal cells severely restricts the allowed temperature range. We will thereby limit ourselves to a concise discussion of some of the most general frameworks. The large values of thermal conductivity that a carbon nanotube can take on may find a principal explanation in the ballistic heat transport regime which occurs, apart from some restrictions, over rather large length scales [169]. Experimental and theoretical studies of carbon nanotubes with different characteristics assigned to their thermal conductivity a number of values with orders of magnitude ranging in $(10^2 - 10^4)$ W $(m\ K)^{-1}$ [170,171].[6] We do not focus here on heat conduction in nanotubes, but generally remember that two kinds of interaction should be accounted for, the electron-phonon, where electron scattering and energy bands play a central role, and phonon-phonon, which prevails in semiconducting species at room temperatures [172]. Obviously, changing the substrate material can alter remarkably the phonon properties and cutoff frequency, bringing about some thermal effect [173]. Nanotube-nanotube and nanotube-substrate conductivities may have competing roles in thermal transport and, just at the film percolation point, their relation may undergo a significant change [174].

It is quite difficult predicting about the likelihood of such perturbations, whether and how they can be more or less central in NCN interphases. We earlier commented on a possible electromechanical coupling of nanotubes with cells while an action potential is fired, and here the attention is turned to thermoelectric cross-terms [175], local electron and ionic heating processes [176], which may also

---

[6] Typical theoretical values at room temperature are 6600 W $(m\ K)^{-1}$ and 3000 W $(m\ K)^{-1}$ for single-walled and multi-walled nanotubes, respectively.

produce a non-negligible feedback among thermal and electrical features at the nanoscale. Nevertheless, the thermoelectric power of intrinsic/undoped tubes is ideally zero. This is due to equal and opposite hole and electron contributions, for having non-vanishing Seebeck's coefficients should require somehow an electron-hole symmetry breaking [177] (by resorting e.g. to chemical dopants). Local temperature variations can affect the energetics of membrane proteins, inducing geometrical and activation energy changes. For example, the sensitivity of A-type K^+ channels and voltage-gated Na^+ channels to cooling temperatures imply somatosensory neuron excitability [178]. The fact that the ionic hypothesis alone appears to be insufficient for a satisfactory understanding of nerve pulse propagation then raised the interest into thermodynamic aspects [179], where entropy, energy and ad-hoc criticality concepts suggest novel descriptions of neural network activity [180]. A thermodynamic account of the role covered by membrane lipids better explains how an action potential is elicited, with concepts like local nerve cooling (during induction), geometric swelling, reversible heat production and zero heat release (during propagation) coming into play. The effect of molecular effusion was evaluated numerically, and regarded to be dominant in the entire thermal exchange [181]. Molecular migrations across axon nanochannels, driven by a filtering process of water molecules and metal cations, would rearrange the implied velocity distributions, with a consequent thermal energy exchange. The related temperature difference turned out approximately to be $(0.02 - 0.03)$ mK, in fair agreement with the orders of magnitude extrapolated from several experiments.

To sum up, despite thermal behaviors might be of secondary importance at the outset, their investigation can be helpful to let the nature of other mechanisms emerge (for instance, electrical). Moreover, use of carbon nanotubes may be promising to look further into several aspects of cell thermodynamics. They could act as 'thermoelectric amplifiers' or 'probes', which not only alter the electrical connectivity of neurons, but effectively transport thermodynamic and thermomechanical states across the neuronal network.

6. Electron Conduction and Solid State Physics of 'Pin Nanoelectrodes'

6.1. Introductory Considerations

Consider Fig. (11a-c), illustrating for simplicity two general configurations of NCN electrical couplings between soma and dendritic trees. In the first (2a), nanotubes or their bundles get into the cell, for the three phases in which the system is divided, soft biological, carbon-based and liquid solutions, all come into contact in a couple of points connected by nanotubes. In the second, soft and hard phases are pulled apart by the extracellular liquid diffusing in between, partly (2b) when the membrane is only anchored at one end of the nanotube bundle, or totally (2c), when membrane and nanotubes remain physically separated. In Fig. (11c), triple contact regions or points vanish, only the nanotube/liquid interface and neuron/liquid interphase lying by. Evidently, when nanotubes pinch or penetrate into a cell, they can both reach the cytoplasm solution and remain inside or strictly adhere to the membrane, in the liphophilic region, giving rise to a soft/hard interphase. Needless to say that all these situations will tend to coexist and mix their effects, having each a given likelihood to occur. Notwithstanding, one can make a first simplification into a couple of separate frameworks, one electronic and the other electrochemical, the latter regulating electron transfers in solution and, as such, being of a greater generality for the NCN interphase. Out of equilibrium thermodynamic equations for membrane electrodiffusion get modified by the presence of nanotubes. To ascertain if quantities such as ion transport and solvent transference numbers get sensitively varied by the presence of nanotubes, an analysis of force-flux relationships is needed [182]. The assumption of linearity will plausibly rest on small enough Gibbs's free energy perturbations [183].

The first case (Fig. 11a) yields a more direct NCN coupling and, as tubes pinch or penetrate cells, any bioelectrical signal will fast run along the connected molecular paths, to come back into a more direct contact with the neuronal network. This will also take place in proximity of cells, where nanotube clusters can accumulate charge at the interface with the bathing extracellular solution. At
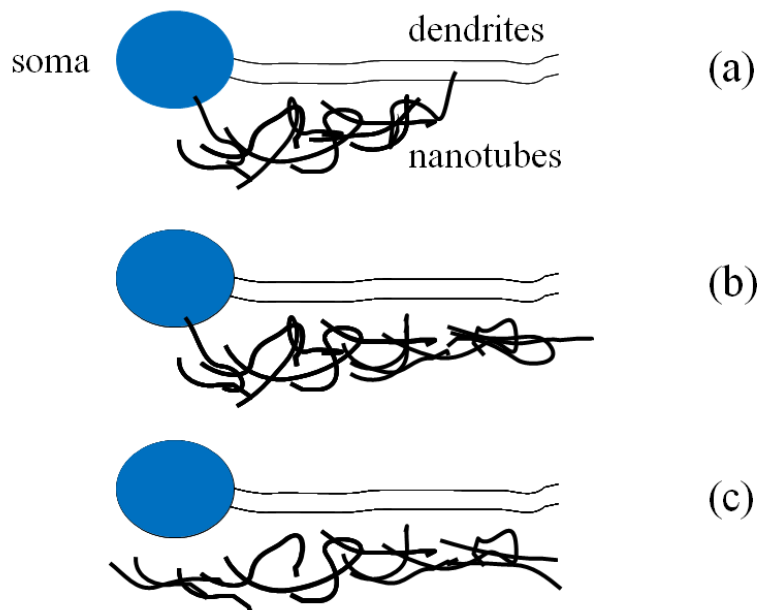
Figure 11. Soma-dendrite coupling mechanism of nanotubes functioning as (a-b) pin-nanoelectrodes and (c) nanocapacitors embedding a cellular bath. This scheme is also representative of reverted one-end configurations, anchored to dendrites alone.

any rate, as electron conduction is much faster than ion's, the nanotube film will crudely act in the first configuration (2a) as a sort of equipotential line, quickly shortcutting the portion of neuronal network that is reached by it. This view would find a simple interpretation in terms of current electrophysiology experiments, bringing the existence of backpropagating potentials to light: An ad-hoc microelectrode injects electrical energy, suitably applied to those regions of the cell believed to trigger or elicit the response [184]. For an action potential to backpropagate into dendritic trees, it is necessary to initiate them somewhere in the region proximal to cell's body. Backpropagating signals then may be amplified by a process that is timely pairing with excitatory post-synaptic potentials, returning a somatic afterdepolarization increase [185]. According to this interpretation, the carbon-based film would stand for a matrix of nanoelectrodes, making and iterating artificially a large number of electrophysiology stimuli.

To prove that this configuration is a primary cause for the present NCN interaction, a couple of strategies may be adopted. First of all, other nanorod or particle species should be checked, provided they are electrically active and similarly able to enter the biological membrane. A comparison among nanomaterials (i.e. solid-state properties of molecular building blocks, geometry and topology of nanostructure) then will allow to conclude about the strict necessity to work with 'pin nanoelectrodes', endowed with a minimum penetration power inside the cells. If this were not the case, nothing may guarantee that the detected biological enhancement is circumscribed to some nanoscale effect, neither to the rod-like shape nor to the extraordinary electronic properties of carbon nanotubes. Any conducting form of matter, directly attachable to neuron cells, would be instead a promising candidate for a meaningful check. Think, for instance, of conducting polymers [186], vertical nanowire electrode arrays [187], nanoparticles with needle-like ends, hybrid materials made of array of molecular units attached to a planar lattice, just as carbon molecules of a graphene sheet [188,189]. We should care, of course, of circumventing any interference with percolation effects, the easiest way to do that just being to start from mats prepared well above the critical volume fraction. What could not be prevented, however, is the coincidental electrochemistry contribution from the solid/liquid interface. Another important aim is to confirm that pin-like nanoelectrodes provide with a larger coupling than the electrochemical one. Alongside, when cells are punctured or pinched, investigating on topological and

geometric particle features (e.g. average dimensions and shape) will supply further indications on toxicity, i.e. if and how it may be or may be not geometry- or topology-dependent.

6.2. Individual Single-Wall Nanotubes

We focus here on a few- and many-carbon nanotube systems, that is junctions and networks, passing through an account of electrical features of single molecules. Individual properties do not form in this context an independent subject of research, but may be important in view to control the samples from a nanometric/molecular level.

Two are the main families of tubes, with smaller ($d \approx 0.4 - 2$ nm; single-wall) and larger ($d \approx 2 - 100$ nm; multi-wall) diameters depending on the number of molecular walls or shells they consist of, while their length can measure up to several hundreds of μm. They are composed by rolled up graphene sheets, thus can assume the shape of a single-walled cylinder, or multi-walled co-axial cylinders. A single-walled molecule, with chiral vector (n, m), can be metallic when $n - m \in 3N$, including a subclass of semiconducting tubes with narrow band energy gaps ($E_g \propto 1/d^2$), otherwise it is semiconducting, with moderate energy gaps ($E_g \propto 1/d$) [190]. Central to such numerical rules is clearly the electron structure, especially, the density of energy states $\nu = \nu(E)$ in graphene sheets, from which these tubular shapes come geometrically by a wrapping operation. As usual in one-dimensional structures, ν shows singularities of the van Hove's type, where the density of states $\sim$ differential conductance $\sim 1/\sqrt{E}$. At Fermi's energy ($E = E_F$) it vanishes in semiconducting tubes but remains finite in metal samples [191]. In particular, metallic single-walled molecules display a long electron elastic mean free paths (> 1 μm), identifying quasi-ideal one-dimensional systems, where charge and spin transport is highly affected by electron-electron interactions in a special liquid-like state of matter, bearing the name of J.M. Luttinger [192]. Armchair nanotubes ($n = m$), for instance, are truly metallic and excellent realizations of 'quantum-ballistic wires'. In a bundle of metal single-walled molecules, instead, their van der Waals' interactions can bring to a pseudogap (~ 0.1 eV in $(10, 10)$ armchairs) at Fermi's level, responsible for a semimetal behavior [193]. To measure the intrinsic resistance of such systems, however, may not be free from shortcomings or misinterpretations. Establishing more contacts than tube ends can strongly interfere with its one-dimensional nature, and the analysis of individual molecules could mix up to a certain extent with junction phenomena.

In NCN interphases, carbon nanotubes do not embed an electrically neutral environment. Cells produce transient and stationary fields, which get somehow to nanotubes in the form of action (V_a) and rest membrane (E_m) potentials. electrical and magnetic fields can be rather influential on nanotube electron structures [194], where band gap opening and closing, for example, are predicted in zig-zag molecules (see Fig. 12) [195]. They can modify the intensity, position and number of prominent peaks in the density of states [196]. In double-wall nanotubes, which are the smallest multi-walled structure, external fields can remarkably alter the electronic properties [197] while single-walled metal-semiconductor junctions appear to be sensitive to positive longitudinal electrical fields, producing electron delocalization and interfacial charge accumulation [198]. It is concluded that transverse fields of $\sim (0.1 - 0.2)$ V nm^{-1} may suffice to significantly increase the density of electron states at $E \sim E_F$, enhancing the junction conductance. Despite biological potentials are rather weak as well ($|E_m| \approx 45 - 90$ mV, $\delta V_a \sim 100$ mV in amplitude) [199], a discussion of their effect is anyway in order. What would be interesting to figure out is whether a biologically-driven modulation of carbon nanotube properties may occur during the cell functioning (e.g. a 'switch'-like behavior). A directional analysis of electrical fields and signals in NCN systems would be tough, but action potentials and their reverse backpropagations point out a preferred direction on their own right. Note that the electrophysical behavior of nerve membranes was already confronted to electrical diodes, with which they seem to share a number of trends [200]. An analysis of data below the percolation point will be helpful to test the electrical contributions, to the NCN interaction, which may locally depend on network or meshwork orientation.

If all chiral vectors of a distribution of single-walled molecules were equiprobable, the average fractions
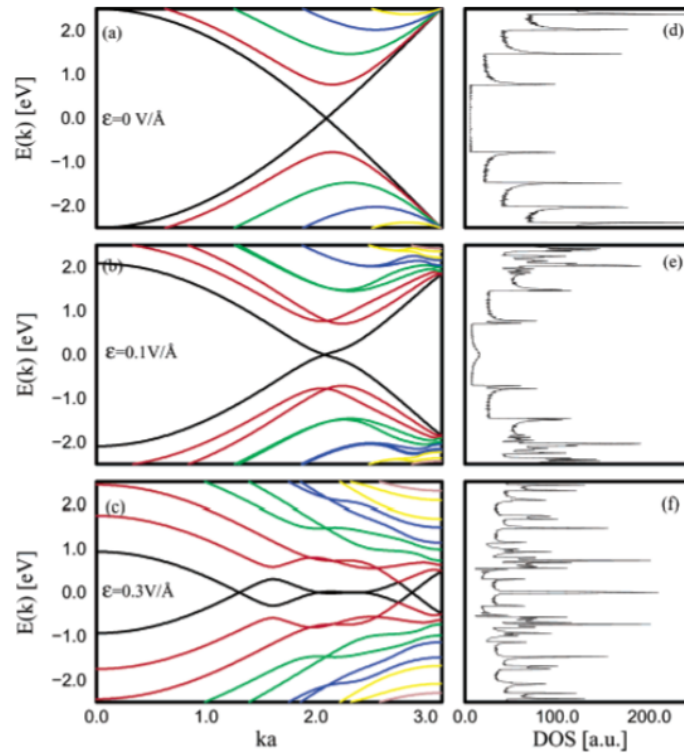
Figure 12. Band structures (left) and density of states (right) of a $[10, 10]$ armchair nanotube ($|E| \leq 2.5\ eV$). Here ε denotes the transverse electrical field intensity and ka is the wavenumber (adapted from ref. [153]).

of its metallic and semiconducting units would tend to $\frac{1}{3}$ and $\frac{2}{3}$, respectively [201]. The effect of their local fluctuations should clearly become more appreciable when the substrate coverage is low or reduced below the percolation point. On the other hand, an investigation of neuronal activity as a function of the electrical character of (single-wall) nanotubes would undoubtedly deserve some attention, especially to focus on the roles of E_g and other energy band properties. A reasonable way to do that is adopting the tube diameter as an independent variable in electrophysiology experiments. Changing d generally affects the energy spacing between van Hove's singularities. In particular, for a semiconducting molecule it turns out $E_g \approx (0.88/d)$ eV [202]. Remember that electronic and electrical properties can be related through the connection between density of states and differential conductance.

Unveiling the relations among neuronal or cell features and solid state tools like electron structures in carbon nanotubes or other nanoparticles is an intriguing program that is still in its infancy, whose significance is yet to be fully unravelled. While an ionic/electron coupling may be expected to hold in NCN interactions, mediated by the electrochemical species diffusing in the liquid phase, an interesting prospect would be the search for new hypothesis in neuro- and nano-sciences of a more theoretical nature, as they may benefit from combining different theoretical cores together (i.e. ionic hypothesis, quasi-particles and energy band models).

6.3. Individual Multi-Wall Nanotubes

Multi-walled molecules are formed by coaxial nanotubes, cylindric shells or layers, whose spacing ($\approx 0.34\ nm$) follows from the graphite interlayer distance ($\approx 0.335\ nm$) [201]. These structures are 'chirally irregular', in that the sequence of tubes, from the innermost one to that outermost, exhibit different chiral vectors and thence different electrical features. No chiral angle correlation was also found along the constituent tubes of double-walled molecules [203]. Walls give rise to a non-trivial

interacting system, where intertube coupling tends to remarkably alter the band structure and to strengthen with decreasing d [204]. The density of states was suggested not to be additive in the wall number, the transport properties of any single layer being dissimilar from those of identical single-walled nanotubes [205]. The electrical conduction of double-wall molecules thus was proposed to sensitively depend on the layers' character, whether metal or semiconductor, and on their interwall spacing, as it affects the overlap of orbitals ($2p_z$) perpendicular to wall surfaces [206]. On decreasing such a separation, density functional techniques predict the occurrence of semiconductor $\leftrightarrow$ metal phase transitions. This may be equally achieved by chemical means, e.g. by heavily exposing initially metallic multi-walled molecules to oxygen [207]. As Luttinger's model does not suffice as well to a complete description, other frameworks were offered as alternatives, like environmental quantum fluctuation [208] and Egger-Gogolin's [209] theories. Multi-walled architectures can benefit at times from one-dimensional reductions, for example, a set of independent graphene sheets [191].

Carbon nanotubes with diameter of (5~25) nm can bear high electric current densities, ($107 - 109$) A cm^{-2}), with no evident destruction in their structure [210,211]. In a first basic view, the mechanism of electron conduction in a nanotube may be described to vary from a ballistic-like ($l/d > 1$; one-dimensional) to a diffusive-like ($l/d < 1$; two-dimensional) regime on the basis of the ratio between tube diameter and (elastic) mean free path (l). It can then be ballistic ($l/l_\phi > 1$) or diffusive ($l/l_\phi < 1$) with respect to phase breaking, where l_ϕ is the phase coherence length [212]. In ballistic transport, normally realized when temperature is low, defect density and size are small, electrons can flow with a few scattering collisions over a length scale of up to ~ 10 μm, while in diffusive conductors they move at the expense of many scattering events. It follows that, on connecting a diffusive wire to a couple of electrodes, the resistance is proportional to its length (L). For a perfectly ballistic wire, it would be independent instead of wire length and equate $1/(kG_0)$, where k gives the number of conduction channels and G_0 is an intrinsic (quantum-like) conductance. For a single-walled tube $k = 2$ and $G_0 = e^2/(\pi\hbar)$ is the conductance quantum unit ($e = $ electron charge). In multi-walled tubes, channels are forming a network of parallel circuits, separated by energy barriers throughout the whole molecular domain [213]. Fig. (13) illustrates the diffusion coefficient in typical conduction regimes at a long time scale, specialized to a $[10, 10]$ metallic nanotube.
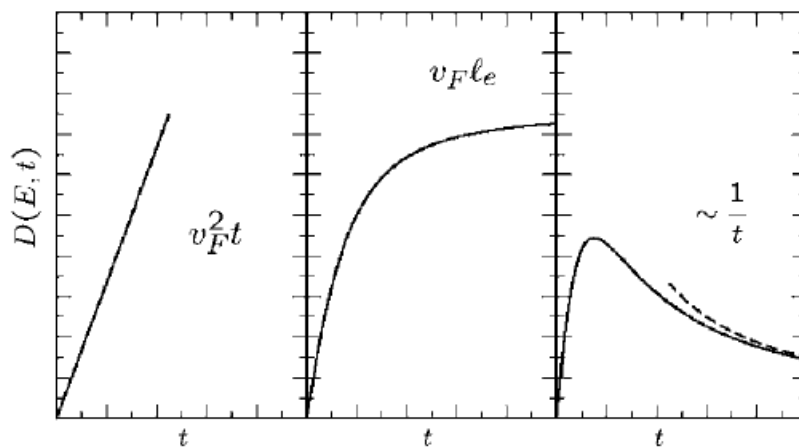

Figure 13. Diffusion coefficient versus time in ballistic (left), diffusive (middle; $\ell_e = $ elastic mean free path) and localized regimes (adapted from ref. [172]).

On adopting such a scheme, two hints may be pursued in the study of NCN interphases. A first would be inquiring if neuronal interphases can recognize different phenomenologies of charge transport in nanotubes, still for instance as a function of d. We remind to this aim that electron currents in a multi-walled molecule, with a contact on the outer wall, may not necessarily flow into the outermost shell [205], as previous Aharonov-Bohm experiments put forward [210,214]. Significant contributions may also come from intershell tunneling among the innermost layers [215], a phenomenon that may

itself promote a NCN interaction. A second hint is to study the NCN coupling dependence on L. In the framework of interconnect applications, it was suggested that multi-wall systems exhibit a critical length ($L_c \approx 7 \, \mu m$) below/above which the conductivity would decrease/increase with increasing d [216]. This effect should be more pronounced for $L > L_c$, when nanotubes approach the larger length scales of a neuronal network, favoring ampler shortcuts within it.

To sum up, because of a more controllable phenomenology and molecular disorder, single-walled nanotubes should be preferred in principle to multi-walled. This may be especially helpful at the outset of a chemical physics research, e.g. on a quantitative characterization of spatiotemporal scales and concentration regimes.

6.4. Junction Effects

Generally, interfacing nerve cells with nanomaterials is affected by the resistance of cell-solid junctions and the spectrum of thermally-induced voltage fluctuations [217]. Metal and semiconducting tubes then can be used to create intramolecular (multiterminal) junctions, comprising molecules of distinct chirality but equivalent diameters [218]. There can be various configurations (pictorially, L, T, Y, X, ..., up to multibranched, ring-like, tetrahedral, octahedral, icosahedral, and so on), providing with the basis for the study of a few (branched) nanotube-systems (see Fig. (14)). In NCN interphases,
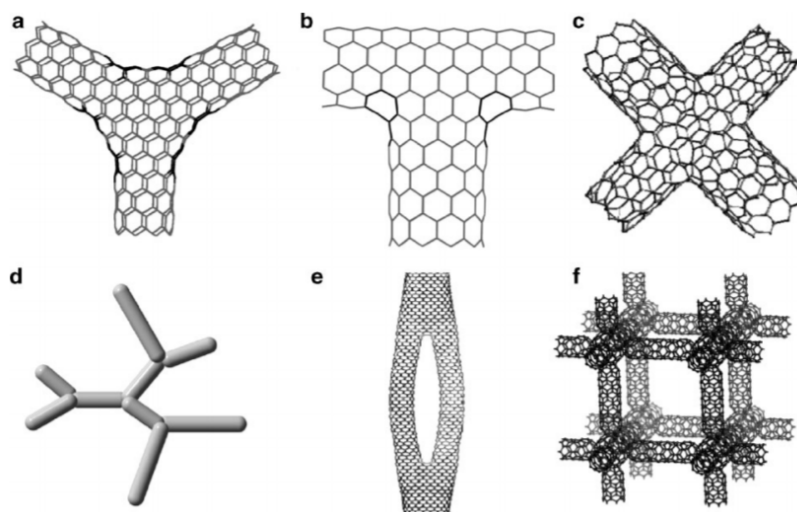

Figure 14. Different configurations of multiterminal intramolecular junctions in carbon nanotubes: Y-shaped (a), T-shaped (b), X-shaped (c), multibranched (d), ring-like and (e) network junction in three dimensions (adapted from ref. [218]).

transmission electron microscopy analyses are helpful to ascertain whether and which intramolecular configurations are formed preferentially onto the substrates. Furthermore, nanotube-based junctions may be also intermolecular, giving rise to contact resistances between nanotubes and/or between a nanotube and the electrical terminal acting as the current source, such as a metal electrode, a cell soma or axon. Wishing to improve the sample homogeneity and exploit the properties of branched systems, multiterminal configurations may be obtained by welding the joint nanotube surface area at high temperature, for example, by electron or ion beam irradiation. Their phenomenology should better emerge from an analysis of biological responses with dilute or semidilute substrate coverages. Nanotubes in a given configuration can be generally modeled as a nanodevice with fixed number of terminals, each identifying a conductance G_{hk} for the kinetic process $k \to h$. In two single-walled nanotubes in cross-configuration, for instance, G_{21} gives the conductance for electron transmission from tube 1 to 2, whose junction behaves as a gate for electrical transport. It is interesting to observe that its maximum value was predicted to be one unit of the conductance quantum, $G_0 \approx 1/(12.9 \, k\Omega)$, in agreement with experimental data on crossed nanotubes ($1/G_0 \leq 16.8 \, k\Omega$ at $T = 4.2 \, K$) [219]. However,

theoretical predictions and experimental data on contact resistances often show large discrepancies, the main reason behind being ascribed to diverse contributions taking part in such phenomena. The total resistance, $R = R_0 + R_s + R_m$, comprises not only an intrinsic length-independent part, $R_0 = G_0^{-1}/2$ ($\approx 6.45\ k\Omega$), but two additional terms that arise from linking the (one-dimensional) conductor with external contacts [191]. The first, $R_s \approx (L/l)R_0$, is of Ohmic nature and set by the ratio between the mean free paths for electron scattering and tube length. Similar laws formally hold for other free path dependencies (e.g. inelastic) [220] or situations (low-bias interconnect resistance) [221]. The second (R_m) is the material contact resistance, quite delicate to be addressed. Particularly, an analysis of the crossover regime between Coulomb's blockade and the nearly perfect contacts seems to be not straightforward at all [222]. In electrophysiology experiments, with 'pin nanorods', R_m is supposed to embody a contribution from the biological tissue, which can be interesting for ascertaining if and how it can be reduced.

Another point to remark is how a crossed junction may depend on the intrinsic electrical characteristics of individual molecules. With single-walled tubes, kept at room temperatures, it turns out in several cases [223] that metal-metal and semiconductor-semiconductor junctions have rather large linear conductances, $G_{mm} \approx (0.05 - 0.15)\ G_0$ and $G_{ss} \geq 0.01\ G_0$. Semiconductor-metal junctions behave as Schottky diodes of the p-type, with $G_{sm} \approx (0.3 - 0.4) \cdot 10^{-3}\ G_0$. Contacting single-walled semiconducting molecules are often of p-type, their processed solutions acting excellently as a p-type/ambipolar material, also for their ability to conform over arbitrary non-planar interfaces [224]. Semiconducting carbon nanotubes can work as Schottky barrier transistors, with metal-nanotube barrier height that is tunable by the metal work function [225]. These findings suggest that crossed single-walled junctions may be exploited to obtain quantitative information on the electrical nature of their units. From a molecular point of view, junction resistances get strongly dependent on nanostructure at the contact zone, changing by several orders of magnitude with manipulations or movements at the atomic scale [226]. Optimal electron transport is thus predicted when tubes are in atomic scale registry (like in a stacking of graphite layers), where modest pressures are able to remarkably enhance the electron transfer. Negative differential resistances would also arise from contacts of the end-end type, prompting applications as amplifiers, switches and memory devices. In armchair-based crossed junctions, intertube conductance versus the applied force (F_a) seems to behave approximately as a convex function, decaying from $\approx 0.2\ G_0$ to a minimum of $\approx 0.1\ G_0$ at $F_a \approx (10 - 15)\ nN$ [227]. Vice versa, the intratube conductance appears to be concave with a maximum rising from zero at $\approx 0.18\ G_0$ to a value slightly above $\approx 0.2\ G_0$. Based on such first-principle calculations, small pressures may be applied to test which conduction mechanism is predominant in the meshwork and to modulate conductance in NCN systems.

Configuration changes can modify the working characteristics. Single-walled Y junctions, for instance, were suggested to behave as ambipolar devices, whereas in the same conditions those of crossed-type would rather be unipolar [228]. About the mechanism of charge injection, both configurations would show the existence of a threshold temperature for the transition from electron tunneling to thermionic emission. When energy barriers ($\sim 110\ meV$ for the Y-type and $\sim (150 - 230)\ meV$ for the crossed-type) are overcome nearly above $T \approx 100\ K$, the dominant conduction process is expected to be thermionic emission. Below this threshold value, electron tunneling prevails, at least until the tunnel resistance gets large enough ($\gg R_0$) to cause Coulomb's blockade [229]. Thermionic properties are sensitive to several factors, such as dopants [230], and were also studied in multi-walled molecules [231]. This is to say that, if a similar threshold phenomenon were applying as well to NCN systems, the percolation picture would change more in favor of thermodynamic aspects. Actually, to well discriminate thermionic emission from (thermally assisted) tunneling would demand a thorough discussion of electrical properties and material-specific parameters, as it is shown by an analysis of metal charge injection into a low-dimensional semiconductor [232]. A temperature-dependent 'zero-bias' anomaly also arises in single-walled cross configurations from an intertube electrostatic barrier lying along the tube, or at the interface with electrodes. This feature, visible from plotting the differential conductance against

voltage dI_1/dV_1 vs V_1, may be gradually suppressed by a temperature increase, or by increasing the electrical current flowing across the second tube [233].

Extrinsic properties of nanotubes seem to matter more in multi-wall than single-walled systems. For instance, the room temperature (zero-bias) conductance of nanotube/metal electrode would be dominated by the resistance of contact regions, set essentially by the length of nanotube portions that are covered by the electrode [234]. Similarly, the rectifying behavior found in multi-walled Y-junctions (see Fig. 15) would be not an intrinsic characteristics of molecular branching, but a property of the nanotube/metal interface [235]. Wishing to check up the effects of the main nanotube features (e.g.
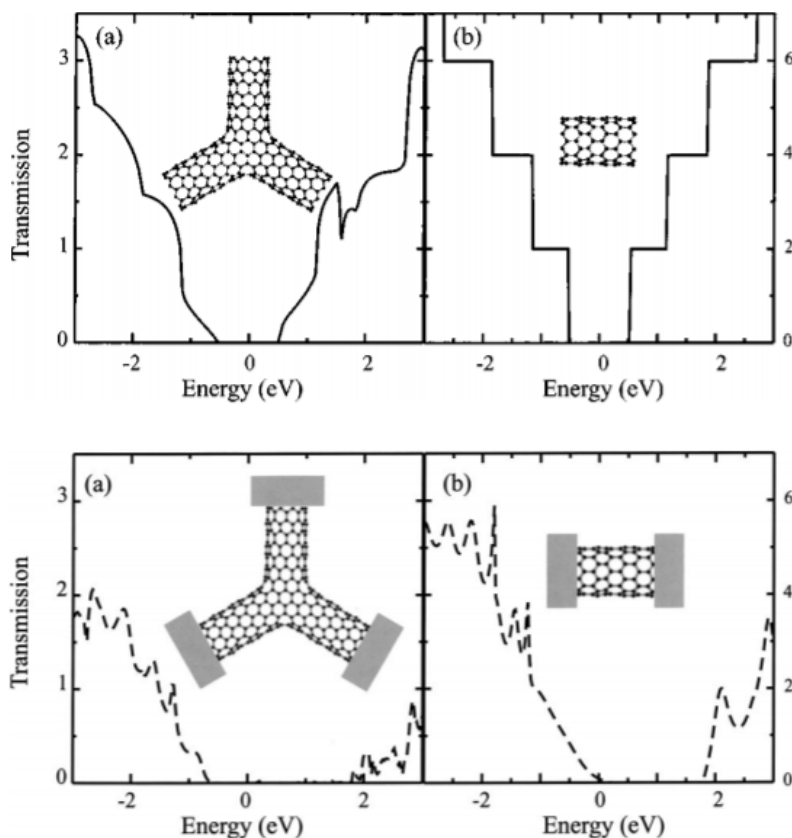

Figure 15. Electron transmission between any two terminals of the nanotube-terminated (a, top) and metal-terminated (a, bottom) symmetric Y-junction of three $[10, 0]$ nanotubes (adapted from ref. [235]). The same calculations were performed for a perfect $[10, 0]$ semiconducting nanotube (b, top and bottom).

chiral vector, diameter, defect concentration, bending), one should conclude again that an analysis with single-walled molecules is preferable, at least at the outset of an investigation. In this line, experiments on the NCN interphase may furnish information on the relative weight of intrinsic and extrinsic factors, keeping in mind that, unlike the single-walled, multi-walled nanotubes are normally diffusive or quasi-ballistic conductors.

The notions of tunneling density of states and the related tunneling conductance here may be equally noteworthy. They provide with the ground for a comparison of Luttinger's liquid theory, well matching single-walled tubes, with competing models that can predict the power law $\sim V^{1+\alpha}$ (and identically in T) for the tunneling density of states in multi-wall systems [236]. Tunneling conductance is vanishing as energy decreases (zero bias anomaly) with an exponent that, besides the number of walls, is influenced by the zone which electrons tunnel through, whether at the middle of tubes or their ends. This behavior can be reproduced from an environmental Coulomb's blockade, multi-walled nanotubes acting as effective LC transmission lines in series with the junction ($1 \leq E\ [meV] \leq 100$) [237]. A similar problem

seems to be issued by thick single-walled bundles, whose zero-bias anomaly is well interpreted both in terms of Luttinger's theory and transport properties of barriers at the nanotube/metal contact interface [238]. In metal impurities lying at a junction, electrons are described by Fermi's liquid theory. Performing electrophysiology experiments in which nanotubes are kept at different dc voltages may thus inquiry into the relevance of tunneling conductance changes. Such an investigation can promptly be extended to account for ac potentials in the frequency domain. In general, dielectric spectra of multi-walled molecules (up to $0.1\ MHz$) should exhibit a couple of separated modes [239]. The slower ones (dozens of Hz) reveals the space charge polarization at the interface with the electrode, and couple the electrical field component in phase with the measurement. Those faster (some or dozens of kHz) reflects permanent and induced orientational polarization states, coupling the oscillating field in the complex rotating measurement frame. In the higher frequency domain both single- and multi-walled tubes showed, independently of their length, an intrinsic resonance state ($f_r \approx 37.6\ kHz$) that points out an important oscillatory regime [240]. The resonance amplitude would be sensitive to temperature variations, progressively approaching zero on increasing T (from ~ 248 to $298\ K$), representative of a thermally activated impedance. Furthermore, from the response of metal-nanotube contacts, a negative capacitance ($4.46 \leq -C\ [pF] \leq 5.15$) turned out in the range $0.1 \leq f\ [kHz] \leq 8 \cdot 10^3$. This last aspect, potentially relevant also in electrochemistry, should not be underestimated. Figuring out a regime where nanoparticles behave as active electrical components can be of a certain importance. This would set a suggestive analogy just with neurons which, despite by different working principles, encompass both active and passive behaviors too.

Before turning to an analysis of networks and films, some notes on the relation between chemistry of carbon nanotubes and their band structure are being briefly recalled. Chemical modifications are used to get robust changes of electronic (and electrochemical) properties, like in intercalation/encapsulation [241] doping [242], adsorption [243] and functionalization [244] or modification reactions [245]. Usually, one recalculates Fermi's energy, density of states and work function, verifying the conductance perturbation and if a phase transition (e.g. semiconductor-metal) has occurred. Related to these points is the influence of structural defects [246,247], usually more located at the ends than walls [248], which supply scattering centers for electron transport and reduce the conductance by means of a smaller mean free path. Each of these transformations allow for a modulation of energy band properties, with interesting prospects to link solid state physics to neurosciences. This, clearly, would not be limited to electrical conductances alone. Seebeck's coefficient, for example, stems from Mott's relation as [249]:

$$S \ \propto \ T \left(\frac{d \ln \nu}{dE} \right)_{E_F} \tag{3}$$

the derivative of density of states equating zero for a pure/intrinsic metallic nanotube, and being sensitive to the presence of dopants and impurities.

Another process to be recalled here, both with respect to electronic and electrochemical properties, is adsorption from (aqueous) solution. Physical or chemical interactions of tube walls with water molecules, whether solvated or not, and metal ions (e.g. Na^+ [250]) can affect the electronic features to an extent depending on helicity and nanostructural details. For example, to explain the enhancement of field emission current in zig-zag structures [251], chemisorption of H_2O molecules was studied at the open ends of $(5,5)$ and $(9,0)$ nanotubes. The outcomes contemplated two positive Fermi's energy shifts, $\delta E_F\ (5,5) \approx 0.12$ eV and $\delta E_F\ (9,0) \approx 0.17$ eV, but a local increase of ν near $E = E_F$ only occurred in the second case [252]. It should also be reminded that thin layers of high-purity metallic single-walled molecules display an extremely stable conductivity, owing likely to a locally constant density of states [253]. Sensitivity of electrical conductance to molecular adsorption increased with addition of semiconducting tubes.

6.5. Many-Nanotube Systems

In the outline of percolation phenomena, the role of the (insulating) medium was not regarded. Measurements, in fact, were performed with contacting particles and electrified interfaces that are not in vacuum or air, but in (aqueous electrolyte) solution. Whatever the electron mechanism is, the cellular liquid will be involved directly into an interface charge transfer [254]. The picture to work with better emerges from discussing electrochemistry in light of electron properties (see next section), but some considerations may be usefully anticipated. From the theory of scanning tunneling microscopy, it turns out that the orientation polarizability of a solvent results into non-negligible effects [255]. Liquid molecules exert a random barrier on charge transfer, giving rise to a stochastic dynamics with a much longer time scale than the electronic's, and ultimately promoting the tunneling current. Since, in comparison with vacuum, a host dielectric medium usually lowers the work function, thermionic emission from a metal/semiconductor will follow as a rule a similar qualitative trend [256]. The presence of membrane fields across interfaces with charge fluctuations in solution then should further interact with electron transmission, including the potential drop caused by the electrical double layer in Helmholtz's plane and Gouy's region. On the other hand, the phenomenologies displayed by quantum conductors in electrolyte solution and by nanoscale electron transfers deserve to be remarked. For instance, a process of quantum interference was advanced to explain the conductance decrease of (Ni) nanobridges in solution [257]. It may be striking to realize that addition of electrolytes has not only a positive ('effective medium') effect on the electrical conduction. At the nanoscale, it would imply a 'compression' of Fermi's surface, augmenting the electron backscattering across nanojunctions.

Many-nanotube systems here represent a last analysis step. Increasing the nanotube density (ρ), or the film thickness (s) if they do not form a pair of independent variables, will presumably suppress or make individual nanotube features less detectable, particularly if samples are inspected by macroscopic measurements. Needless to say, however, that nanotubes and their clusters will not cease to locally interact with neurons or finite regions of cell cultures. In general, borrowing some fundamental assumptions from the scaling theory, e.g. from polymer science [258], there will be a set of characteristic lengths:

$$\xi_k \;=\; \xi_k\,(d, L, s, \rho, T, V, ...) \tag{4}$$

by which the main quantities describing the electrical conduction in a rod-like network can be expressed and may vary with nanostructural, thermodynamic, and further interaction parameters. As a function of density, for example, one would expect a value above which the phenomenon gets mainly affected by properties of individual tubes (or their bundles), leaving the scaling regime behind, $\xi_k \neq \xi_k(\rho)$. It is clear that increasing a characteristic length does not bring necessarily to an enhanced spatial order in the network. For instance, interjunction distance and mesh correlation length stand, in principle, for distinct statistical concepts. Furthermore, strong dependencies $\xi_k = \xi_k(s)$ may also be indicative of poor intertube or interbundle contacts, which are often unavoidable in real systems.

electrical conduction in single-walled networks was studied as a function of thickness and temperature, assuming the ideal 1 : 2 proportion between metallic and semiconducting units [259], meaning that the first percolation clusters will be mainly semiconducting, while metallic tubes behave as interconnects. With increasing density of nanotubes, the effect of interfacial and junction Schottky's barriers is superimposed to the formation of metallic paths, giving rise to a higher Ohmic character of the mat. This picture, which may equally hold in NCN systems, led in brief to the following conclusions. At a fixed temperature value, in the range $0 \leq T\,[K] \leq 300$, conductivity (σ) increases with s (i.e. with the net metal content). Conversely, σ increases with T, a larger conductivity reduction being measured with decreasing T as films get thinner and thinner. This behavior is well approximated by Mott's variable-range-hopping equation, where σ is coupled with T via the hopping conduction dimensionality [260]. A similar conclusion was also drawn upon comparing the charge transports in (i) transparent conducting films made by single-walled molecules, (ii) the conducting polymer poly(3,4-ethylenedioxythiopene):polystyrene sulfonate (PEDOT:PSS) and (iii)

indium tin oxide (ITO) [261,262]. The latter displays metallic behavior, with monotonically increasing $R = R(T)$ in $100 \leq T \, [K] \leq 300$, and is the inorganic compound unsuccessfully coupled in [4] to the neuronal network. The nanotube sheet resistance was about sixty times larger than in indium tin oxide samples, showing a monotonically decreasing $R = R(T)$ and hopping transport, a feature of disordered electron systems. Finally, a phase diagram for the electronic behavior of mixed nanotube
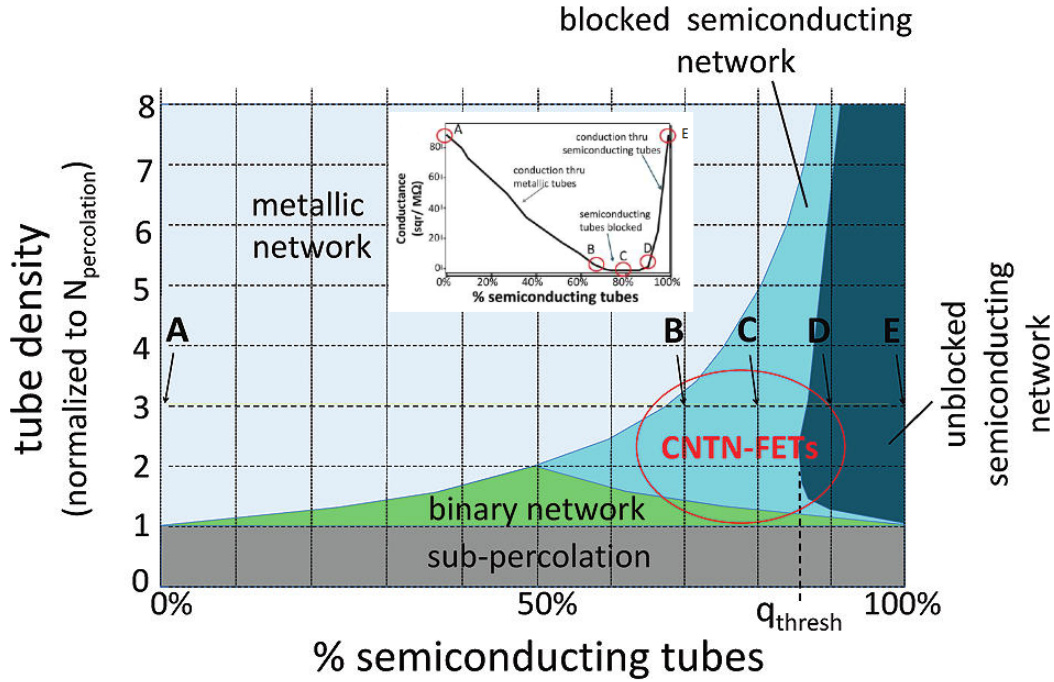

Figure 16. Electronic phase diagram for a metallic-semiconducting carbon nanotube system. Density (y-axis) is normalized to the percolation threshold. Green, light blue and dark blue areas stand for different types of carbon nanotube network field effect transistor(CNTN-FET), the last two being blocked by Schottky barriers. In the inset the conductance behavior through points $A - E$, at three times the concentration threshold, is depicted (adapted from ref. [263]).

network is depicted in Fig. (16).

In the thickest freestanding films tested in [259], the behavior $\sigma = \sigma(T)$ suggests a thermally-assisted electron tunneling by thin metallic barriers. At higher temperatures, the augmenting charge carrier-phonon backscattering causes a conductivity decrease and a peak, i.e. $\sigma^* = \sigma(T^*)$. In the thinnest layers, the I vs V plot showed to be nonlinear at low temperatures ($T = 4.3 \, K$), resembling individual semiconducting single-walled molecules and allowing current modulations by a gate voltage. With increasing temperatures such nonlinearities tend to disappear, being slightly retained at the room value ($T = 291 \, K$). This implies, upon alike assumptions, that electrical features of thin single-walled layers can be regarded as nearly Ohmic. Despite the carbon nanotube mats interphased with neurons are either contacting with a liquid or a soft biological phase, such an approximation may be anyway relevant to describe the behavior at the largest length scales.

In the frequency domain, the difference between ac and dc conductances of single-walled nanotube networks is found to increase according to the 'extended pair approximation':

$$G(f) \, - \, G_0 \, \propto \, (f/f_0)^{\gamma} \qquad (5)$$

f_0 being the onset frequency ($\gamma \leq 1$) [264]. This conclusion does not apply to the THz domain, where conductivity was found to diminish with increasing frequency ($f \geq 1 \, THz$) [265]. The typical relation met in disordered solids [266], $f_0 \approx G_0$, then is verified over a wide experimental range. Conductance

increases are regulated by the onset frequency, and it cannot be ruled out that processing history and purification of nanotubes may strongly affect it, as it seems to happen elsewhere [267] with $G(f) \approx G_0$ (at $f = 10 \, GHz$). According to a scaling approach, based on Einstein's law for the random motion of charge carries, it reads $f_0 \propto \ell^{-2}$, where the proportionality constant stands for a diffusion coefficient and ℓ is the average size of conductive domains in the film. The use of Brownian motion and polymer laws [268,269] is a realistic possibility, to be checked up in modelling NCN interactions as well. Provided the quantities defining criticality are posed consistently, notions like scaling or universality may offer important simplifications and be able to capture a wide phenomenology. Finally, the dc conductance in submonolayers turned out to be a nonlinear increasing function of the electrical field. Another factor expected to sensitively increase the dc conductivity is the bundle aspect ratio. In single-walled networks, with given mean bundle length (L_B) and diameter (d_B), one has:

$$\sigma \sim L_B^p d_B^{-q} \qquad (6)$$

being $p \approx 1.46$ and $0 \leq q \leq 2$ [270]. It does not astonish the two scaling exponents are generally not coincident, for their aspect ratio alone is not sufficient to represent conductivity.

In multi-walled molecules, high aspect ratio-electrodes enhance stimulation efficiency and higher signal-to-noise ratio (S/N) [271]. The mechanism of electrical conduction in such systems, which better resemble a disordered composite material than a classical network, received different interpretations. Among the models found in the literature, we remember again Luttinger's liquid theory, $G_0 \sim T^\alpha$ ($\alpha \sim 0.36 - 0.95$) [272], the one-dimensional disordered wire behavior:

$$G_0 \sim \exp(-\eta/\sqrt{T}) \qquad (7)$$

η being an order parameter [273], and an activation mechanism of Arrhenius's type:

$$G_0 \sim \exp(-\Delta E/T) \qquad (8)$$

with $\Delta E \approx 0.7$ eV [274]. Notwithstanding, a nonmetallic/metallic transition was proposed to hold in aligned multi-walled layers for the conductivity component that is parallel to the tube axis (at $T \approx 280$ K) [275]. This is simply to highlight the gain in operational simplicity and efficiency of samples, which may be achieved by increasing the molecular orientational order along the substrate, ensuring a better exposure/anchorage of neurons to the nanotube surface/pin-like nanoelectrodes. On the other hand, the effect of geometrical order onto the NCN coupling seems to be more articulated and deserving to receive further quantitative assessments. While major neurites of motor neurons eventually grow
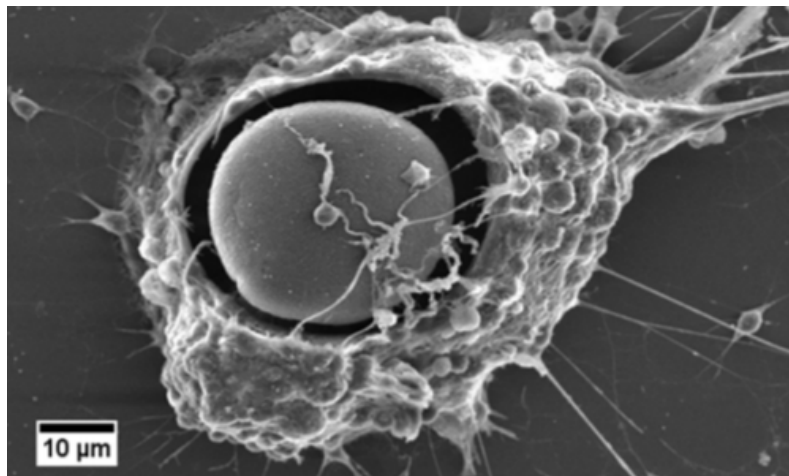

Figure 17. Magnification from top of neurons grown up in the vicinity of vertically aligned nanotube structures (adapted from ref. [276]).

parallel with aligned carbon nanotubes [74], and cortical neurons attach preferentially on the sidewalls of high aspect ratio nanotube structures than over the tips (see Fig. 17), the latter turn out to be more colonised in randomly oriented nanotube clusters than in pillar structures [276].

To conclude this subsection, the electronic properties of carbon nanotubes, mainly considered here as 'pin nanoelectrodes', were discussed in view of inquiring into the effects of individual molecules, junctions and molecular layers on the overall charge transport in NCN interphases. A challenging yet relevant goal would be to introduce language and tools of condensed matter (electron band structure and quasi-particles, just to make an example) at an ever deeper level, turning biological issues into theoretical physics and chemistry relationships.

7. Ionic Conduction and Electrochemistry of Nanoelectrodes and Nanocapacitors

Let's come to the last framework here completing the basis for a quantitative account of NCN interactions. As being in the presence of a liquid phase and electrified interfaces, both electron and ion transfers need an opportune electrochemistry analysis. If nanorods are spaced out enough from the biological matter, an electrochemical model may be afforded independently of the mechanical/adhesive coupling with cells (Fig. 11c). Otherwise the intermediate situation in which they mostly connect cells at one end, should be dealt with (Fig. 11b). As a prototype situation to detect electrochemical contributions to the NCN coupling, one can operate with mats mechanically uncoupled from neurons, the carbon-based molecules acting as nanoelectrodes kept at a variable potential and nanometric separation distances from the cell culture. As for pin-like nanoelectrodes, the molecular film may act here as an electrochemical probe with strong electrocatalytic activity [277], by e.g. increasing admittance, attracting/repelling interfacial ions (capacitive perturbation), inducing electron transfer kinetics and charge transfer through oxidation/reduction at the electrode [278,279], and sensing influences like (periodic) forcing [280] or noise [281].

Carbon nanotubes should not be regarded totally equivalent to glassy carbon electrodes, as they identify electrochemical devices on their own right [282], and an in-depth description of a meshwork interplaying electrochemically with a neuron network remains a tough task. A point to be introduced is how an electrical charge distributes along a nanotube. Charged individual molecules have been studied by means of classical electrostatics, and it turned out that their charge distribution strongly accumulates at their ends, with values depending on the position along the nanotube (length) axis [94]. Such behaviors, which may find an explanation in terms of non-trivial changes of energy levels induced by charging, were either reproduced in infinite or semi-infinite electrical fields [283] (see Fig. 18) and by neutral molecules as well, with slightly negatively charged ends [284]. Intensity of the
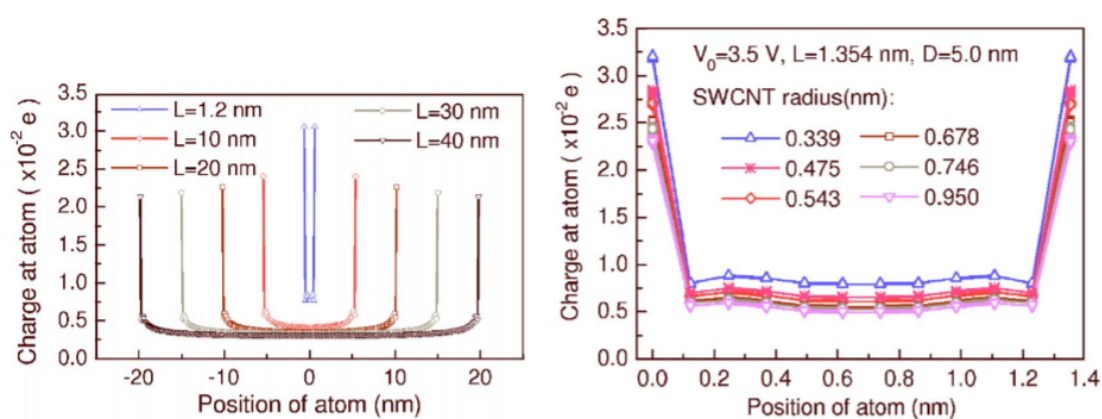

Figure 18. Effects of length (on the left, in an infinite electrical field) and radius (on the right, in a semi-infinite field) on the charge distribution in a single-walled nanotube (adapted from ref. [283]).

charge distribution along the nanotube is globally decreasing with increasing length and, when end

charges are expressed in unit of average atom charge, it was seen that they increase (logarithmically) with L. Charge accumulations were also found in compressed states of cellular assemblies [81], in a number of interfaces ($p - n$ and $n - i$ junctions, metal/nanotube Schottky barriers) [285] and in strongly localized interfacial transfers [286]. These predictions would suggest to model the overall charging process in NCN interphases as it were (ideally) characterized by a two-fold stochastic process, both comprising an ensemble of (almost) uniform density functions (ρ_k) and of pointwise charge distributions (q_k), more concentrated at extremities and junctions. Secondly, one may also include cross-interaction terms. Stochastic properties would both be defined in time and space, modulated by the fields that follow through the neuronal functioning. In this line, an interesting aim to pursue by a mean-field approach would be reducing the meshwork to an equivalent nanotube cluster with given charge density, conductivity and topology, and studying the resultant NCN coupling.

7.1. Electrochemical Charge Transfers

When nanotubes embed an electrolyte solution, an electrochemical double layer establish at the solid/liquid interface. To examine it in detail is part of electrochemistry at semiconductor and metal electrodes [287], a classification certainly matching nanotubes as well. Here only follow some fundamental notes on it, bearing in mind that a mere electrochemical analysis of nanotubes may not suffice for a proper electrochemistry characterization of the biological NCN interphase. electrical charging is supplied by a voltage of biological origin, reaching the nanoelectrode (previous schemes in Figs. 11a-b) and continuously evolving, from the rest membrane to action potentials and vice versa. Nearby the surface, for instance of a metal nanoelectrode in aqueous solution, the liquid phase is structured into three layers, delimited by two Helmholtz's, inner (iH) and outer (oH), planes. The outer plane demarcates Stern's 'compact' layer, close to the surface, comprising polar and oriented solvent molecules, as well as molecules and/or ions which undergo selective adsorption. The first monomolecular adsorption layer is lying at a distance $r = r_{iH}$ from the surface (typically, $r_{iH} \sim 0.2\ nm$). The maximum charge density is stored at the outer plane, at $r' = r_{oH} > r_{iH}$, identifying the distance of the closest approach to the surface of mobile counterions in solvated states ($r_{oH} \sim (0.3 - 0.5)$ nm). They spread up towards the unperturbed bulk phase through the third 'diffuse' (or Gouy-Chapman) double layer, hosting an ion excess of the same sign. The thickness of Gouy's region delimits the layer structure at $r'' = r_l \equiv r_{oH} + \Delta d$ and depends on the ion concentration ($\Delta d \sim (10 - 100)$ nm, in low concentrated aqueous solutions). With increasing concentration the diffuse double layer becomes increasingly thinner, until it gets circumscribed by the outer Helmholtz plane ($r_l \sim r_{oH}$). An analysis of Gouy's region thus is more important in the dilute regime. In a limiting case, from Gouy-Chapman's theory, high enough values of the electrical potential can maintain a constant counterion surface concentration (contact value theorem) [288]. Another interfacial excess charge then can distribute from the surface to the solid bulk, creating a diffuse layer of electrons or holes (up to $r''' \sim -d_{sc}$). Similarly to Gouy's region, the thickness of this 'space charge layer' is more pronounced in semiconductors ($d_{sc} \sim (0.1 - 1)$ μm), for low electron and hole concentrations), where it is expected to augment the sensitivity of surface carriers to the applied potential, and becomes negligible in metal electrodes ($d_{sc} <$ monoatomic layer thickness). In principle, space charge, compact and diffuse layers contribute to the total (or apparent) interfacial capacitance by a connection in series of three separate capacitors. In the complementary case (Fig. 11c), electrical charging arises from two main stages, i.e. dissociation/ionization of surface groups and ion adsorption (binding) from solution onto an uncharged surface [288,289]. A phenomenon of ion exchange then takes place whenever anions/cations are adsorbed onto cationic/anionic sites. These processes separate the surface from counter charges and, analogously to the previous case, a double layer region forms. The counterion cloud, in rapid thermal motion at the solid/liquid interface, will spread in space with decreasing concentration to balance the surface charge and screen the electrical field in solution. The length over which significant deviations from charge neutrality can occur is often identified with Debye's screening radius, predicting the diffuse double layer size from the solution dielectric constant and salt concentration (typically, $\ell_D \approx 1\ nm - 1\ \mu m$). Counterions may also be

adsorbed into Stern's layer, and take place in a structure with own dielectric properties.

A first consequence of the double layer picture, to be recalled here, is about the electrical conductivity of a particle in an electrolyte solution, which is set by the sum of internal and surface conductivities. The second term, accounting for the interfacial excess conductivity from moving counterions in the double layer, in turn represents the sum of the diffuse zone contribution and Stern's layer conductance. Although this portion of liquid is practically stagnant, ions were proved to move inside it by diffusion and electromigration [290]. In the context of NCN interactions, to assume the separation of bulk from interfacial terms may also be helpful to further clarify where the enhancement of biological activity is mostly developing or originating from, whether in cellular membranes or some interphase domain. When nanotubes interact with neurons, charge accumulation phenomena may render the interfacial region inhomogeneous and require (at least) a two-dimensional description. Action potentials would elicit a longitudinal perturbation, altering the charge density along the tube axis, e.g. $\delta\rho_l = \delta\rho_l(z, r)$. These areas may identify possible preferential sites for the NCN coupling, concentrating the electrostatic energy that is made available by the double layer capacitance. A way may be paved by suitable chemical modifications of the substrate or nanotube meshwork, bridging the latter with cells through the most active sites (for example, by ad-hoc functionalization routes).

In general, two are the central contributions to an electrochemical charge transfer [291]. An electrical current originating from oxidation/reduction of some chemical substance at an electrode is named Faradaic, and accompanied by matter transformation. Otherwise, non-Faradaic currents are those arising, out of chemical reactions, from charging/discharging of the double layer, with given capacitance C_{dl}. In Helmholtz-Perrin's description [292], this brings to a parallel plate capacitor, with specific $C_{dl}/A \approx \epsilon/r_{oH} \sim (0.1 - 0.3)$ F m^{-2} (A is layer's area) [293], but more accurate expressions may be obviously afforded upon a thorough characterization of the counterion profile (namely, ℓ_D) [294]. Faradaic processes are highly surface-specific, but their basic principles follow at once from solid state physics. The current in fact is anodic [cathodic] when $E_F < E_H$ [$E_L < E_F$], where Fermi's energy refers to the electrode, E_H and E_L denote respectively the energies of the highest occupied (HOMO) and lowest unoccupied orbitals (LUMO) of a redox molecule (in solution). Electrode and solution in this way undergo an equilibration of their energy levels. Interactions of charged nanotubes with ions and solvent molecules may obviously alter the electron density of states (E_L and E_H) while, for each electrolyte, van Hove's singularities are attained (in single-walled tubes) at different applied potentials [295]. The relative position of Fermi's level, as compared to another band edge, yields an acceptable criterion in standard three-dimensional cases, but it is not completely clear if it can match molecular or one-dimensional systems. A lower dimensionality lies itself at the basis of a capacitance of quantum origin, as it emerges from charging a single-walled nanotube. Large energy spacings between adjacent states imply that a fraction of the electrical potential, applied over the nanotube/solution interface, will take the form of a chemical potential drop [296]. This resembles a space charge layer-induced band which is bending at a semiconductor surface, similarly producing a chemical potential variation (see Fig. 19). One is therefore led to introduce a Faradaic-like term, strongly dependent on the electron band structure, and expressible like a quantum capacitance (C_q) in series with the geometric/electrostatic one (C_{dl}), with total value:

$$C^{-1} = C_q^{-1} + C_{dl}^{-1} \tag{9}$$

Two limiting regimes are promptly recovered, classical ($C \approx C_{dl} \ll C_q$), as for instance in usual metal electrodes, and quantum ($C_{dl} \gg C_q \approx C$). However, discussing the orders of magnitude of C_q and C_{dl} requires some care. In general, C_q ($= e^2\nu$) should increase with the density of states, thence with any related quantity (e.g. wall number). Single-wall and multi-wall systems may show situations in which the prevailing term is, respectively, $1/C_q$ or $1/C_{dl}$. For isolated single-walled molecules, typical values are $C_q \sim 1$ fF μm^{-1} and $C_{dl} \sim 10$ fF μm^{-1} [296], but it turned also out that $C_q \sim (0.01 - 0.1)$ fF μm^{-1} [297], the discrepancy being ascribed to strong electron correlations. Furthermore, a double-walled molecule modeled as a quantum capacitor would exhibit a large bias dependence and an enhanced capacitance value due to a quantum-mechanical spill of the charge density accumulated at the walls
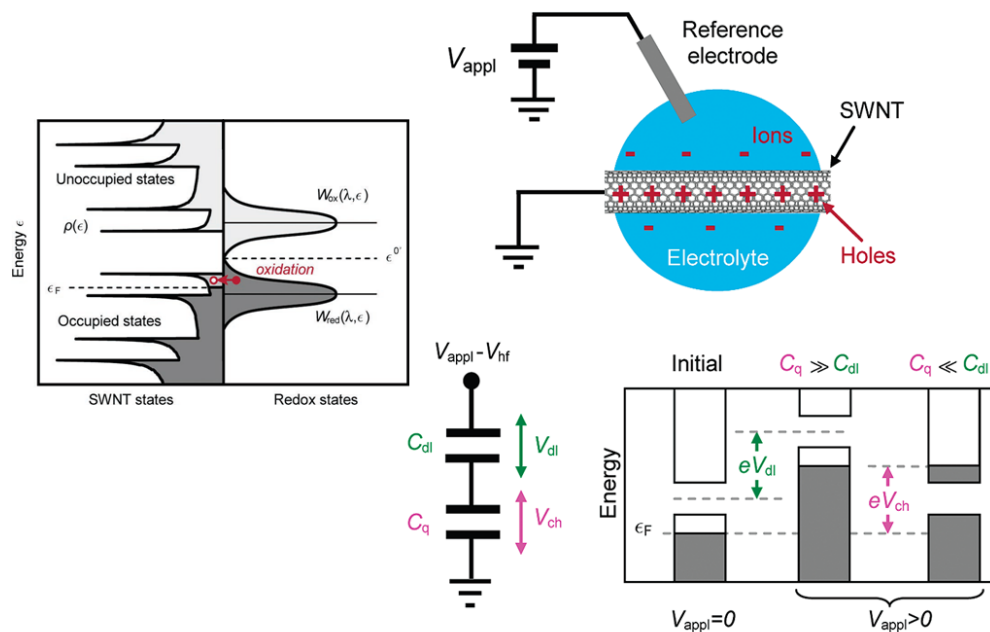
Figure 19. Interplay of double-layer charging, redox reactions and quantum capacitance in single-walled carbon nanotubes (adapted from ref. [296]).

[298]. Overall, the electric capacitance of nanotube arrays can be 10 times higher than noble-metal microelectrodes, and may even take larger values upon ad-hoc functionalization (e.g. $40 - 100$ times higher with polypyrrole, PPy, at least with a 20-fold decrease in impedance) [171,299]. In our case, for a local NCN description, it can be opportune to work in an intermediate semiclassical regime, where both capacitive elements are implied. This was partly done already by a quantum/semiclassical model, employing a thermodynamic uncertainty relation for a cell [300]. The duration of a biological signal was regarded as the average lifetime of a decaying state (or population of states) and the carbon phase effect as a linewidth broadening, propounding a quantitative explanation of the frequency enhancement for the spontaneous activity of neuronal cultures interfaced with carbon nanotubes (Fig. 20). The importance of thermodynamic uncertainty relations, to study current fluctuation constraints in steady states which are arbitrarily far from equilibrium, was progressively scrutinized until recently [301], and is awaiting more established applications to life sciences as well. There may
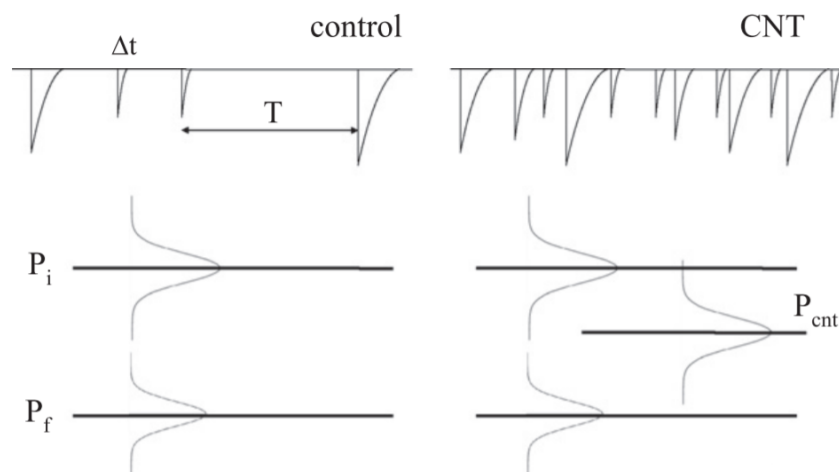

Figure 20. Cell frequency enhancement by a carbon nanotube phase (CNT) as a bandwidth broadening (P denotes power = energy/time. Adapted from ref. [300]).

also be the intriguing possibility to work with $C_q < 0$, and find negative capacitances to be a signature or requirement of certain biological electrochemistry processes. This regime, corresponding to very high charge accumulations, was proposed to happen in gated nanotubes with reduced carrier density [302].

Besides the double-layer picture, Faradaic pseudocapacitance reactions may obviously take place. The electrochemistry of carbon nanotubes, as well as its dependence on fundamental quantities (such as pH), is tough however to be treated in a systematic way, and is dramatically affected by chemical and structural details. In general, it is dominated by double-layer charging, with residual contributions from surface oxides [303], and is sensitive to electrolytes [304], transition metal complexes [305], functional groups (like oxygen-containing) and impurities [306]. Thermal annealing should increase hydrophobicity and favor the release of electroactive groups, thus reducing the electrochemical reactivity [307]. In aqueous media, the potential range set by the evolution of molecular hydrogen and oxygen is expected to fix another constraint [308]. When the environment, for instance, is alkaline and a cathodic current is applied, water should reduce at the carbon nanotube/electrolyte interface, with formation of hydrogen adatoms [309]. They were conjectured to recombine into molecular hydrogen stored at the tube surface [310], but this conclusion was afterwards criticized [311]. A dual oxidation mechanism with molecular oxygen was also proposed to occur in acid environment (O_2/H_2O) [308]. It is interesting to note that, in a redox chemistry study of nanotube-mediated reactions, physically distinct multi-walled molecules seemed to be incapable of exchanging electrons [312]. An investigation of this phenomenon in NCN interphases may contribute to decouple the electron and electrochemical scales for charge transfer.

Faradaic processes can be enhanced by covalent or physical modifications of the nanotube surface, or by altering the ionic environment, but this could raise biocompatibility issues or undesired neuronal effects. Treatments, normally useful in carbon-based materials [313], such as oxidation reactions increasing the surface functionality, the creation of conducting polymer interfaces, and intercalation of electroactive compounds (e.g. transition metal oxides), may be totally unsuitable here. Cell physiology is affected by the chemical composition and purity degree of carbon nanotubes, as it turns out for amorphous carbon or catalytic metal impurities [314]. On the other hand, oxidative thresholds for electrochemical potentials, above which the electrical conductance of single-walled molecules vanishes [304], were derived for different electrolytes. Alongside, the saline bath can't be altered arbitrarily. Within the limits and variations dictated by neuronal cultures, an investigation on the electrochemical potential, even for slight electrolyte concentration and composition changes, may be a further step to be made in the characterization of NCN interphases, especially as a function of nanotube diameter or chirality. Because $E_g = E_g(d)$ is a decreasing function, the reduction/oxidation of molecules with larger d should be promoted. Fermi's levels, in turn, can be tuned by (donor/acceptor) counterions of different redox potentials and detected by in situ Raman scattering [315], the energy shift being proportional to the electrode potential ($\Delta E_F \leq 1\,\mathrm{eV}\,V^{-1}$) [316]. The C-C bond length elongates/shortens upon transferring an amount of extra-electron/holes to a carbon atom (in π orbitals), yielding an actuation process in which charge injection and strain rates may be strictly related and tailored e.g. by electrochemical doping. In carbon nanotube systems, charging and actuating can couple in fact on the *ms* scale [317]. Aligned multi-walled molecules, for instance, were proven to work as an electrochemical actuator in a 2 M Na^+Cl^- solution. Employing a 2 V square wave excitation, they actuate up to 10 Hz with a strain reduction of $\approx 0.15\,\%$ [318]. Carbon nanotube cellular structures in a dilute acid electrolyte solution displayed a high electrostriction-induced actuation even with no mechanical load [319]. At any rate, tuning of Fermi's energy by electrolyte solution gating is itself an interesting issue to link band structure properties to the electrochemistry of NCN coupling. To this aim, it may be useful to remind that Raman responses from metallic tubes were more sensitive to electrode potential changes than from semiconducting ones [320].

Associated to the overall charging there is clearly an equivalent circuit that, because of the complex physical nature of electrified interfaces, is often dealt with as a distributed parameter system. Double

layer charge separations are described by a capacitance (C) in parallel to a leakage resistance (R_F) responsible for the self-discharge. They are both in series to the electrolyte solution resistance (R_s), which stands basically for a heat loss term to be evaluated between the nanoelectrode position and infinity. An equivalent inductance may also be found in series with the former elements [313]. The Faradaic R_F component should vary with the nanotube surface density of electroactive functional groups, and governs the self-discharge, with time constant $\sim R_F C$. Charge and discharge relaxation times follow instead from the spreading resistance ($\sim R_s C$). Faradaic processes then requires the insertion of pseudocapacitances (C_p), in series with R_F, while a film deposited on nanoelectrodes can be represented, as a further element in series, by another parallel RC circuit [321]. Examples of pseudocapacitive materials are ZnO-MnO$_2$, ZnCo$_2$O$_4$ and polyaniline, which were implemented successfully in the form of nanorods array and nanowires, respectively [322]. Warburg's impedances [323] can also be employed, in series with R_F, to model concentration polarization and passive coating (in surface films) and finite ion diffusion (in saline baths). A more thorough analysis of semiconductor electrodes with given surface state distribution then leads to an equivalent representation in terms of compact layer and space charge capacitances, surface site capacitance and charging/discharging resistance [324]. To represent the NCN interaction by an equivalent scheme similarly requires the formulation of an equivalent cell model. While this was partly done from a neurophysiology point of view [4,122,123], one of the most complete interpretation scheme certainly remains the electrochemical. We also note that the two circuits could be not independent, for instance, the neuronal field may couple or modulate the nanotube capacitance. In an adhesion model for cell-solid junctions, for example, cell interactions in tissues turned out to be dominated by an extracellular region, displaying the electrical properties of the bulk solution [325]. In another model membrane, the resistance (R_m) as a function of bathing electrolyte concentration ($c_\pm$) then obeyed [326]:

$$\left(\frac{d \ln R_m}{d \ln c_\pm} \right) \ \leq \ 1 \tag{10}$$

A review of electric circuit-equivalent models for interfacing cultured neurons to microtransducers may be found in [15]. At any rate, unless enough realistic information be provided, it may be useful perhaps to recall that the search for an equivalent circuit may result into an ill-posed inverse problem, able to furnish a description but not necessarily a physical or chemical explanation. As a basic electrophysiology example, it was prompted that any resistive coupling between biomembranes and (single-walled) nanotubes could be qualitatively indistinguishable from coupling nanotubes to the patch pipette through the patchseal path to ground [123].

7.2. Carbon Nanotube Systems

In turning the attention onto the characteristics of carbon nanotube systems, recall that not only single-walled [327] but multi-walled molecules too [328] were used individually as nano/micro-electrodes or coating materials for them. By means of a suitable materials processing (e.g. deposition, functionalization, coating routes), it was reported they are better than Au or standard TiN electrodes. Their impedance, at a physiologically relevant spiking frequency of neurons (~ 1 kHz), does not change meaningfully in time and, overall, their behavior in saline is stable. Variations in capacity and electron transfer resistance may be produced by salt residues accumulated on the electrodes during the experiment. Noise was lowered from (16.1 ± 7.8) μV in planar Au electrodes to (2.61 ± 0.51) μV in carbon nanotube's, with an enhancement of S/N ratio > 6 [329]. In functionalised nanotubes investigated by voltammetric techniques [330], the redox behavior of multi-walled molecules dispersed in solution resulted into single-electron transfers, a quantum charging phenomenon. If voltammetry is not enough effective, resorting to spectroelectrochemistry can usually provide with a wider electrochemical characterization [282]. We also remind that (carboxyl-functionalized) carbon nanotubes, likely due to their large electrochemically accessible surface area (e.g. $(700\tilde{\ }1000)$ m^2 g^{-1}) [331] and oxygen containing surface groups, were unveiled to trigger electron transfer reactions and important

negative shifts (< -0.05 V) of the anodic potential of compounds such as ascorbic acid, epinephrine, dopamine [332,333], enabling a selective sensing of electroactive neurochemicals [278]. From a morphological viewpoint, (individual) multi-walled nanotubes can show edge-plane defect sites, consisting of graphite sheets terminating at the tube surface, which were suggested to be responsible for much of their electrochemical behavior [334]. Once again, despite larger wall numbers might better improve the neuronal activity, this wealthy of phenomena still enforces the conviction of giving the priority to a quantitative-mechanistic research based on single-walled molecules. At the larger scales of a nanotube film, multi-walled molecules may have a small specific surface area, thence a small specific capacitance (e.g $\sim 180\ m^2g^{-1}$ and $\sim 15\ Fg^{-1}$) [335]. The relation between such two quantities is constrained by the pore fraction that is actually accessible to electrolytes, and should not be linear. To increase the capacitance, pores should be large enough (in aqueous electrolyte solutions, $\sim 0.5\ nm$) but, at the same time, reasonably small to keep the surface area as large as possible. A process which would vary instead the electrostatic boundary conditions is the (aqueous) electrolyte diffusion inside hollow (single-walled) cavities, which is normally believed to need large defect sites at the walls, or nanotubes with caps removed. However, this point turns out to be non-trivial and required to be addressed for the specific molecules in use, for instance by ultraviolet/visible/near-infrared (UV-Vis-NIR) and Raman spectroscopy [336,337] (see Fig. 21). We remind that simple ions, like Na$^+$
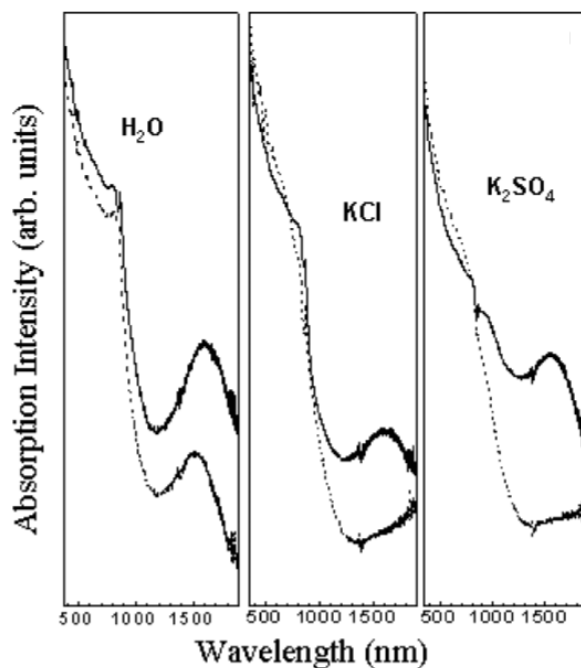

Figure 21. UV-Vis-NIR absorption spectra of single-walled nanotubes synthesized by gas-phase catalysis [338] and treated in oxygen atmosphere (550 C for 5 *min*) for removing caps at tube tips and open holes at defect sites of tube walls (adapted from ref. [336]). Broken lines are the nanotube spectra treated with water, 0.2 N KCl and 0.2 N K$_2$SO$_4$, dried at room temperature. Solid lines show the absorption spectra after a further drying process (200 C in vacuum for 1 *h*).

and Cl$^-$, both intercalated in carbon and boron nitride nanotubes, were considered to solvate at a distance in polarizable nanodroplets [339]. Also, the end charge redistribution in an open tube should be more pronounced than in a closed one [283,284].
The choice of length and time scales to be focused on in a stochastic study obviously remains a primary aim. If measurements were performed at a scale that is too distal/proximal to the coupling events, then experimental responses could be featureless. To enter a more microscopic domain, yet exploiting macroscopic experiments, an inquiry at least into concentration and percolation effects should be in order. In fact, electrochemistry of individual semiconducting and metallic single-walled nanotubes

turned out to be almost identical [327]. Their high-density networks, consisting of a mixture of both species, mostly behaves as they were thin metal films [340]. This conclusion was independent of the redox couple potential and only required a fractional surface coverage $\phi \sim 10^{-2}$. Furthermore, in aqueous electrolyte solutions, their voltammetry and capacitance were only varying a little with charge, hydrophobicity, anion or cation molar mass changes [341]. pH and concentration did not produce as well noteworthy capacitance variations. It was also deduced that ion diffusion into pores was not a rate-limiting step for double layer charge separations. Unless of involving very short time scales, it would be governed by the charging/discharging time constant, bringing to a rather fast process. On the other hand, changing film morphology turned out to be more effective. A comparison between aligned and entangled networks (Fig. 22) ascertained that a higher geometrical order can enhance the electrochemical response [342]. The interplay of nanostructure and morphology may be equally important for establishing the roles of pore size and conductivity path distributions in films with given orientational degree. Still, at the level of molecular layers, a broad investigation conducted on fifteen different materials led to conclude that electrochemistry of carbon nanotubes would be solely determined by the electrostatic charging of double layers and redox reactions of impurities [311]. This may suggest to conduct experiments on the NCN interphase at different substrate morphology and purity degree, to attempt a separate analysis of Faradaic versus non-Faradaic contributions to electrophysiology results. Titration techniques will be helpful, to this end, to determine the partition into acid and basic sites [343].
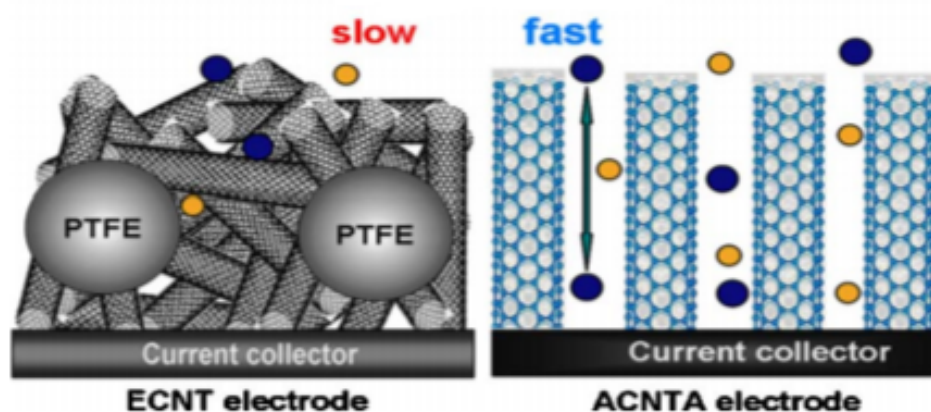

Figure 22. Comparison scheme for ion diffusion in aligned array (ACNTA) and entangled (ECNT) electrodes of carbon nanotubes in ionic liquid electrolyte (PTFE = polytetrafluoroethylene binder, 10% wt. Adapted from ref. [342]).

More generally, the influence of the charge amount (reversibly) stored by nanotubes should be dealt with, either as an initial condition, when they only come in contact with cellular solutions, or during the electrical functioning of cells. An estimation of double layer charge can be performed by an analysis of zeta potentials (typically, dozens of mV) that, at least for substrates alone, should be made affordable by techniques like electrophoresis or electroosmotic flow [344]. It will account for the effect of the layer charge and the interfacial contribution from solvent dipoles (dielectric saturation). One may also be interested to see whether and how neurons are reacting at (or slightly below/above) the sample isoelectric point. In the course of signaling, mechanisms of charge accumulation then will be affected by the chemical composition of the solution. For instance, when nanotubes and neurons are disconnected (Fig. 11c) and discharge rate is ruled by the difference between action and rest membrane potentials, positive and negative charges should better be stored in acid and basic environments, respectively [341]. During a cycle of negative sign, the presence of oxygen dissolved in the bath should make the storage less efficient. Dealing opportunely with solution chemistry thus can furnish other indications about the NCN interphase.

7.3. Physical Chemistry Considerations

To complete this paragraph, a number of physical chemistry details are addressed for the experimental system and NCN interactions under focus. First of all, the affinity of the solid with solvent molecules should not be overlooked. The immiscibility of an inert compound with water lies at the basis of the so-called hydrophobic effect, i.e. the resulting entropy-driven attraction among hydrophobic molecules or surfaces in water. Pristine carbon nanotubes are unsoluble/indispersable in any ordinary solvent/liquid, thus their electrochemical characterization is limited to the solid state (i.e. as molecular layers at an electrode surface). The functionalization reaction by which molecules are processed [113] globally reduces the hydrophobicity degree, which could not be relevant to the film electrochemical response [341]. Reorientation of water molecules, as usual at a hydrophobic surface, could however persist to some extent, with the consequent phenomenon of solvent ordering at the interface with nanotubes and of solvent disordering at the interphase with membrane regions, which are instead hydrophilic [288]. Hydrophobicity of cavities, anyway, does not prevent water molecules from getting inside narrow nanotube pores, the rotational entropy being able to increase remarkably upon this internalization [345]. The work accounting on the whole for such entropy variations may supply a contribution to thermal energy exchanges in the NCN system.

We then generally have two global double-layer structures, one adjacent to carbon nanotubes and one other to the membrane, in proximity to the extracellular side where inhomogeneities are local and at the nanoscale [346]. In Fig. (11b) carbon molecules act at one end as nanoelectrodes, while in Fig. (11c) they mostly behave as capacitors, charged/discharged by neuronal electrical fields and Faradaic currents. Similarly to surfaces approaching each other in a liquid, neuron and nanotube double layers will couple and eventually overlap, with implications on their interaction picture. In double layers of biological membranes, pressure contributions to the ion potential energy are normally neglected [347]. Here, additional thermodynamic countereffects, structural and hydrophobic forces may arise near the ion channels, membrane and nanotube walls, and should anyway be checked.

An account of Debye's, Bjerrum's and Gouy-Chapman's lengths will also be useful to discuss the extent of the implied electrostatic interactions. The latter is inversely proportional to the surface charge, and defines the spreading range of the counterion cloud. The second is the distance (in water, typically ~ 0.7 nm) below which two ions are regarded to be associated (and Debye-Huckel's theory is invalidated). To have many screening ions within $\sim \ell_D$ is equivalent to require Bjerrum's length being much smaller than the mean ion spacing in solution. The ends of nanoelectrodes penetrating into membranes will sense instead, apart from a contact impedance, the effect of a third double layer located in the cytoplasmic domain (Fig. 23). Describing the ion atmospheres, inside and outside the cell, can be fairly afforded by Gouy-Chapman's mean field theory, or its extension to mixed valency electrolytes (Gouy-Chapman-Grahame's approach). At a first approximation, the electrical field in each biological phase will have the same mathematical form, provided with distinct electrostatic details. Inner (ψ_i) and outer (ψ_o) diffuse double layer potentials display their own polarization contributions (i.e. Stern's layers $\psi_{\delta i}$ and $\psi_{\delta e}$), with a diffusion membrane potential (E_D) joining intracellular and extracellular fields [348]. A reasonable estimation of the voltage at nanotube ends thus is:

$$\psi_o - \psi_i \sim E - E_D \tag{11}$$

where E is the total 'transmembrane' potential, accounting for the potential difference of the two bulk phases in aqueous compartments. Otherwise, when the inner end just arrests at the membrane, a similar evaluation returns $\sim E + \psi_i - 2E_D$. These potential drops further enrich the picture of chemical polarization of nanoelectrodes, as it is met by any signal traveling along a pinned membrane. We remind that the ionic permeability of a channel is sensitive to dipole moments (~ 50 D) lying near its neck [349]. The selectivity of anions and cations should then be influenced by the polarity of charge groups and/or dipole orientations. It was also put forward that internal and external membrane sides may be intrinsically linked by capacitive surface charges [350], in which case carbon nanotubes would
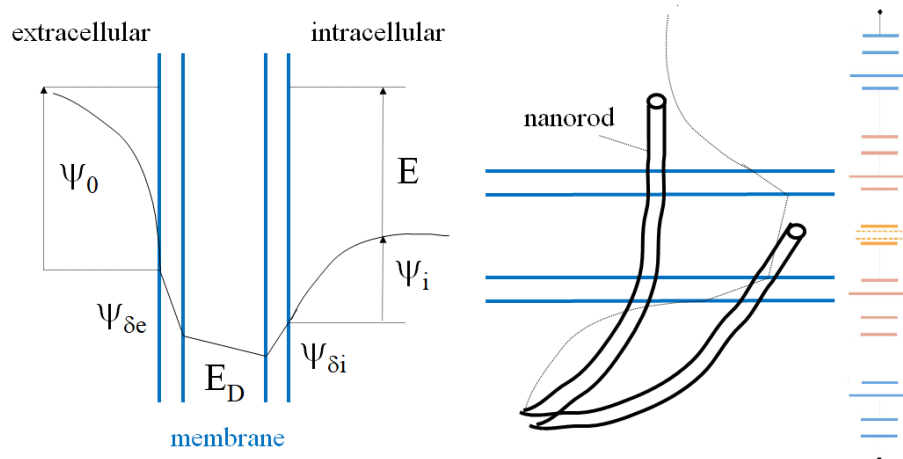
Figure 23. Electrostatic picture of (left) surface and diffusion potential theories of extra- and intracellular sides, and (right) scheme of carbon nanotube molecules approaching the membrane ($\psi_{0/i}$ = outer/inner diffuse double layer potential; $\psi_{\delta e/\delta i}$ = extra/intra cellular asymmetric polarization potential; E/E_D = transmembrane/diffusion potential). Capacitors/batteries in the inset on the right adapted from ref. [167].

likely supply an extrinsic coupling source. Finally, several effects such as surface charge discreteness or finite ion size could be more pronounced and thus reconsidered at the NCN nanoscale. Whenever the dielectric medium would cease to be well represented by a continuum, and ions would no longer behave as pointwise charges, the usual electrostatics picture may need a reformulation. This criticism is equally met in the calculation of electrical potentials in ion channels, for instance in the vestibular region [351] or in highly heterogeneous charge distributions of a biological membrane [352].

Imagine now that some biological signal, like an action potential, is elicited when the film molecules mainly act as a capacitor (Fig. 11c). Any transient field will induce a polarization perturbation, propagating and fluctuating through the bath electrolyte solution by a stochastic dynamics. Dealing with time dependence of polarization, its relaxation times and the attainment of equilibrium will establish how much the electrochemical coupling can effectively store and release electrostatic energy for the neuronal network. Whenever redox semireactions would develop at molecular walls, the relaxation dynamics will have to be endowed with the resulting (Nernst-like) reduction potential at nanoelectrodes. If the voltage is supplied by cells (Fig. 11b), the potential profiles at the neuron and nanotube extremities will vary with the biological activity. This case, which is likely the most complex if we consider that nanoelectrode potentials may also originate from distal neural regions, points out a sort of stochastic capacitor with spatial and temporal random inhomogeneities, each obeying Hodgkin-Huxley's or some suitable biophysical model. When this picture is superimposed to Faradaic charge transfers, to ascertain the role of cells in nanotube reactivity, the involved overpotential value (η) can be compared to the biological voltage (V). Note that, in a linear regime for the polarization resistance, Butler-Volmer's equation for the electrode current density reads:

$$i \propto \eta = V - V_e \tag{12}$$

where V_e is the equilibrium potential for the electron transfer (redox) reaction. This potential difference stands evidently for an activation energy, and it cannot be said in advance that cells will always contribute favorably to it. Biomolecules, whose size is typically comparable with nanotubes', are also expected to set unfavorable electrochemical interactions. When implanted in the neighborhood of a nanotube, they may promote an electrochemical gating that lowers conductance. We finally speculate on a possible electrochemical interaction with negative capacitance values, as former frequency analyses [240] and investigations of C_q [302] already conjectured for gated carbon nanotubes. In

semiconducting single-walled tubes strongly coupled to a metallic gate, the quantum capacitance was separated into a couple of terms, one ascribed to the density of states (electron kinetic energy) and the other, with negative values, to motion correlations (electron interactions) [353]. The signature of $C < 0$ is a negative transient current following a positive voltage jump that, in mechanical words, reflects the inertia of the associated process. Under a step function bias, current will be initially falling, then rising transiently and finally decaying to zero. A number of examples of such a behavior may be found in charge transport phenomena at relatively low frequencies, generally originating from dc/ac signal mixing by means of nonlinear conductors [354,355]. A pertinent example is provided by electrorheological fluids (Fig. 24), characterized by a complex dielectric response [356]. In addition,
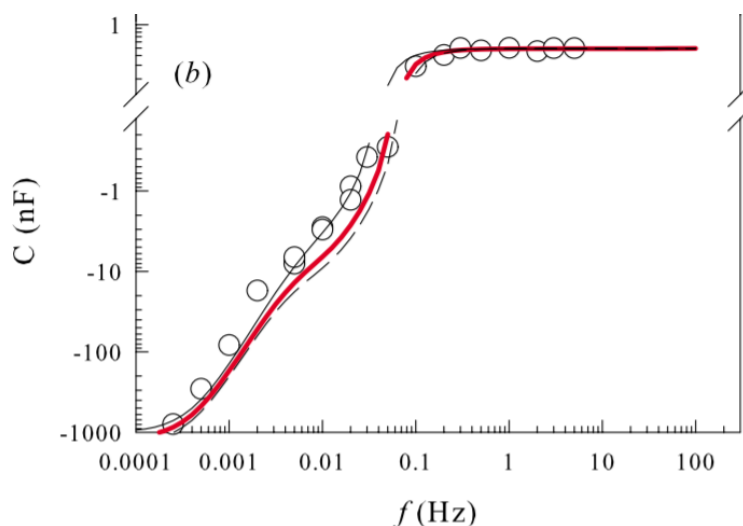

Figure 24. Negative capacitance in an electrorheological fluid at 50 V (adapted from ref. [355]). Symbols are measured data, lines are fits (with upper and lower boundaries) as they stem from the nonlinear frequency behavior of fluid conductance with three superimposed plasma-like relaxations.

in a dipole capacitor model at the metal/electrolyte solution interface, negative values were also put forward for the compact layer capacitance [357]. Now, if this were somewhat the case of NCN systems as well, carbon nanotubes interfaced with neuron cells would stand not only for ordinary electrodes or capacitors, but also for dual energy accumulation/conversion devices. During the falling/rising phase of a biological signal, for example, energy would be stored/released to the neuronal network, modulating the overall inertia of the polarization process. An interesting application, in this respect, would be resorting to nanosystems with ferroelectric properties and investigating on the induced memory effects.

This section, in conclusion, drew part of the complex view arising from charge transmission phenomena in NCN systems at the solid/solid and solid/liquid interfaces or interphases. A number of ad-hoc experiments will be useful to clarify in depth classical electrochemistry issues, such as the implication of Faradaic and non-Faradaic charge separation couplings, the structure of double layers and surface potentials. A more mechanistic approach to electrochemistry and electrokinetic processes in nanostructures and cells may be helpful e.g. to shed further light on ionic conductivity variations in a neuronal system upon interaction with carbon nanotubes – i.e. whether and to which quantitative extent they interplay with ion channel pores, cell permeability, cytoplasmic Ca^{2+} elevation, neuron polarization – and on the possible solutions to restore the activity of cells inadvertently impaired.

8. Blood-brain Barrier, Functionalization and Biocompatibility

8.1. Blood-brain Barrier

Blood-brain barrier (Bbb) (see e.g. [358,359] and portrait in Fig. 25) is a neurovascular unit surrounding the brain, preventing the reach of toxic materials, assuring nutrients (e.g. glucose, oxygen, etc.) to the brain tissues, a proper osmolarity and homeostasis for neuronal functions. Its structural
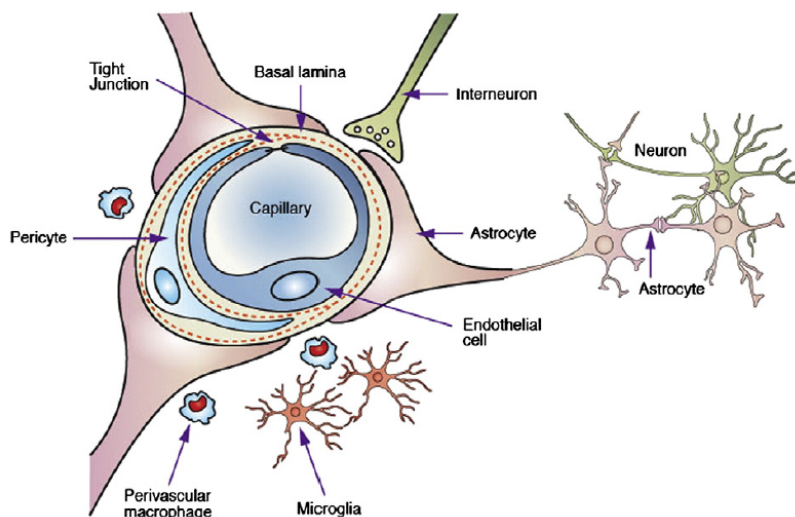

Figure 25. Scheme of blood–brain barrier (Bbb) and other components of neurovascular units (adapted from ref. [360]).

elements are astrocytes (i.e. a sub-type of glial cells), the microvascular endothelium, basement membrane, neurons in endothelium and pericytes (specialized cells surrounding brain capillaries), signaling pathways and correlations among them specifying a fundamental research area on its own (e.g. [361]). Brain microvessel endothelial cells tightly connect by apical adherent junctions and junctional adhesion molecules, generating a continuous and relatively permeable barrier. Owing to a deficit of surface cytoplasm, they have high density in mithocondria, smaller diameter and thinner walls than other vessels in the organism. Portions of pericytes may carry macrophages and phagocytose exogenous proteins and antigens (e.g. [362] and references therein). Molecules crossing Bbb then undergo a high enzymatic and macrophage degradation [363,364]. Note that Bbb is not a merely static lipid membrane barrier, as the functioning of cerebral endothelial cells involves a number of metabolic enzymes (alkaline phosphatase, glutathione transferases, etc.) and an asymmetrical arrangement of energy-dependent efflux transport pumps (i.e. P-gp and further multidrug-resistance proteins) [365]. There is actually a second barrier after Bbb, separating the blood from the central nervous system, which a molecule would meet prior to getting to the brain: The blood-cerebrospinal fluid barrier (Bcfb), gathering epithelial cells of the choroid plexus and being sealed as well by tight junctions between adjacent cells. It was suggested that to target both Bcfb and Bbb may be more effective for therapeutic interventions [366].

Molecular exchanges between blood and brain interstitium thus are very selective, ruled by several families of solute transporters for small molecules (e.g. glucose or amino acids) and by endo/trans-cytosis systems for protein molecules [362,367]. Nutrients and ions are said to cross Bbb via paracellular or transcellular pathways. Paracellular transport is a concentration-dependent passive diffusion for lipophilic or low molecular weight solute compounds. It is affected by features like geometrical constraints, substance quantity and type, the spatial polarity profile, and is contained by the expression of tight junctional proteins that lend high electric resistance to the cell. Reported values of transendothelial electrical resistivity spam within $(1.5 - 8) \cdot 10^3$ Ω cm^{-2} [368], three orders of magnitude higher than in other tissues $(3 - 33$ Ω cm$^{-2})$. Only small hydrophilic compounds with

molecular weight < 150 Da and highly hydrophobic compounds weighing $< (400 - 600)$ Da can enter Bbb by passive diffusion. Lipophilic molecules may cross as well Bbb by getting solubilized in lipid bilayers of endothelial membranes [362,369]. Transcellular pathway is a major transport system in the brain, comprising mechanisms as diffusion, receptor-mediated endocytosis, efflux, and carrier-mediated transport processes [370]. Transportation through luminal and abluminal membrane of brain endothelial cells may bear the name of transcellular diffusion. Receptor-mediated transcytosis instead is a saturable active mechanism with high specificity, independent of size and lipophilicity [371], where ligand molecules interact with receptors on the brain endothelial surface for producing endocytic vesicles to be transported into the cell. The receptor afterwards separates from the ligand and releases it out from the endosome by exocytosis. In efflux transportation, accumulation of damaging substances in the brain is disallowed by flowing out of substances from the brain into systemic circulation. Carrier-mediated processes, lastly, form a class of saturable transport mechanisms activated by different types of transporters, which may be dependent on or independent of energy [362,372,373]. A synoptic picture reporting the crossing pathways across Bbb is available in Fig. (26).

8.2. Bbb Crossing Phenomenology of Nanoparticles and Carbon Nanotubes

Nanoparticles may access the brain by penetrating Bbb or circumventing it via peripheral nerves. The reach of central nervous system through translocation routes along neuronal dendrites and axons was noticed in [374]. It isn't said, however, that particles which are able to mediate biological interactions with neuronal bodies may travel via peripheral nerves [363,375]. Nanoparticles can cross Bbb via transcytosis (say, direct penetration) [376], partially prevented by efflux transport proteins as P-glycoprotein (P-gp) [377], and especially via passive/simple diffusion (adsorptive transcytosis) and receptor-mediated endocytosis [363,378,379].[7] The former can take advantage of the electrostatic attraction between (positive) surface ligands and the oppositely charged endothelial cells. The latter relies on overexpressed cellular receptors for selectively transporting nanoparticles across Bbb.

To understand the tendency of a particle to escape the endo/lysosomal pathway, phenomenological views based on membrane fusion and/or destabilization, particle swelling and osmotic rupture were supposed [380]. Before a molecules of any kind, internalized by endocytosis, is inactivated by entering lysosomes (with low pH and a lot of degrading enzymes), it should free in fact from the vesicle it is trapped into, and it turned out that functionalizations carrying positive charges (for instance, polyethylenimine – PEI [381], polylysine – PL [171], etc.) may endow the nanoparticle with a more effective transfection activity. In the so-called proton sponge hypothesis, the positive surface charge lowers the endosomal pH, implying water influx, osmotic swelling and, finally, vacuole disruption with cytoplasmic release of nanoparticle/cargo systems [381,382]. This view remains unsuitable to suggest a valid interpretation key in any circumstance, but represents a promising framework for applying physical chemistry tools to the quantification of nanoparticle effects on endo/lysosomal escape pathways. Nanocarriers can also transiently, reversibly and moderately (20 nm) open up the tight Bbb junctions, augmenting the paracellular permeability of endothelial cells and perycites [382]. A number of diseases (e.g. infections, multiple sclerosis, glioblastomas) can likewise weaken Bbb to some extent, easing nanoparticle entries into the brain parenchyma, while altered permeabilities may generally be tied to neuroinflammatory events [383].

As a rule of thumb, particles with size not exceeding $(200 - 250)$ nm may be not recognized by macrophages and therefore cross Bbb with good biodistribution [362], while rather small nanoparticles (say < 6 nm) should be cleared to the kidneys [384]. Also carbon nanotubes can be quite generally uptaken by cells by active transport through endocytosis/phagocytosis and passive transport/simple diffusion (nano- or needle-like penetration), to be afterwards translocated into different subcellular

---

[7] We omit, from the present discussion, the basic notions behind the nomenclature of these biological processes, with its subcases and ramifications, which are therefore referred to dedicated texts.
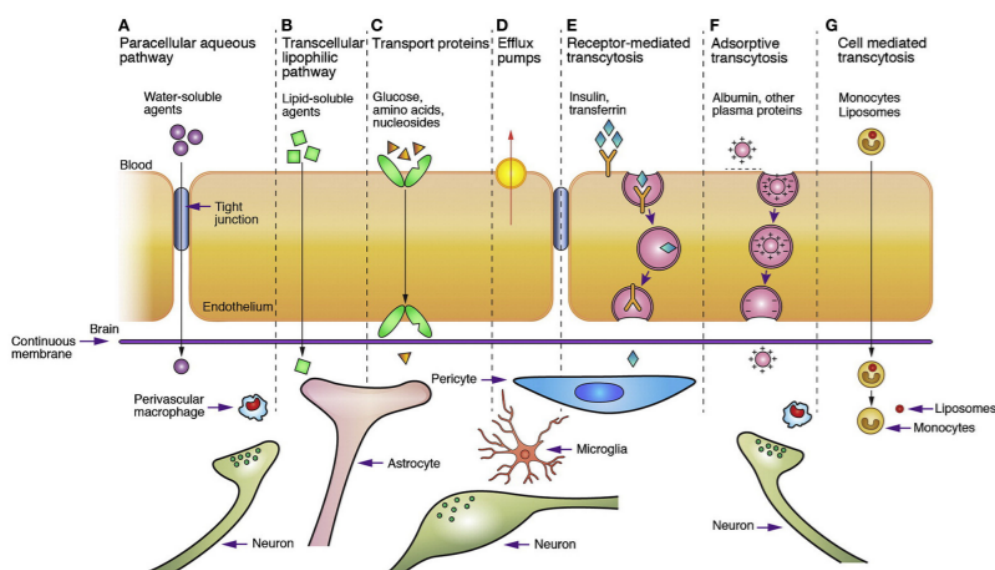
Figure 26. Crossing mechanisms through Bbb (adapted from ref. [360]). Routes (a-f) are commonly by solute molecules. Route (g), where monocytes, macrophages and other immune cells take place, is for drugs and incorporated drugs (e.g. by liposomes or nanoparticles).

compartments (e.g. [363,385–388] and references therein). Their ability to cross Bbb was proven in a number of in-vivo and in-vitro studies and can successfully be employed in therapies of central nervous system disorders and brain glioma (see e.g. [362,363]). Either mechanisms, active or passive, can give rise to a number of simultaneous transport routes and, consequently, to different immune reactions. Passive nanopenetration across phospholipid bilayers of a membrane, being akin to simple diffusion, does not require vescicle generations. It is energy-independent and develops upon interactions of nanotubes, highly hydrophobic, with plasma membranes. Once in the cytoplasm, carbon nanotubes undergo the usual autophagocytic processes over time, as it was just ascertained in a number of situations (i.e. horseradish peroxidase [389,390], human neutrophil myeloperoxidase [391], upon microglia [392] and eosinophils [393]) [394]. In endocytosis, nanotube molecules are first internalized in endosomes, then merged with lysosomes into endolysosomes. This phenomenon, for both single- and multi-walled nanotubes, depends on energy (ATP), temperature, and is clathrin-mediated [395]. Phagocytosis resembles endocytosis but is driven by exogenous material of larger size, as bacteria or microorganisms, and it turns out that internalization of nanotubes is also affected by the phagocytic cell nature. When e.g. professional phagocytes are concerned, they mainly enter cells via phagocytosis, to accumulate into lysosomal compartments. Passive penetration into non-phagocytic cells of single-walled nanotubes was reported instead to be followed by accumulation into mitochondria [386,387]. It is also interesting to note that, when cells are exposed to soluble (PEG-functionalized) carbon nanotubes, stimulated endocytosis was supposed to be inhibited [396], allowing for a net incorporation of plasma membrane by vesicle fusion or exocytosis. In other words, exocytotic inclusion of vesicles (diameter ≈ 50 nm) into the cell would not be balanced by the endocytotic reverse process in the presence of single-walled nanotubes (diameter $= 2 - 11$ nm, length $= 0.1 - 2.2\ \mu$m), whose relatively long length would constrain the vesicle by preventing it from closing and pinching off the membrane. This would justify an increase in the net neurite length and a principle of constant cell surface/volume ratio, also explaining why the number of neurites would correspondingly decrease, as propounded elsewhere [397].

Penetration mechanisms and kinetics can generally be influenced by relevant features like dispersion state, molecular length, diameter, surface properties (charge, chemistry, geometry), concentration and time exposure. Clearly, biokinetics of nanoparticles is also a function of in-vivo surface modifications (see e.g. the 'protein corona' concept, see below) and specific surface areas. Chemically

identical particles with larger surface area per mass will tend to be biologically more active. Clusters, bundles, aggregates are normally internalised through endocytic/phagocytic processes, whereas single nanotubes, especially whether functionalized, mainly resort to passive pathways, which avoid lysosomial leakages in endocytosis-mediated mechanisms and lower toxycity (e.g. [387,398]). Unpurified multi-walled molecules may get through plasma membranes into cytoplasm and nucleus, both actively and passively, indicating possible harmful effects as incomplete phagocytosis or energy-independent mechanical piercing mechanisms [274,399,400]. About geometric effects, shortening carbon nanotubes favours their uptake by passive diffusion, and in phagocytic cells as well. In studying the uptake into human monocyte-derived macrophages, lengths > 400 nm were mainly localised in endosomes, shorter molecules diffusing throughout the cytosol and suggesting their extravesicular localisation [401]. An entry route for smaller nanoparticles may be also provided by neuron synaptic transmission and cell membrane with ion channels (Ca^{2+}, Na^+, K^+, Cl^-) [1]. On the other hand, conjugation of multi-walled nanotubes with Angiopep-2 (ANG, a ligand for low-density lipoprotein receptor-related protein-1, LRP1) turned out to be selective towards the wide-type nanotubes (diameter ≈ 23.8 nm) as those of the thin-type (diameter ≈ 7.9 nm) were not uptaken [402].

The work that was done in relation to surface chemistry and charge against Bbb crossing is noteworthy, and below are again some relevant examples. Single-walled molecules (diameter ≈ 1.5 nm, length $= 10 - 100$ nm) were proposed to act as intracellular transporters via the endocytosis mechanism for protein molecules (of molecular weight 80 kDa) that are non-covalently and non-specifically bound to nanotube sidewalls [403]. Endocytosed carboxyl-functionalized multi-walled molecules then were found to strongly stimulate migration of macrophages (RAW264.7) [404]. In another cellular environment, both negatively and positively charged multi-walled nanotubes were able to reach human embryonic kidney epithelial cells (HEK293) by direct penetration, their bundles being instead endocytosed [395]. Cell penetrating peptide TAT (trans-activating transcriptional activator) and cancer targeted molecule biotin-functionalized multi-walled molecules were also designed to augment Bbb penetration [405]. Multi-walled molecules conjugated with gadolinium L2 (amyloid beta targeting agent) were able as well to cross Bbb via receptor-mediated transcytosis (in therapeutic Alzheimer's mice model) [406] and, coated with Pluronic (PF127) surfactant, did not produce neuronal degeneration close to the injection site [407]. Bbb penetration was also observed when multi-walled nanotubes were functionalized with fluorescein isothiocyanate (FITC) [408], with no evident toxicity from cell viability studies, and with dethylenetriaminepentadianhydride/antibody fragment antigen binding region (FAB), which entered the mice brain and distributed into the parenchyma [409]. Polysorbates can facilitate the transport of nanotubes to the brain by adsorption of apolipoprotein-E (APO-E) from blood plasma onto the nanoparticle surface [379]. Sometimes, interaction of charged groups with the negatively charged cell membrane may yield non-specific crossing mechanisms, like with cell-penetrating peptides (CPP) [405]. CPP form a class of short (generally not exceeding 30 residues), water-soluble and partly hydrophobic, and/or polybasic peptides, which are rich in basic amino acids (e.g. arginine and lysine) and have the ability to enter Bbb by electrostatic interactions [365]. Finally, an interesting heuristic surface-chemistry law holds for the H-bonding extent versus Bbb penetration. It applies to compounds with high H-bond forming capacity (e.g. peptides with amide groups), displaying a minimal distribution within Bbb [410]. Lipinski's rule says in fact that molecules develop a decreased absorption and permeability when the numbers of H-bond donors/acceptors are larger respectively than 5/10, each pair of H-bonds bringing to a permeability decrease equal to 1 log of magnitude [362,369].

A crucial variable is also represented by the nanoparticle concentration, as it was shown in various contexts. Carbon nanotubes versus viability of PC12-cell lines was strongly dose-dependent [411]. Impairment of axonal regeneration in low density dorsal root ganglia (DRG) neurons upon incubation with multi-walled molecules (10% of surfactant in saline) was detected over a dose range $1 - 10$ μg ml^{-1}, stepping back to be safe at 0.1 μg ml^{-1} [412]. Similarly, exposure of postnatal mouse DRG

neurons to multi-walled nanotubes dispersed in culture medium was definitely toxic at 250 μg ml^{-1}, with aberrant neurite morphologies, but got back to be nontoxic at 5 μg ml^{-1} over 14 days [413]. Dose and time thus may be conceived forming a joint experimental variable, suggesting researchers to investigate both on acute and chronic cytotoxicity to avoid inappropriate conclusions related to nanomaterials accumulation and delayed toxicity. Sometimes, impairment can come along large doses of administered molecules, but could not be an intrinsic effect of nanotubes per se [374]. Neuronal excitability in CA1 pyramidal neurons in rat hippocampus was inferred by means of whole-cell patch-clamp techniques, providing with an assessment of carbon nanotube neurotoxicity. From an analysis of action potentials and signal patterns, spike half-width and repetitive firing frequencies turned out to remarkably increase and still depend upon concentration ($= 50, 100, 400$ μg ml^{-1}) of multi-walled molecules suspended in an artificial cerebrospinal fluid [42]. A dose-dependence was also registered in the gradual amplitude suppression of voltage-gated transient outward and delayed rectifier K$^+$ currents, which affect several processes in excitable and non-excitable cells (e.g. setting/resetting membrane potential and action potential duration, discharge patterning, delaying between stimulus and the first action potential) [1].

A hurdle in investigating on realistic nanoparticle biokinetics is to figure out which in-vitro model may actually rebuild up the in-vivo behavior. Permeability index and (transepithelial/transendothelial)
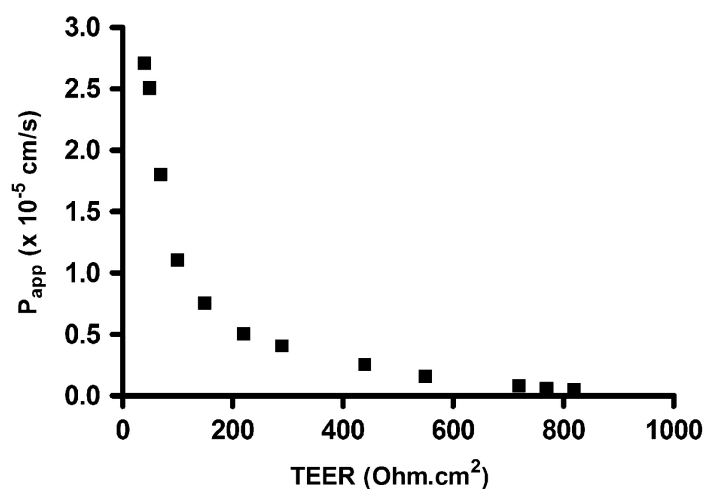

Figure 27. Permeability versus TEER in monolayers of primary cultured porcine brain endothelial cells (adapted from ref. [414]).

electric resistance across cellular layers (TEER, see example in Fig. 27), helpful to characterize the microstructure (e.g. tightness of junctions among cells), are two noteworthy parameters assisting the model interpretation [414]. There are many studies reporting in-vitro models (see e.g. [415,416]) with various types of cell line of different origins and culture environments. This may apply too to the assessment of neural biocompatibility, as e.g. neurons and astrocytes grow differently on biomaterials. The former require more specific properties for their adhesion and differentiation. Astrocytes – guiding the neuronal growth by expressing and secreting molecules which are essential to neurite adhesion, growth and branching [417,418] – were found to preferentially adhere to carbon nanotubes with larger diameter and low surface energy scaffolds [419]. Primary endothelial cell cultures thus mimic the in-vivo Bbb behavior better than immortalized endothelial lines, as they form tight junctions that express surface receptors and can demonstrate transcytosis. On the other hand, model examples where Bbb's failure or disruption is a crucial limiting step in pathology development and/or progression may be found e.g. in [378]. A further potential pitfall is that experimental analysis of internalization is not straightforward and strongly depend upon cellular/molecular details. It can rely e.g. on labeling protocols to track transport – which may bias however the physical chemistry characteristics of nanotubes, the NCN interaction and thus the quantitative description of translocation or toxicity mechanisms – or on electron microscopy e.g. to qualitatively assess transcytosis. Unfortunately,

whenever certain biological details were required (e.g. to discriminate nanotubes endocytosed into endothelial cells from those interacting with apical cell membranes, or nanotubes in intracellular space from those exocytosed via basolateral cell membranes but trapped within basolateral space before crossing the transwell filter, etc.), UV-Vis spectroscopy methods alone (i.e. without secondary carbon nanotubes labeling) could no longer suffice and should be complemented by quantitative TEM analysis [388]. It was shown accordingly that a majority of cationic-functionalized multi-walled molecules was strongly adsorbed onto the negatively-charged glycocalyx structure, staying trapped onto the apical cell phase without an actual internalization.

8.3. General on Cytotoxicity Effects

The dual chemical/geometrical nature of carbon nanotubes, which is graphitic/fiber-like (as asbestos), may be responsible for a behavior which is toxic and biopersistent [363], potentially inducing inflammation, angiogenesis or fibrosis [420], and especially in systems that are sensitive to toxicants, such as neuronal cells (see the synoptic picture in Fig. 28). The high hydrophobicity and aspect ratio give these structures the ability to cross biological membranes, threatening the living organism with a number of potentially harmful effects (see e.g. [386] and references therein). Carbon nanotubes generally reach subcellular compartments (cytosol, endosomes, perinuclear region, mitochondria, see e.g. [386,395]), single-walled molecules being proved to raise oxidative stress in a number of cellular lines, like human keratinocytes, rat lung epithelial and mesothelial cells ([399] and references therein). Carbon nanotubes also distribute in many organs and tissues (e.g. transiently in lungs, spleen, kidneys; long-term and dose-dependent in the liver, see [421] on CD1 mice), including a detectable ($1.0 - 3.3$ % ID/g) accumulation in brain over 28 days of pulmonary exposure [422]. Acute pulmunary exposure to multi-walled nanotubes−7 fibers was found, still in mice, to cause indirect (extra-pulmonary) neuroinflammation, as they showed a minimal translocation from the lung into systemic circulation. After 4 h of exposure, impairment of Bbb integrity was detected, the largest-diameter vessels and the immediate branches that feed the microvasculature sustaining a greater Bbb disruption [383]. The mechanistic link of neuroinflammation (and a possibly worsened proinflammatory phenotype), cytotoxicity and genotoxicity versus Bbb permeability is an issue worth to be further investigated. Still in this line, single-walled nanotubes turned out to diminish the cell adhesiveness and thence the proliferation of human embryo kidney cells (HEK293) [423], while multi-walled molecules induced apoptosis in mouse embryonic stem cells [424]. Surface oxidation in amino-functionalized multi-walled molecules induced significant levels of glial fibrillary acidic proteins (GFAP) and integrin family member CD11b (marker of macrophages and microglia), prompting it may be responsible of inflammatory reactions in a healthy brain [425]. Other researchers claimed
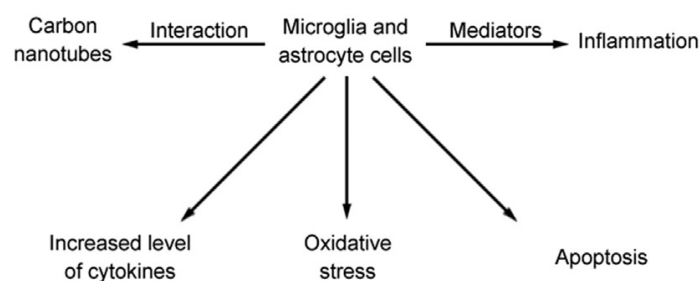
Figure 28. Connections among carbon nanotubes and toxicity on brain cells upon entering Bbb (according to ref. [426]).

that electro-conductive multi-walled nanotubes, as opposed to redoxactive and non-conductive – can change the phenotype and function of microglia cells from rat brain cortex without cytotoxicity, switching from pro-inflammatory to anti-inflammatory/neuroprotective microglia phenotypes within $(24 - 48)$ h cell exposure [427] – and were suggested to be electrochemically interacting with human macrophages [428]. Finally, the (in-vitro) toxicological impact of functionalized and pristine nanotubes

returned some differences once it is tested on neuron-, mixed glial- and microglial-like cultures. While specific cytotoxicity effects emerged from mixed glial cultures according to the brain region of origin (they were lesser in fetal rat frontal cortex (FCO) cells than striatum's (ST)), the influence of exposure of mixed glial cells to multi-walled molecules was independent of surface chemistry. A number of types of functionalized nanotubes (carboxylated, amino-functionalized, amino-functionalized oxidized) seemed not to elicit harmful effects up to a dose of 100 μg ml^{-1} (within 24 h) in isolated neuronal cultures from FCO and ST, but triggered a cytotoxic response in microglia-containing cultures [429]. Oxidation (e.g. redox imbalance, DNA oxidative damage) is not the only mechanism causing toxicity and different immunological responses [430], since aggregation, number of walls, chirality and crystal structure can contribute on their own [420,431]. Nanotubes in aggregated ropes are more toxic than in dispersion states, even μm-sized dispersed carbon nanotubes were reported to be less toxic than aggregated ones [138,432]. A relationship between the dispersion state of as-prepared, purified, carboxylated multi-walled nanotubes and the pro-fibrogenic response was also proposed in tissue culture cells [433]. Molecules with smaller surface areas seemed to be more toxic as well. Single-walled nanotubes elicited a greater toxicity than multi-walled [434], maybe because of a certain geometric resemblance with some virus molecule [138,435]. Impurities like metal catalyst residues incorporated during the synthesis (e.g. Fe, Co, Ni, Y) take also a central role in cellular toxicity [385]. For example, cationic Y traces released from aryl-sulphonate functionalyzed single-walled nanotubes inhibited the neuronal voltage-gated Ca^{2+} ion channels in a nanotube dose- and sample-dependent fashion with inhibitory efficacy (IC50) of 0.07 ppm (w/w) [436]. Metal ions can also influence gene expression by triggering ROS, affecting NGF, or acting as enzyme cofactors (see [437] and references therein). A pro-oxidant activity can be ascribed as well to surface erosion in functionalized molecules upon strong reaction conditions (by disrupting the sp^2 hybridisation of carbon atoms and, jointly to unavoidable hexagon ring defects, increasing chemical reactivity) and to molecular length [398,438]. While shorter nanotubes enter cells more easily, lowering the host immune response, longer nanotubes can get bundled in extracellular space, giving rise to ROS and oxidative stress [426,439]. It is known moreover that an excessive length may deform cell walls [379]. To reduce the aspect ratio, strong oxidation, ultrasonication, steam-purification and mechanical methods are available (e.g. [386]). In any case, even if carbon nanotubes were completely degradable (e.g. to CO2), their cytotoxicity would not be zero but should be re-assessed in terms of further aromatic molecules (e.g. rings or polyciclic hydrocarbons) that could be produced consequently. There is also an issue related to the toxicity of surfactants, employed to stabilize nanotube suspensions, and generally capable to permeabilize plasma membranes. Sodium dodecyl sulfate (SDS), sodium dodecylbenzene sulfonate (SDBS) and sodium cholate (SC) are surfactant molecules for dispersing bundles of entangled nanotubes into aqueous dispersions of individual units. However, only SC and carbon nanotubes conjugated with it did not affect morphology, proliferation and growth of (1321N1) human astrocytoma cells [440]. A more recent biocompatible surfactant is the non-ionic triblock copolymers Pluronics. Further references about in-vivo and in-vitro biocompatibility/toxicity of carbon nanostructures, are gathered e.g. in [441,442], keeping in mind a promising molecular system to repair a damaged nervous tissue does not mean it won't necessarily ruin the activity of cells it is interfaced with. Carboxyl-terminated multi-walled nanotubes (diameter $40 - 50$ nm, length $300 - 800$ nm, 5 mg/ml, 24 h exposure) incubated with immortalized rat PC12 neuronal pheochromocytoma cells produced in fact a time-dependent depolarization state that irreversibly inhibited the activity of three kinds of K^+ ion channels (transient outward, delayed rectifier and inward rectifier currents), apparently with no oxidative stress (ROS), modifications in intracellular Ca^{2+} concentration and mitochondrial membrane potential [443]. A discussion of inhibition effects of carbon nanotubes on depolarization-dependent ion channels and transmembrane ion fluxes (Ca^{2+}, K^+), as formerly noticed in [397,444] may be found in [445].

8.4. Functionalization and Biofunctionalization

To limit cytotoxycity researchers work with high-purity and/or functionalized carbon nanotubes (e.g. [446,447] and references that follow). Purification routes, such as acid treatment and vacuum heating/thermal annealing [333], can reduce toxicity to a meaningful extent [448]. Regarding functionalization, it has been known for more than twenty years (e.g. [3]) that neurons grown on nanotubes coated with bioactive molecules (in that case, 4-hydroxynonenal/4-HNE, a lipid peroxidation product which can trigger an increase of intracellular Ca^{2+} concentration levels, modify cytoskeletal proteins and signaling mechanisms that govern neurite outgrowth [171]) may produce multiple neurites with extensive branching. As we have seen, insoluble raw nanotubes may trigger harmful effects to cells and tissues especially in the form of bundles or aggregates, and even at low concentrations [449]. Surface functionalization is the technique ordinarily in use for enhancing dispersability (i.e. hydrophilicity) and translocation ability in biological media/plasma membranes, facilitating cellular internalization, protein adsorption, biodegradation and excretion, thence prompting NCN interactions and reducing toxicity.

Functionalization can be accomplished by the incorporation of pendant units such as amino and carboxyl groups [450]. Normally, these modifications may be carried out covalently if they give rise to chemical alterations of the surface structure (e.g. by stably incorporating reactive groups as amine $-NH_2$, thiol $-SH$, carboxyl $-COOH$) or non-covalently, by means of coating or wrapping procedures relying on electrostatic, π-π, van der Waals or H-bond interactions between nanotube surface and hydrophobic/aromatic sites of amphiphilic organic molecules [363]. Two main protocols to get covalent functionalization of carbon nanotubes are i.) sidewall and tip covalent conjugation of functional groups, which may be carried out by chemical reactions (see e.g. the 1,3-dipolar cycloaddition of azomethine ylides in Fig. 29) and ii.) strong acidic oxidation followed by modification, generally producing purified and shorter nanotubes [430]. Strategy i.) is quite simple but is not versatile when
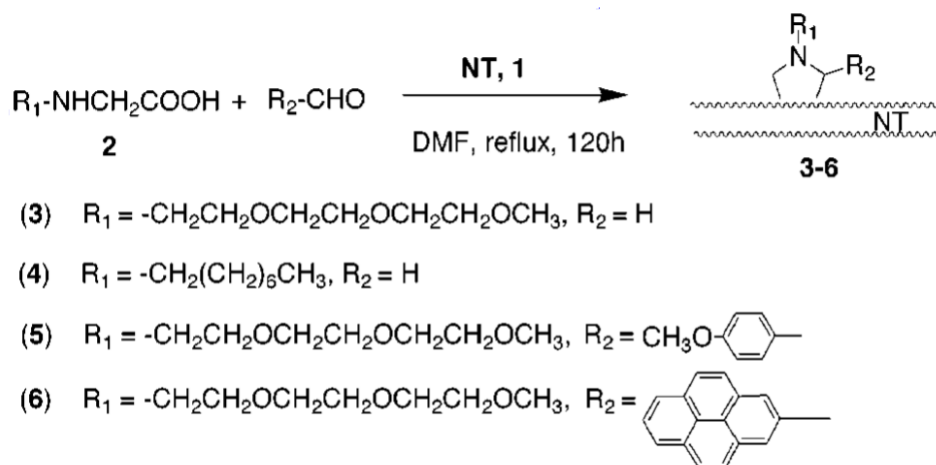

Figure 29. Carbon nanotube (NT) functionalization scheme based on 1,3-dipolar cycloaddition of azomethine ylides, produced by condensation of an R-amino acid and an aldehyde (adapted from ref. [113]). This reaction is widely in use for modifying fullerenes C_{60}.

additional insertions are desired, whereas in ii.) tube cap openings/sidewall holes are formed. For instance, in case of oxidation followed by carboxyl-based couplings, nanotubes may be covalently conjugated with biological molecules by amide and ester bonds. Oxygen plasma treatment is also used [102] but there may be cases in which it does not return the expected beneficial effects. Dissociated retinal cells were cultured in vitro on oxygen plasma functionalized vertically aligned nanotubes grown from a Fe catalyst and a Fe catalyst with an Al underlayer (Al/Fe). The extent of neurite outgrowth was larger in Al/Fe samples than upon plasma preparation, suggesting that plasma functionalization, usually meant to positively alter surface topography, increase surface roughness

and hydrophilicity [451,452], could in some situation inhibit neurite outgrowth [453]. Dendrimers (e.g. protonable groups) can also be exploited as an alternative to remedy to the possible damage produced by an excessive covalent functionalization, yet retaining a high dispersability [454]. Generally, the (adsorption) affinity of carbon nanotubes with hydrophilic macromolecules such as surfactants, polymers, peptides/proteins, lipids, and nucleic acids, particularly single-stranded DNA, can be pronounced enough to give rise to a wealthy of mixed bionanomaterials (e.g. [455]. Coating and wrapping conjugations preserve the aromatic structure of nanotubes without affecting their electronic properties [456]. Examples of stable non-toxic polymers involved in non-covalent functionalization are poly-L-ornithine (PLO), poly(acrylic acid) (PAA), poly(diallyldimethylammonium chloride) (PDDC), polyoxyethylene sorbitan mono-oleate (PS-80), polyvinylpyrrolidone (PPY), and the above-mentioned PEI (polyethylenimine), PEG (polyethylene glycol), PABS (poly-m-aminobenzene sulphonic acid), PL (polylysine) and poly(L-lactic acid-co-caprolactone) [386,457]. However, the weak forces between these complex elements or physisorption interactions could not assure the necessary stability for a biomedical use and a long-lasting retention to nanotubes [386]. Noncovalent functionalization was also achieved in multi-walled nanotubes upon incubation e.g. in trimethyl-(2-oxo-2-pyren-1-yl-ethyl)-ammonium and 1-pyrenebutyric acid solutions, carrying respectively positive and negative charge units [102].

As it was previously pointed out, a property of the utmost importance here is surface charge (at physiological conditions, e.g. pH values), whose manipulation may be effective to enhance neurite outgrowth, to get longer average neurite length, and elaborate neurite branching. Generally, as cell membranes mostly consist of negatively-charged phospholipids, more positive/less negative surface charges may yield a more favorable niche [458]. As examples, multi-walled nanotubes functionalized with PABS and ethylenediamine (EN) were able to induce a higher number of growth cones than those grown on functionalized with carboxylic groups (COOH) that, in a culture media with pH $= 7.35$, are negatively charged as a consequence of the surface charge density $(0.2 - 0.5 \%)$ induced by deprotonation (pKa $= 4.5$) [459]. The positive charge carried by nanotubes/EN stems from the larger pKa of amine groups (pKa $= 9.9$). PABS, containing amine and sulfonic groups, are nearly zwitterionic, being electoneutral at pH $= 7.35$. As a result, neurite branching showed a graded dependence on charge in the order EN > PABS > COOH. Note that use of EN proved to be more effective in giving multi-walled nanotubes a higher dispersibility and lower cytotoxicity than carboxyl functional groups [460]. Positively charged multi-walled nanotubes, amino-functionalized by 1,4-diaminobutane, grew and adhered to neuronal cells too, acting as good electrodes for extracellular recording as well. The amino-functionalization increases interfacial capacitance (from 2.1 to 22 F mm^{-2}, between nanotube and buffer electrolyte solution) and lowers the interfacial impedance (from 0.37 to 0.19 kΩ mm^{-2}). These nanotubes exhibited higher sensitivity of neural signals (i.e. larger S/N ratio) than standard suction glass pipettes [461]. Finally, the adverse impact of neutral and negatively charged nanotubes, onto cell survival and growth, was also put forward in a study on functionalized 4-tert-butylphenyl- and 4-benzoic acid single-walled molecules [462]. To afford a thorough analysis of how the biophysical chemistry behavior changes upon insertion of surface moieties and/or drug molecules, suitable quantum-like approaches (i.e. ab-initio simulations and density functional theories, DFT) can be exploited. A comparison between adsorption energies, intra/inter-molecular interactions, density of electronic states (DOS, see e.g. Fig. 30), Fermi's levels, HOMO/LUMO energy gaps, as well as an analysis of the conformational statistics of functional groups, chemical reactivity and stability, provide with useful control information about functionalization effects. In carboxylated carbon nanotubes, the difference between HOMO and LUMO values in functionalized and pristine nanotubes amounts to -0.07 eV, and it is known that a lower band gap could affect the activity/reactivity in biological environments [463].

More heterogeneous structures, with polymer molecules, supramolecular complexes or more than one functional group [362], can be also created to endow the nanostructure with advanced properties. For instance, covalent functionalization with carboxyl groups allows the insertion of amine and thiols [401], while covalent attachment of macromolecules to the carbon nanotube surface can be carried out
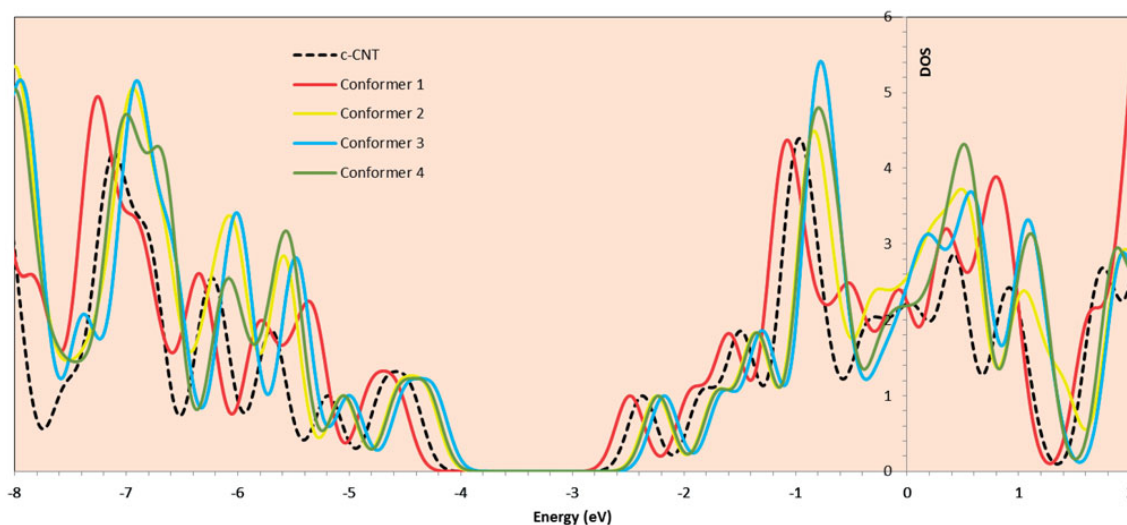
Figure 30. Example of total DOS of a carboxylated carbon nanotube (c-CNT) and of c-CNT conformers with benserazide molecule adsorbed (BZ/c-CNT) (adapted from ref. [463]). BZ ($C_{10}H_{15}N_3O_5$) is an irreversible inhibitor of peripheral aromatic L-amino acid decarboxylase, useful in combination with L-Dopa in the therapy of neurodegenerative diseases.

by 'grafting to' or 'grafting from' procedures (e.g. [464]). In the first, polymers with a reactive group is linked to functionalized nanotubes by a chemical reaction. The second, where polymerization of a given monomer is started from reactive nanotube sites, is characterized by a higher grafting density and better nanostructural control. Polymer grafting methods can be used to adjust surface chemistry, polarity and charge density by either using homo-polymers or random co-polymers encoded with desirable moieties.[8] About polymer materials, PEI, PEG and PLO were noticed to promote neural cell attachment, neurite outgrowth, and increasing biocompatibility of carbon nanotubes [465]. With PEI/functionalization (see Fig. 31), carrying positive charge, a modulation of neurite outgrowth and branching was observed, as opposed to zwitterionic or negatively charged nanotubes [466]. PEG chain attachment to nanotubes with large enough molecular mass is an extensively used technique to promote their elimination from the body and decrease toxicity [467]. PEGylation increases the nanotube half-life in blood vessels, preventing the immunological clearance upon opsonisation [386]. In another investigation, single-walled molecules were coated with electro-active polyaniline (PANI) by in-situ chemical polymerization and employing sodium dodecylsulfate (SDS) as a surfactant template for monomer assembly/polymerization. In-vitro biocompatibility with primary immune cells turned out to be affected by the dosage and cell type [468]. Cross-linked poly(3,4-ethylenedioxythiophene) polystyrene sulfonate (PEDOT:PSS) [469] then was observed to elongate neural stem cells, impacting on their differentiations to neurons and eliciting longer neurites [470]. It showed good (in-vitro) biocompatibility, high stability upon long-term biphasic pulse stimulation and aggressive cyclic voltammetric stimulation. As a relevant example, single-walled nanotubes carrying carboxylic end groups were functionalized with PABS and PEG. Addition of these nanotube graft copolymers, to cultured neonatal rat hippocampal neurons grown on PEI-coated coverslips, increased the length of a number of neuronal processes [397], highlighting in this case too dose-dependent phenomena to light. The neurite number/neuron diminished at 1 μg ml^{-1}, but no meaningful variation in the total neurite length/neuron occurred, as neurons evidenced an increase in the average neurite length. Treated neurons had sparser yet longer neurites. This was ascribed to a modulation of intracellular Ca^{2+}

---

[8] See e.g. [458], on the effect of grafted polymers/carbon nanotubes onto human embryonic stem cell differentiation into neurons
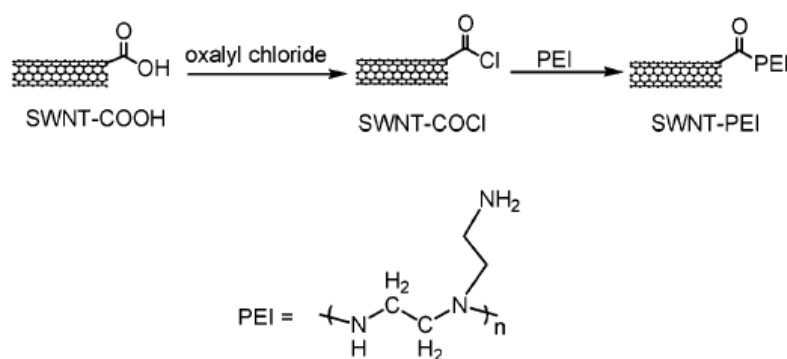
Figure 31. Reaction scheme for single-walled graft copolymer (SWNT-PEI) synthesis, functionalized with branched polyethyleneimine (adapted from ref. [466]). A similar schematic could also be drawn e.g. for PABS, PEG, EN [397,459].

homeostasis, known to be implicated in neurite elongation kinetics, as single-walled/PEG nanotubes may inhibit the depolarization-dependent Ca^{2+} influx from extracellular space to the cytosol.

Incorporation of functionalized nanotubes into hybrid structures or nanocomposites then can be promising to create nanostructures with enhanced features (e.g. mechanical strength, biodegradability, electric conductivity, cytocompatibility, etc.) and/or for drug delivery. This was the case e.g. of the multifunctional biodegradable elastomer poly(glycerol sebacate urethane) (PSGU, 4 wt. %), strengthened by carbon nanotubes functionalized with PEDOT:PSS [471]. Charge storage capacity, (1508 ± 4) μC cm^{-2}, and electrochemical impedance at 10 kHz of this nanocomposite, (204 ± 44) Ω, outperformed pristine Pt electrodes. Other examples bringing to alike conclusions are the trihybrid electroactive material formed by Iridium Oxide (IrOx), carbon nanotubes and PEDOT - that is, an inorganic metal oxide, a carbon nanostructure and a flexible polymer, to be exposed at the interface with the biological system [418] - and the electrically conductive hydrogel, with specific conductance (5.75 ± 3.23) mS m^{-1}, fabricated by covalently embedding functionalized graphene oxide acrylate (GOA) and carbon nanotube/poly(ethylene glycol) acrylate (PEGA) within an oligo(poly(ethylene glycol) fumarate) (OPF) hydrogel via chemical cross-linking followed by in-situ reduction of GOA in L-ascorbic acid solution [472]. Without resorting to PEDOT chains, the IrOx/single-walled nanotube hybrids deposited as three-dimensional thin film structures by dynamic electrochemical methods [473], and conventional multi-electrode arrays of IrOx and W/stainless-steel microelectrodes, modified with multi-walled nanotubes still by electrochemical means [331], are further noteworthy examples of bioelectroactive carbon-based nanomaterials. In this latter case, electric measurements at a frequency of 1 kHz returned a decreased impedance (from 940 kΩ to 38 kΩ) and an increased charge transfer (40-fold) for multi-electrode arrays. In order to create a composite hydrogel equipped with electric conductivity and surface charge, positive charges were embodied through 2-(methacryloyloxy)ethyltrimethylammonium chloride (MTAC), yielding a stiffer interface for cells to adhere, spread, proliferate and differentiate. Finally, a nanohybrid of carboxylated single-walled nanotubes and levodopa (LD, for Parkinson's disease) was built up by π-π stacking interactions [474], while oxaliplatin (OXA, for orthotopic glioma therapy) was incorporated into a cell penetrating peptide- and cancer-targeted molecule carboxyl-functionalized multi-walled carbon nanotube [362,405].

A last strategy to improve NCN interphases, for an effective repair and regeneration of neuronal tissues, is resorting to biofunctionalization [465], i.e. the provision of compounds as proteins, genes or therapeutic molecules, giving rise to a nanomaterial with a biological activity that, normally, tends to increase with their volume [475]. A conceptually simple first example of it is just binding carbon nanotubes to blood proteins [476] or globular heads [477]. Amino-functionalized multi-walled nanotubes, administered with nerve growth factor (NGF, an endogenous soluble protein for the

survival, growth, plasticity, and protein synthesis of differentiated neurons), increased the number of neurons with neurite outgrowth when compared to the addition of NGF alone and their concentration in the culture medium was ranging in (0.11-1.7) μg ml^{-1}. The extracellular signal-regulated kinase (ERK) signaling pathway was in that case activated [478]. In another study, neurotrophin (NGF, or brain-derived neurotrophic factor BDNF) was covalently bound to amino-group-functionalized multi-walled carbon nanotubes to form a coated nanostructure (diameter $\approx$ 25 nm, length $\leq$ 2 μm) that elicited neurite outgrowth likewise the soluble NGF and BDNF. A maximum bioactivity was detected at a given neurotrophin concentration (10 ng ml^{-1}) in the culture medium, but the relatively large size of these nanostructures was incompatible with transportation inside cells. As neurotrophin may internalize upon binding to its receptor, neurotrophin-coated nanotubes was deduced to be internalized by endocytosis [475]. About the carboxyl functionalization, it turned out that functionalized multi-walled carbon nanotubes didn't alter the neurotrophin expression level, but elicited neurotrophic factor release (BDNF) from cortical and hippocampal neurons (isolated from embryonic mice) regardless of their cellular type [479]. Overall, their influence on cultured neurons seemed to resemble Matrigel's, a soluble basal membrane (comprising laminin, collagen IV, heparin sulfate, proteoglycans, entactin, and nidogen [480]) that was acting effectively as a coating substrate for primary neuron cultures.

8.5. Morphological Notes

One of the ultimate goals of a thorough mechanistic analysis of NCN interphases is to collect all the atomistic/molecular knowledge for a morphological/morphogenetic comprehension of either NCN interactions or neuronal media themselves. The brain, inclusive of its extracellular space (i.e. 1/5 of brain volume), obviously forms a highly coordinated system, where neurons and glial cells generate electrical fields in a concerted fashion and little is still known of its space structure and time-spiking dynamics [108,481]. A 'morphological' problem may clearly arise whenever one asks about the rise of a functioning neural network from an assembly of single neurons, growing and structuring up to get to an astonishingly intricate molecular system [482]. Researchers started challenging analysis of form-function interactions and the underlying molecular and cellular mechanisms to inquiry their roles in the morphogenetic growth and differentiation into ordered neuronal networks, where a fundamental understanding of basic points – such as a full dynamical description of microtubule rearrangements (nucleation, stabilization and transport, see Fig. 32), the creation/destruction of synaptic connections, and the basic knowledge to precisely calibrate stimulus parameters (e.g. stimulation type, power and duration) for avoiding inappropriate perturbations bringing to apoptosis – is still lacking [12]. In this case too, however, carbon nanotube interphases may offer suitable testing systems with stable topology and a consistent recording of electric bioactivity (as in small interconnected neuronal circuits morphed by one-to-one neuron-electrode interphases [482]). Similarly to the scaling and universality notions met in macromolecular sciences [269], NCN interactions may be expected to include both specific terms, dependent upon the types of biological cells and nanotubes employed [484], and invariant contributions, linked to the transition to larger spacetime scales, i.e. from single neuron cells to synaptic connections and three-dimensional tissues. According to a minimal basic scheme to model how a NCN interacting picture may develop at diverse scales, there emerge the cell body region, for localization and selectivity events, and the growth-dependent neurite's. Let cell membranes then to stay stable – as long as suitable differences in charge density (linked e.g. to concentration, charge type and size of inorganic and betaine ions) and stability (i.e. the hydrophilic colloidal fluids of proteins/polysaccharides) are maintained [485] – carbon nanotubes should potentially interact with neuronal electrogenic responses at any scale.

The relative arrangement of carbon nanotubes with neurons and/or non-neuronal cells was ascertained to be essential to morph the properties of the system as a whole. Neuron-carbon nanotube or neuron-glial interactions cell can contribute differently to the behavior of a NCN interphase [486]. The importance of the latter was documented e.g. in neuron migration phenomena [487], in synchronization
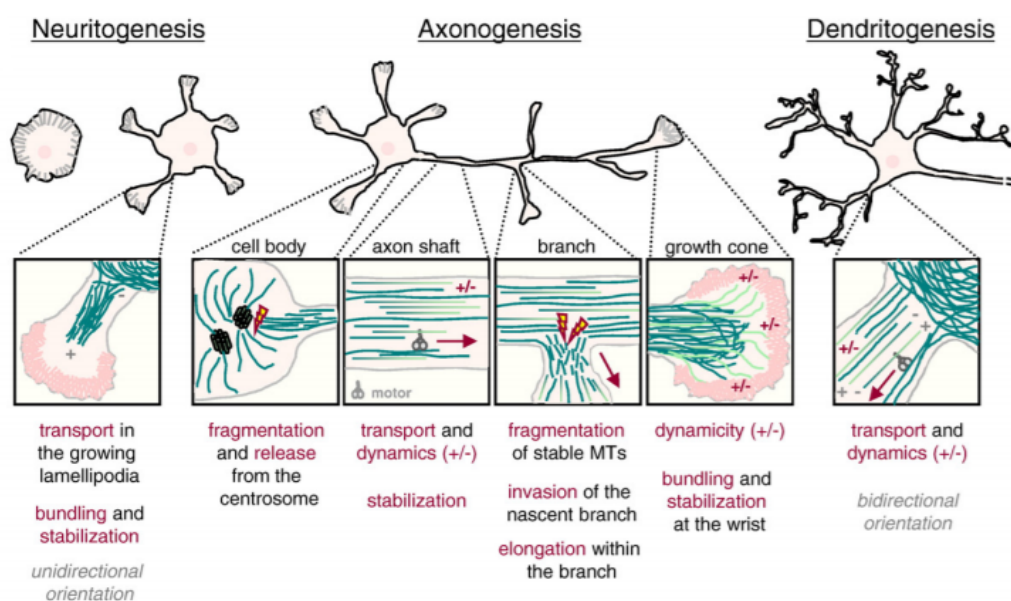
Figure 32. Microtubule reorganization in neuronal morphogenesis (adapted from ref. [483]).

of firing patterns from neurons in regions of non-synaptic glutamate-release astrocytes [299] and in the propagation of intercellular Ca^{2+} signaling between astrocyte networks and distal neurons [488]. The behavior of neuronal cells at an interphase was also studied for different substrates/arrays (in Fig. 33), highlighting a certain complexity of diverse clustering trends, and suggesting a phenomenology of the many-body type [451]. An unexpected collective behavior of neurons was detected at 8 days in-vitro, ruling out a major effect of serum protein deposition in the modulation of neuronal adhesion, migration and neurite extension. The relative affinity between neuron–neuron and neuron–substrate was varied by means of five multi-walled nanotube arrays, with different surface chemistry, bringing to the appearance of variable neuronal organizations with intermediate phenotypes. For instance, when neuron-substrate interactions were augmented by oxygen plasma treatment, neuronal cluster and neurite bundle formation were gradually lowered. In another extreme case, settled by treatment with PEG5000, good cell viability is observed accompanied however by a total absence of neuronal differentiation, clustering and lack of neurites on the surface. Changes in cell adhesion upon different surface chemistries eventually resulted into clusters of various morphology (e.g. fractal-, sunshine- and ball-like), while bundle-like organizations come from neurite–neurite interaction preferred over neurite–surface's. All surface chemistries produced neurite fascicles, but displayed remarkable differences in the fraction of fascicles linking two distinct neuronal clusters (it was 100 % maximum for silicon wafers with a raw nanotube array, and minimum, 10 %, for a treatment in 2 mM pyrene–PEG5000 aqueous solutions) [451]. Needless to say that unnatural cellular constraints will negatively impact the system bioactivity. When quantities like length, diameter, roughness, stiffness, wetting angle, surface-to-volume ratio, electric conductivity and surface charge of carbon nanotubes (and their substrates) are on scale with neuronal systems, NCN interphases will better match the prerequisites of the biological matter. For instance, on varying the copolymer PEI/single-walled nanotube ratio, we have seen in ref. [466] that neurite branching and outgrowth could be somehow modulated. Alongside, carbon nanotubes are reported to modulate glial cell morphology and gliotransmitters, enhance glutamate uptake, regulate the intracellular gamma amino-butyric acid (GABA) distribution in astrocytes, and set an interaction between adenosine triphosphate (ATP) release of astrocytes and neurons [489]. Neuronal interaction and information exchanges proceed in fact by releasing chemical messengers (neurotransmitters) at synapses and their reception in specific proteins (receptors), triggering a physiology reponse. After an action potential gets to a synapse,
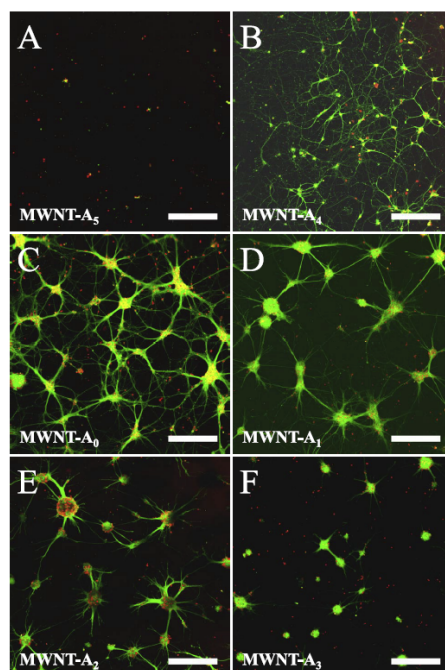
Figure 33. Hippocampal neurons clustering on raw (A_0) and functionalized (A_{1-5}) multi-walled nanotube substrates (adapted from ref. [451]). (A) Non-differentiated neurons, (B) network built by individual neurons and neurites, (C) network-like clusters linked by numerous neurite fascicles, (D) sunshine-like neuronal clustering, (E) fractal-like clusters and (F) ball-like cluster structure (fluorescent confocal microscopy images at 8 days in vitro, bar $= 250$ μm). $A_{1,2,3}$ were non-covalently functionalized by positively charged trimethyl-(2-oxo-2-pyren-1-yl-ethyl)-ammonium (A_1), negatively charged 1-pyrenebutyric acid (A_2) or pyrene– PEG5000 (A_3). A_4 was covalently modified by treating A_0 with plasma oxygen (getting a mixture of carboxyl, carbonyl and hydroxide groups), while A_5 was obtained by covalently coupling A_4 to PEG5000. Further substrate details are found in [451].

neurons undergo depolarization and neurotransmitter release. Thus, neurons interphased with carbon nanotubes may own a reasonably equipped machinery to keep functional and display a long-range interaction.

Processes like neuritogenesis, neurite growth, synaptogenesis, synaptic stabilization, axon formation, neuronal polarization and dendritogenesis (see Fig. 32) should be correlated as well to topology (e.g. intertwining) and geometry (spatial organization) of both the endogenous extracellular matrix elements and growing environment, giving rise to a shape-like (nanotopography) interaction affecting local and directional growth of cells and their adhesion to the NCN interphase via physical confinement, chemical functionalizion and electric charge [2,12,138,445], as neural cells were suggested to prefer surface-treated larger-scale nanomaterials [490]. Low circularity distributions of neural cells were detected on positively charged (conductive) hydrogels, characteristic of a more linear shape as confronted with electrically neutral hydrogels [472]. Exposure to multi-walled nanotubes tended to unbalance a population of bipolar/rodshaped and amoeboid microglial cell phenotypes towards the amoeboid shape (after 24 h), to produce an almost stationary distribution from 48 h of exposure onwards [427]. It was also noticed that neuronal cells interphased to a substrate or film are inclined to intertwine, bend and curl when they meet a roughness comparable with the length scale of the biological process [491]. An established nanotopography interaction developed when membrane contacts afford focal adhesion sites ranging in $\approx$ $(5 - 200)$ nm (e.g. [492]), while a mean roughness of tens of nm is able to electrically couple nanotubes to neurons [171,493]. Increasing the flexibility of carbon nanotubes, as it is related e.g. to their length, normally increases the surface roughness and favors the formation of a porous network (i.e. a 'sponge') that elicits the adsorption of culture medium proteins. This NCN interaction creates protein concentration gradients along carbon nanotube patterns,

where cells turn out to preferentially grow and neurites are guided by μm paths, even at angles close to 90° [494]. Extracellular proteins are known in fact to promote neuron adhesion to substrates (e.g. laminin, with size $\approx$ 70 nm) [495], their adsorption onto carbon nanotubes being governed by hydrophobic and electrostatic forces [496]. Equilibrium isotherms (e.g. Langmuir's, Fröhlich, Van der Waals, etc.) and thermodynamic stability criteria [497] then may be exploited to deduce adsorption features (e.g. monolayer fractions) and the equilibrium constant, inversely proportional to the rate of attainment of equilibrium in a reversible adsorption/desorption phenomenon [498]. The morphology of carbon nanotubes was suggested as well to regulate stem cell differentiation [7,138,499], nanoparticles being generally able to activate one or more transcription factors increasing the fraction of neurons carrying neurites (e.g. [437,500]). Mesenchymal stem cells cultured on carboxylic single-walled molecules attached preferentially to nanopatterns, spreading and elongating with development of focal adhesion contacts along the pattern axis [501,502]. NCN interphases are most easily studied by means of standalone carbon nanotubes (i.e. linear morphologies) and two-dimensional structures. The former, normally, promotes the generation of directional signalling pathways among cells, the latter tending to grow neurons and dendrites in radial directions [496]. Three dimensional organizations, which are proven to play important effects on NCN interactions [503] and where in-vivo conditions are better inquired, cells seem to develop more branching points and elongation [504]. It is interesting to note that more elongated neuron morphologies offer a better directional impulse conduction and dictate a larger mechanical rigidity of the final tissues [496,505]. Conversely, a lower neuronal branching decreases detrimental effects on nerve regeneration, sets a connection between neuronal network and target innervation and leads to a better axonal pathfinding [506,507]. In comparison with randomly aligned multi-walled molecules, directional effects induced by nanotubes tend to suppress axonal branching [508].

As it may be argued from the previous contents, further length scales may be clearly designed and investigated. For instance, crinkling of carbon nanotube films, by swelling/shrinking nanotube-coated substrates, yielded mesoscale ridges featuring $(300 - 500)$ nm in height, tens of nm in width and a few μm in length [509]. These mesostructures too were beneficial for neuronal development, the growing cells fastly assuming (in 24 h) a highly polarized geometric shape with numerous neuritic protrusions. On the contrary, neurons cultivated on non-crinckly substrates retained a radially symmetric, unpolarized morphology. In multi-walled nanotubes coated with poly-L-lysine (PLL), a positively charged synthetic amino-acid chain, cells displayed neurite growth along the edges of substrate patterns only onto long enough nanotubes [510]. Neurite-pattern bridges extended over 20 m or so to create synaptic links. Over the years, researchers have built up increasingly sophisticated nanomaterials and have moved from carbon nanotube sheets and yarns, endowed with directional orientation [511], to embracing architectures as carbon nanotube scaffolds or layer-by-layer assembled nanotube composites, which can mimic the electric features of nerves, electrically stimulate neurons and/or trigger the differentiation of multipotent cells [512]. To make the usual model examples, anisotropically conductive hydrogel scaffolds (e.g. multi-walled nanotube/chitosan) proved to be effective in neural regeneration and directional outgrowth by action potential transmission between neighbouring neurons, first generated by depolarization/repolarization across axon membranes and afterwards sent across synapses via voltage-gated Ca^{2+} channels [507,513]. Pillar nano/micropatterning (i.e. ridge–groove–ridge) was found to govern the neuronal growth by giving a surface contact guidance to neurite attachment and extra/intracellular protein alignment [514]. On cytocompatible multi-walled nanotube/chitosan scaffolds, hyppocampal neurons (HT-22) acquire elongated geometry, the insertion of graphene nanoplatelet reinforcement driving them to spread radially [496]. NCN interactions within these nanostructures can be even augmented by electric or laser stimulation, enhancing proliferation, neurite length kinetics and differentiation [12]. In testing the joint effect of substrate stiffness, electric conductivity and relative composition on neurite outgrowth phenomena in neuronal PC12 cells cultured on nanocomposite hydrogels, the electric stimulation induced neurite alignments at an angle $(60° - 90°)$ to the applied electric current/field, produced primary and longer neurites $(20 - 46$ %

more) and a larger net outgrowth ($18 - 49$ %) than in non-stimulated control states, where neurites were multiple, shorter and randomly oriented [515]. Hydrogels with high PEG fraction (20 % w/v) and multi-walled nanotubes at 0.1 % w/v displayed the highest total outgrowth and mean neurite length within the whole class of soft and stiff hydrogel materials investigated, to be further increased upon electrical stimulation by 2- and 1.8-fold, respectively. Polyurethane (PU) and silk fibroin were combined with multi-walled nanotubes functionalized with carboxylic group by electrospinning technique. The obtained electrospun scaffold was tested in-vitro with Schwann cells, stimulating their growth, proliferation, and improving axonal growth, neural cell sensitivity and expression [516]. Scaffolds in fact can also mimic the tubular organization of axon and dendrites [138,517].

Overall, nanotopography and physics/chemistry (see the scheme in Fig. 34) should better go hand in hand, i.e. a matching in only one of the two could not return a NCN interface with the expected performance. A good example of this is given by the electric and mechanical coupling. Neuronal
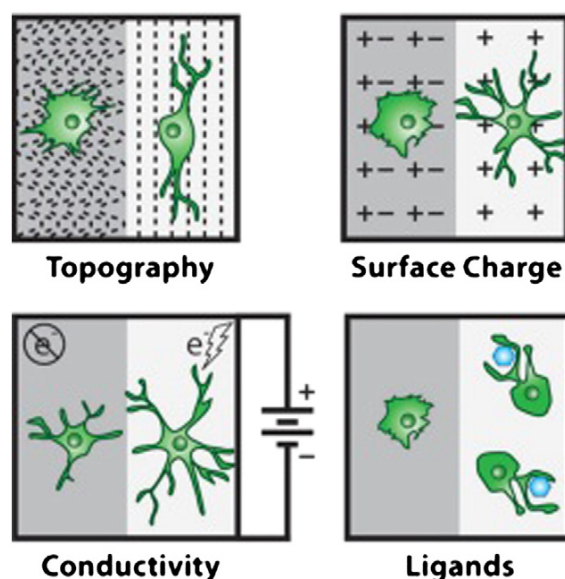

Figure 34. Pictorial representation of some features of carbon nanotube substrates for establishing NCN interactions and assisting cell attachment, growth and function (adapted from ref. [171]).

growth and morphology was confronted on substrates coated to PEI and single-walled nanotubes/PEG films with different thicknesses, thence at different electric conductivities. An akin investigation could be made e.g. by changing the surface-to-volume ratio, greatly reducing the contacting electrical impedance [171]. The outcome anyway was that low conductivity-substrates (i.e. 0.3 S cm^{-1}) could only promote a meaningful neurite extension/outgrowth [518]. In thicker, more conductive films, neurite outgrowth was limited, with an increase in the mean area of cell body and a decrease in the number of growth cones at neurite tips. The latter is known to control neurite outgrowth and synaptic formation [519], while neurite patterns get influenced by molecular signaling (e.g. neurotrophic factors) and tubulin/actin dynamics [465]. In addition, it is interesting to recall the electrical conductivity of nerve tissues was reported in the range ($1.0 \cdot 10^{-2} - 5.7 \cdot 10^{-1}$) S m^{-1} [472]. A further compliance phenomenon stems from mechanics. The outstanding properties of carbon nanotubes (i.e. roughly five times mechanically stronger than steels) descend from a strong interaction between C atoms in sp^2 hybridization. For defectless nanotubes, Young's modulus would be 1.80 TPa in multi-walled molecules and 1.25 TPa in single-walled, to be reduced by the presence of defects to ($10 - 50$) GPa [171]. In spite of that, long enough carbon nanotubes may be nicely twistable and bendable to a large extent, they can deform when in contact to growth cone structures, whereas short nanotubes may be too stiff to support axon extension [520]. A problem thus may stem from the mismatch with

the much softer elasticity range, (0.1–6) kPa,[9] applying to neurons, the central nervous system and brain tissues [452,522], as several cell functions are sensitive to mechanical properties of the cellular environment, especially in the long-term [521,523]. Substrates matching these values elicited higher expression of neuronal early markers (i.e. βIII-tubulin and MAP2, microtubule-associated protein 2) for the maturation of stem cell-derived neurons, with long neurites and presynaptic terminals, while cell morphologies on stiff substrates were bipolar and immature [524]. Also, neural cells turned out to correlate with the substrate stiffness according to the cell type. Hippocampal neurite outgrowth didn't depend on Young modulus, unlike dorsal root ganglion (DRG) neurons that displayed a maximum outgrowth on substrates of stiffness $\sim$ 1 kPa [515,525]. A final point that should be realistically considered, and which certainly raises the complexity of NCN interactions, comes from phenomena ascribed to the formation of a 'protein corona'. In practice, it would stand for what cells (and organs) 'see' or 'perceive' in-vivo, as nanoparticles embedding a biological fluid are normally enshrouded by an adsorbed layer of biomolecules [526] that may further be enriched by other molecular species interacting with it (e.g. lipids [527]). Protein corona affects nanoparticle interactions with the cell environment (e.g. cellular receptors) to even revert their in-vitro behavior [528]. Conceptually, it stands in a certain relation with opsonization and clearance by phagocytic cells [529,530]. When nanoparticles are endowed with a barrier layer inhibiting opsonin adhesion in blood serum, they stay hidden to the phagocytic system [531]. The mechanistic origin of protein corona falls to a large extent into physics and chemistry, like thermodynamics and chemical kinetics [529]. Given the biomolecular compositions and concentrations, concepts like hydrophobicity/hydrophilicity, hydrogen bonding, solvation and van der Waals forces are surely expected to take place in its formation, with possible structural changes in protein chains as well (e.g. in secondary structures, with denaturation). Whatever factor may be involved, it will strongly depend on differences in plasma, serum, species, and circulation but, quite interestingly, corona interactions seems to be not exclusively electrostatic, as there would be little correlation of them with protein charges (i.e. positively charged nanoparticles do not have coronas dominated by negatively charged proteins, and vice versa) (see e.g. [532]).

This research, given so far its lack of predictability, may be told to be still in its infancy, and expected to benefit from advanced computational approaches, likely machine-learning techniques. An outlook of open prospects and questions can be found in [529]. Ad-hoc theoretical methods and nanostructural design are desired to control protein corona formations, i.e. what and how proteins will interact to a given nanoparticle surface/functionalization. To report some example of basic carbon nanotube-protein interaction, one may resume amyloid diseases and remind that nanomaterials can disturb the β-sheet conformation of amyloid monomer, suppress or slow down oligomer and protofibril kinetics, and even disassemble pre-existing fibrils and plaques [379]. Nanotubes were found as well to enhance nucleation of protein fibrillization. Molecular dynamics simulations (MD), an efficient tool to inquiry carbon nanotube-protein interactions at the single molecule level, highlighted in fact that single-walled molecules inhibit amyloid Aβ_{16-22} peptide and full-length Aβ fibrillization by destabilizing the β-sheet structure through hydrophobic forces and π–stacking interactions [533]. Carbon nanotubes own conjugated π-electron structures, thus a polypeptide with aromatic moieties could generally interplay with them via π–π stacking forces. They were also established to interact with amyloid Aβ_{25-35} oligomers to form β-barrel structure by curving Aβ_{25-35} β-sheets and to interfere with fibril formation by affecting the kinetics of intersheet H-bond backbones [534]. Adsorption mechanisms of Aβ_{1-42} on the single-walled nanotube surface initiated by interactions with the hydrophobic core while hydrophobicity was generally governing the collapse of the amyloid chain [535,536]. Similarly, and still by means of MD computations, the interaction of single-walled molecules with Aβ peptides (whose misfolding was linked to Alzheimer's disease) turns out to compete with Aβ–Aβ's, preventing

---

[9]   With the critical rupture strength of brain tissues being $\sim$ 3 kPa [521].

the formations of intra/inter-chain H-bonds, of α-helix and β-sheet structures of the Aβ trimer, and increasing the likelihood of random-coil configurations [537].

In conclusion to Section 8, owing to the many factors that can participate in here, it is tough to draw an unequivocal opinion on the in-vitro versus in-vivo neuronal biocompatibility of carbon nanotubes, especially if one regards their long-term fate in-vivo and the lack of a precise correlation between in-vitro and in-vivo biological responses [12]. To devise procedures for assessing, confronting, reducing and possibly eliminating nanotoxicity remains an open research area, intimately connected to a quantitative/mechanistic understanding of how carbon nanotubes and other nanostructures interact with neuronal and other biological systems. Investigating further by more mechanistic means on dosing, time- and exposure routes (injection, ingestion, inhalation), physical and surface chemistry (size, distribution, aggregation/adsorption, functionalization) in nanoparticle release phenomena (i.e. dispersed in physiological circulating fluids) are only a few examples in which theory, experiment, pre-clinical and clinical protocols meet [12,385]. For example, the precise nanoparticle amount accumulating in a single neuron cell after circulating through the body, penetrating Bbb and eluding the astrocyte uptake is still unpredictable, as it is influenced by so many factors like protein corona [528]. Very good results (less citotoxicity) on NCN interphases had already come from studying carbon nanotubes trapped within a network (e.g. polymer gels) and/or developing from a surface (substrate or scaffold), despite in-vivo environments are very rough and demanding also for implantation techniques [329]. Continuing with the analysis of three-dimensional media, where NCN interactions may find platforms for a systematic study of many-body and/or collective behaviors, will shed further light on morphological and morphogenetic views. Theoretical physics and chemistry disciplines, for their part, offer rather effective tools that could also find an outlet in nanosciences. Mean field and renormalization theories in fact require an element of randomness (in a way, what is deterministically unknown), various length and/or time scales (certainly applicable to neuronal or NCN interactions) and a bare quantity (e.g. membrane potential, synaptic conductance, etc.) [538], to be rescaled/renormalized into an effective counterpart that depends in turn on a relevant spacetime scale [539].

9. Drug Delivery to Neurons

Many drugs do not accomplish the prerequisites to cross Bbb (i.e. on size, lipophilicity, etc.), thus various protocols were inspected, spamming from more or less invasive administrations to non-invasive drug modifications with larger permeability and/or coupled with compounds to overcome the blood-brain barrier (Bbb). [362,378]. When nanoparticles are adopted, for a safe and responsive use in living systems, they need to be biocompatible/biodegradable (i.e. non-toxic, non-inflammatory, non-immunogenic) and modified at their surface by materials or biomaterials carrying a functional/conjugate group to target/enter Bbb and display a suitable half-life in blood (e.g. by eluding the reticulo-endothelial system). Insulin, transferrin, apolipoprotein E, 2-macroglobulin are examples of chemicals transported by receptor-mediated endocytosis, thus they can be adopted to improve the nanoparticle surface for an efficient Bbb entry [540]. Other suitable ligands are polyethylene glycol (PEG), lactoferrin, peptide angiopep-2 (ANG) and thiamine. In general, for a nanocarrier to act as a delivery carrier to the central nervous system, it should i.) penetrate one or some membrane layers (mucosa, epithelium, endothelium), ii.) cross Bbb or travel by nerve terminals; iii.) diffuse via the neuronal or glial cytoplasmic membrane, and iv.) break free from encapsulation in organelles [382]. Another aspect to be mentioned is the assessment of the ratio between biokinetic rates in relation to the intended aims. A rapid clearance of nanotubes lowers their potential toxicity but may be a disadvantage for delivery purposes due to a smaller circulation time, as it is set by their rapid excretion. This may be the case e.g. of nanotubes functionalized with chemical groups reducing the blood half-life to a meaningful extent [541]. On the other hand, for fast irreversible internalization processes, cargo molecules could need to be quickly released.
Resorting to nanoparticles like carbon nanotubes as drug carriers to neurons and the nervous system

[542,543] (see Fig. 35) has become over the years an important strategy e.g. for the release of active chemicals at specific sites or for direct interaction with disease-related biomolecules [379], and is based on the outstanding properties (geometric, electric, etc.) partly already addressed in the former sections. Normally, carbon nanotubes can load a molecule (e.g. a drug) via physical adsorption by non-covalent
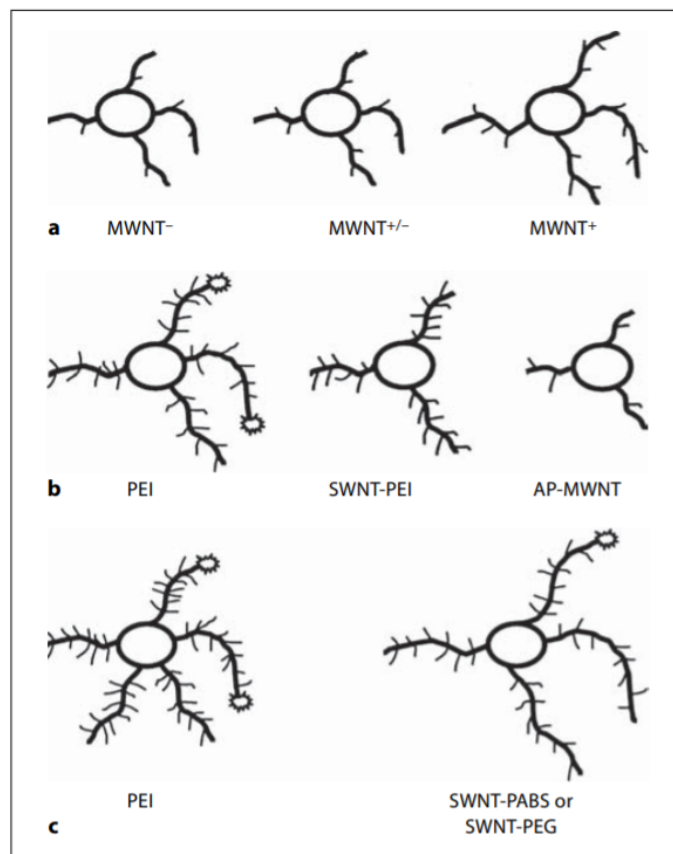

Figure 35. Carbon nanotube effects on neurite outgrowth and growth cones. (a) Surface charge of multi-walled molecules versus neuron outgrowth and branching pattern. (b) Single-walled molecules/ polyethyleneimine (PEI) graft copolymer substrate fosters neurite outgrowth and branching that are intermediate to those displayed by PEI and as prepared multi-walled nanotubes (AP-MWNTs), prompting that neuronal growth may be differentially sensitive to substrate qualities. (c) Adding watersoluble graft copolymers such as single-walled molecules/poly-m-aminobenzene sulfonic acid (SWNT-PABS) and single-walled molecules/polyethylene glycol (SWNT-PEG) enhances the length of the selected neuronal processes and reduces the growth cone number (adapted from ref. [543]).

hydrophobic interaction, encapsulation, surface functionalization, and by other carriers with nanotubes serving as release controllers [544]. The attachment (also covalent) of chemical groups (e.g. lipids, DNA and various peptides) then is useful to improve some features, among which biocompatibility is one of the most important in drug delivery to living cells like neurons. Carbon nanotubes are intrinsically toxic, this being linked to the ability of fullerenes to induce lipid peroxidation, to hydrophobicity, aggregation propensity and interaction with cell membranes, as it was already discussed in subsection 8.3. Further evidences suggest that the presence of metal ion impurities drive fullerenes to generate free radicals. Interestingly, in vitro and in-vivo experiments demonstrate that, in cytoplasm, single-walled carbon nanotubes tend to be actively transported inside lysosomes but not in mithocondria, unless their concentration overcomes a given threshold value, estimated in mice to be $\approx$ 300 mg/kg (mice). This is a relevant aspect because the increase of dangerous ROS would mostly be triggered in mitochondria. A simple decrease of their dosage could therefore prevent from the appearance of toxic effects as 'pharmacological' organelles (lysosomes), and not 'toxicological' ones (mitochondria), would only

be affected by the administration of single-walled nanotubes. Usually, 300 mg/kg is quite above the pharmacological active dose for an effective drug release to neurons,[10] therefore, dose reduction may represent a simple yet reliable manner to improve biocompatibility of carbon nanotubes. To combine this procedure with purification and chemical modifications would then guarantees an even better bioactivity. On the other hand, the enzymatic degradation (i.e. peroxidases) that nanotubes may undergo in extracellular space, immune and glia cells [446] reduced the concerns about their use in neuron therapies. Apart from the regeneration of peripheral nervous system [399], carbon nanotubes may find applications in treating neuro-inflammation (a common aspect of many neurodegenerative disorders) [545] and in the realization of photo-triggered nano-delivery systems [546]. Neuron stem cells moreover can grow and differentiate on carbon nanotube-containing substrates [547]. On the other hand, the enzymatic degradation (i.e. peroxidases) that nanotubes may undergo in extracellular space, immune and glia cells [446] reduced the concerns about their use in neuron therapies. These, as well as further aspects, were discussed in the former section 8.

As we discussed in subsection 8.2, a most intriguing aspect of carbon nanotubes which may be relevant to drug delivery resides in their high efficiency to cross the cellular membrane according to a passive, endocytosis-independent, mechanism [548]. Probably, during uptake, they dispose perpendicularly to the membrane and, by acting as nanoneedles, can penetrate the lipid bilayer without provoking cell death. Dynamic simulations involving amphiphilic nanotubes and experimental techniques (nano-tubes spearing, SEM images and near-infrared fluorescence) support such a mechanism [548]. Length is as well a crucial feature for crossing cellular membranes. Short nanotubes (generally < 1 μm) structures rapidly enter the cytoplasm and nucleus of rat hippocampal cells and PC12 cellular line (neuron progenitors). Other notable carbon nanotube features (namely, high electrical conductivity, mechanical strength, excellent chemical stability, and high surface-to-volume ratio) identify them as promising candidates for the realisation of nanosystems devoted to a targeted drug delivery to neurons. All such characteristics make the design and realization of carbon nanotube-based delivery systems feasible, enabling a precise control of drug transport and a fast response to external stimuli such as pH, temperature, light, magnetic and electrical field [399,546]. For example, electrical conductivity can guide the growth of nerve cells and promote myelination, providing with a new strategy for clinical peripheral nerve regeneration and functional reconstruction [549]. Carbon nanotubes may mimic [550] but also influence the functioning of neuronal ion channels, i.e. transmembrane proteins mediating the passive transport of ions, and involved in a broad range of basic biological processes such as excitation, signalling, secretion, adsorption [1]. Probably, nanotubes sit in or on top of channel pores and interrupt ion fluxes and channel transitions from open to inactive states. Interestingly, electrochemically neutral unmodified single-walled nanotubes with rather small diameter (0.9 nm) displayed a great blockade capability (e.g. on K^+ channels) by a concentration-dependent reversible mechanism, and large-diameter multi-walled nanotubes seemingly showed none [444,542]. Finally, while the chemical stability of carbon nanotubes prevents from transformation into undesirable (toxic) metabolic sub-products, their high surface/volume ratio greatly enhance the effect of surface chemical modifications, prompting them as promising tools for developing specific approaches to different types of injuries in the central nervous system [399]. It was already emphasized how functionalization chemistry opened new horizons in the study of biomedical applications of carbon nanotubes [548]. For instance, the ability of amine-functionalized carbon nanotubes to form stable supramolecular complexes with nucleic acids via electrostatic interactions, can pave the way to different prospects, among which gene therapy, genetic vaccination and immune-potentiation enhancement deserve to be mentioned explicitly.

To sum up, the above considerations and evidences support the idea that carbon nanotubes are very

---

[10] In case of single-walled nanotubes/acetylcholine complex, $25 - 50$ mg/kg is the optimum dosage release to mice neurons.

good candidates for becoming reliable and effective drug delivery systems, as they accomplish the paradigm on which modern concepts of personalized and precision medicine rely.

9.1. Applications

In the last decade, applications of carbon nanotubes to drug delivery have increased so a lot that it is hard, if not impossible, mentioning and commenting on every aspect. For simplicity, one may single out two main strategies. A first regards their direct use, and conceives nanotubes as carriers devoted to transport the desired drugs into cell cytoplasm and/or nucleus [542,545,548], the second is about an indirect use of them. In fact, in the last case, carbon nanotubes serve to modify some of the properties of the delivery system (e.g. such as mechanical strength or electrical conductivity) which, in turn, may affect the release kinetics by modifying the delivery structure and mechanism. In addition, surface-modifications of nanotubes can be helpful to increase the propensity of cells to adhere to the delivery system/scaffold. In other words, they can favour interaction and information exchanges between living (cells) and nonliving matter.

One of the most appealing usage of carbon nanotubes, belonging to the first strategy, is connected with the oral administration of acetylcholine (ACh) [542]. It is a natural transmitter of the cholinergic nervous system, allowing signal transmission between neurons and, thus, lying at the basis of functional activities of neurons such as thinking, memory and learning. As Alzheimer (AD) is a neurodegenerative disease induced by the lack of ACh (neurons fail to correctly synthesize it), ACh administration should be the best treatment of AD, but unfortunately the strong positive charges carried by such a molecule render its delivery into the brain impossible since they hinder the crossing Bbb. In order to solve this problem, a single-walled nanotube/ACh adsorption complex was designed by incubating the two compounds together [542]. Then, the authors induced dementia in mice by an intraperitoneal single dose injection of kainic acid (KA, 20 mg/kg), a neurotoxic amino-acid which is damaging neurons. For evaluating KA effects, mice learning and memory capabilities were tested before injection and after 24 h. While mice belonging to the control group were not treated with the above complex, those belonging to that therapeutic received, after 20 h from KA injection, the single-walled nanotube/ACh complex via gastro gavage ($20 - 50$ mg/kg, corresponding to $4 - 10$ mg/kg ACh). Experimental evidences demonstrated that not only the carbon nanotube-based complex can be absorbed by gastrointestinal mucosa, but it can even get to hippocampal neurons. In fact, learning and memory abilities of the treated mice were similar to those untreated, whereas the control group clearly revealed a learning and memory deficit. Interestingly, a separate administration of single-walled molecules and ACh did not provoke any effect on the cognitive ability.

Another interesting application, falling into the second strategy, is that proposed in refs. [499, 551], where the rat sciatic nerve regeneration was dealt with by releasing different drugs (erythropoietin or curcumin) from a poly-lactic acid (PLA)/multi-walled nanotube or poly-L-lactic acid (PLLA)/multi-walled nanotube guidance conduits containing Schwann cells (SCs). One of the most effective methods, aimed at the treatment of peripheral nerve system (PNS) injuries (microsurgical nerve autographs), is not free in fact from issues such as the limited accessibility of donor sites and the loss of sensation in donor and recipient areas. To this purpose, use of synthetic conduits, built up by proper biomaterials and containing pro-regenerative substrates (stem cells, growth factors), seems to furnish a good alternative. Practically, the conduit hosted the proximal and distal end of nerve stumps into its respective ends, in order to improve and guide the development of the two stumps (see Fig. 36). Aiming to increase the system performance, the inner part of the conduit was filled by a fibrin hydrogel containing SCs. These cells cover a positive role in axonal regeneration, as they secrete neurotrophic factors enhancing the survival of injured neurons, their presence induce considerable macrophage infiltration to the injured nerve, which provides the axonal growth with a favourable environment, and, finally, they release nerve growth factors (NGFs) [551]. Survival and health of SCs was guaranteed by addition of different drugs (such as curcumin and erythropoietin) inside the fibrin gel. While the electrical conductivity of hollow conduit was realized by electrospinning of a PLLA solution containing
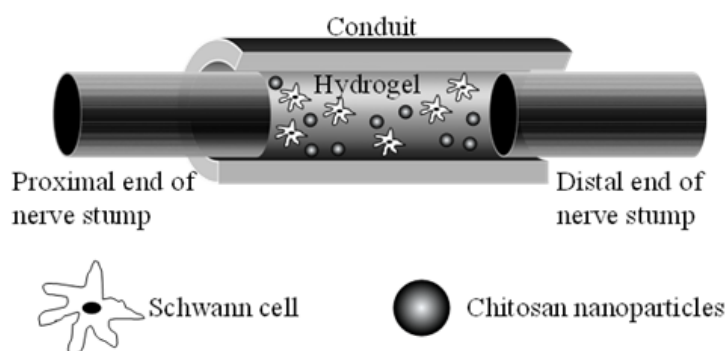
Figure 36. Scheme of proximal and distal ends of nerve stumps inserted in a conduit filled by a fibrin hydrogel containing Schwann cells and chitosan nanoparticles loaded by curcumin, whose release improved the SC survival.

multi-walled carbon nanotubes bearing on their surface different oxygen-containing groups (mainly carboxyl groups), a curcumin-controlled release was achieved by addition of chitosan nanoparticles inside the fibrin hydrogel [551]. Efficacy and reliability of the proposed approach was studied by a random subdivision of rats into seven groups. Group I represented the positive control (rats without any lesion and treatment), group II was constituted by rats injured with 8 mm nerve gap and treated by nerve autograft, group III was the negative control group (rats injured with 10 mm nerve gap and without any following treatment) while other four groups comprised rats injured with 10 mm nerve gap and treated with different formulations, containing or not containing curcumin and SCs. The evaluation of motor functional recovery of injured rats was realized by an account of the value taken by the sciatic function index (SFI). Experiments showed that, after 2 months, there was no significant difference between values associated with group II (autograft samples) and group VII (rats treated with fibrin hydrogel containing curcumin and SCs).

In another study [552], carbon nanotubes act on NGF release kinetics from collagen-nanotube composite matrices. Such materials were realized by mixing, in different proportions, a collagen (type IV from bovine Achilles tendon) solution, containing the desired NGF amount, with an aqueous suspension of surface-functionalized (carboxylic groups) multi-walled molecules (30 nm diameter, 20 μm length). The final product, a dried thin film ($\approx$ 100 mm thick), then was heated to produce crosslinks between collagen chains and carboxylic groups. While collagen was adopted to enhance biocompatibility, functionalized multi-walled carbon nanotubes were aimed to increase the electrical conductivity of the film. It is worthwhile to report that NGF release from the film was ruled by passive diffusion, and the film electrical stimulation considerably increased its release rate. On the other hand, this work did not explain in sufficient depth the reasons behind the release rate enhancement upon electrical stimulation. In our opinion, two possible causes (not mutually exclusive) can be invoked. A first may be an increased NGF mobility upon the electrical field, the second instead being about a possible modification of carbon nanotube-collagen networks, still driven by the electrical field. Should the network modification be permanent, i.e. still present after the electrical stimulation removal, the new structural network characteristics could be detected by means of different techniques such as Low Field Nuclear Magnetic Resonance [553], which may help to discern among the reasons for such an enhanced kinetic rate. Finally, it was also observed that an increase in NGF release stimulated a development of PC12 (neuron progenitors) cells cultured on the film.

The above study, stressing the importance of carbon nanotubes in substrates used for cell cultivation, represents a sort of starting point for realizing scaffolds aimed at neurons culture. For example,

a multi-walled nanotube/agarose scaffold for neuron growth[11] under electrical stimulation was proposed in [549]. This work demonstrated the electroconductive neural scaffold resembles the native three-dimensional extracellular matrix which provides guidance channels to nerve cells. It was shown furthermore that the applied electrical stimulation can recreate a physiological neuronal activity, promoting the directional growth of nerve cells, a very important aspect in regeneration of peripheral nerves. It is easy to understand the incorporation of particular drugs, such as NGF itself, could ameliorate and optimize the scaffold performance. In this light, an electrospun catalpol-loaded composite nanofibrous scaffolds was realized to get stem cells from human adipose cells [554]. Catalpol, an iridoid glycoside isolated from the roots of traditional Chinese medical herb Rehmannia, and acting as neurogenesis inducer, is released from a fibrous scaffold formed by poly(lactic-co-glycolic acid) (PLGA), silk fibroin (SF) and multi-walled carbon nanotubes. A higher percentage of cells ($> 60\%$) with neuronal phenotype then was detected on catalpol-loaded nanofibers as compared with control groups.

9.2. Further on Cytotoxicity and Drug Delivery

As it was discussed throughout the former section, a point which is primarily influencing the application of carbon nanotubes in-vivo, such as drug delivery for the treatment and diagnosis of diseases of the central nervous system, is given by their intrinsic and ultimate cytotoxicity. We have seen how this issue may be complex, depending on the biological environment, and sometimes controversial, with several studies documenting toxic effects and others suggesting very low or even insignificant toxicity (see e.g. [555]). Such an apparent contradiction was explained by reminding that different types of nanotubes, distinct preparation, purification, evaluation methods, and even different exposure conditions were inspected in the literature [556]. Although a definitive systematic approach to this issue does not exist yet, it has been interesting to see how researchers coped with it over the years. In particular, we remind that functionalization with PEG molecules is one of the most common strategies to diminish the toxicity of nanotubes (see also [557]). In targeted drug delivery (methotrexate or siRNa) for rheumatoid arthritis, usage of PEG-functionalized carbon nanotubes furthermore decreases the well-known methotrexate toxicity and guarantees its selective accumulation in inflamed joints within a serum-transfer mouse model [558]. In a further study, of computational nature, a significant toxicity reduction was reached by transporting carnosine dipeptide, an anti-ageing compound and neuron protection in relation to Alzheimer's dementia [559]. Free energy simulations conducted therein revealed in fact that functionalization with such a molecule was beneficial for the solubility of nanotubes. Another investigation [560] focused the attention on the belief that carbon nanotubes do not undergo in-vivo degradation, making them bio-persistent and ultimately akin to asbestos fibres, which are sadly famous for their ability of triggering inflammation and, eventually, lung cancer (mesothelioma) [561]. Conversely, an enzyme that is present in white blood cells (myeloperoxidase) was suggested to be able of converting nanotube molecules into water and carbon dioxide [562].
It is known alongside that a number of workers, researching on drug delivery procedures in anticancer therapies, remarked that in-vivo applications of carbon nanotubes still require a deeper knowledge of their pharmacological/toxicological impact in humans, before clinical trials or a routine practice may be definitely recommended (see e.g. [563]). This precaution partly relies on the formerly discussed ability of nanotube molecules of accumulating in tissues (e.g. heart, spleen, brain), where they might elicit long-term oxidative stress and damage healthy cells. On the other hand, their high potentialities - not only for administration of synthetic drugs such as anticancer (e.g. docetaxel, doxorubicin, methotrexate, paclitaxel), anti-inflammatory and steroids, but also to carry genetic materials (plasmid DNA, micro-RNA, small interfering RNA (siRNA)) [564] - is there for all to see, and remain. A most important reading key for this debate likely resides on the strong individual character of (real) carbon

---

[11] RSC96 - neuronal Schwan cells from rattus norvegicus and PC12 cells.

nanotubes, not infrequently overlooked to some extent. Owing to the various intensive and extensive variables, previously reported to influence the biological response (geometric features, dose, time of exposure, purity, presence of chemical agents bound to their surface, etc.), it may be tough in fact to reliably isolate the effects of each of them [556].

10. Conclusive Remarks

The properties of carbon nanotube materials are outlined in the greatest possible generality in view of a mechanistic inquiry into their effect on the biological activity of neuronal cells, including an outlook on drug delivery. Several frameworks were described, in particular to let percolation, electron and electrochemical processes better emerge. Thermal, mechanical and chemical properties were also discussed, including a comparison among materials of different molecular composition or nanostructure, as well as the processing histories of nanomaterials and substrates. The main biological frameworks (blood-brain barrier and crossing mechanisms, nanotoxicity and biofunctionalization) are gathered in the second part of the review.

1.   Yang, Z.; Liu, Z.W.; Allaker, R.P.; Reip, P.; Oxford, J.; Ahmad, Z.; Ren, G. A review of nanoparticle functionality and toxicity on the central nervous system. *J. R. Soc. Interface* **2010**, *7*, S411–S422. doi:10.1098/rsif.2010.0158.focus.

2.   Fabbro, A.; Prato, M.; Ballerini, L. Carbon nanotubes in neuroregeneration and repair. *Adv. Drug Deliv. Rev.* **2013**, *65*, 2034—2044. doi:10.1016/j.addr.2013.07.002.

3.   Mattson, M.; Haddon, R.; Rao, A. Molecular Functionalization of Carbon Nanotubes and Use as Substrates for Neuronal Growth. *J. Mol Neurosci.* **2000**, *14*, 175–82. doi:10.1385/JMN:14:3:175.

4.   Cellot, G.; Cilia, E.; Cipollone, S.; Rancic, V.; Sucapane, A.; Giordani, S.; Gambazzi, L.; Markram, H.; Grandolfo, M.; Scaini, D.; Gelain, F.; Casalis, L.; Prato, M.; Giugliano, M.; Ballerini, L. Carbon nanotubes might improve neuronal performance by favouring electrical shortcuts. *Nat. Nanotechnol.* **2009**, *4*, 126–33. doi:10.1038/nnano.2008.374.

5.   Kotov, N.A.; Winter, J.O.; Clements, I.P.; Jan, E.; Timko, B.P.; Campidelli, S.; Pathak, S.; Mazzatenta, A.; Lieber, C.M.; Prato, M.; Bellamkonda, R.V.; Silva, G.A.; Kam, N.W.S.; Patolsky, F.; Ballerini, L. Nanomaterials for Neural Interfaces. *Adv. Mater.* **2009**, *21*, 3970–4004. doi:10.1002/adma.200801984.

6.   Rago, I.; Rauti, R.; Bevilacqua, M.; Calaresu, I.; Pozzato, A.; Cibinel, M.; Dalmiglio, M.; Tavagnacco, C.; Goldoni, A.; Scaini, D. Carbon Nanotubes, Directly Grown on Supporting Surfaces, Improve Neuronal Activity in Hippocampal Neuronal Networks. *Adv. Biosyst.* **2019**, *3*, 1800286. doi:10.1002/adbi.201800286.

7.   Kumar, R.; Aadil, K.; Ranjan, S.; Kumar, V.B. Advances of nanotechnology and nanomaterials based strategies for neural tissue engineering. *J. Drug Deliv. Sci. Tech.* **2020**, *57*, 101617. doi:10.1016/j.jddst.2020.101617.

8.   Negri, V.; Pacheco-Torres, J.; Calle, D.; López-Larrubia, P. Carbon Nanotubes in Biomedicine. *Top. Curr. Chem.* **2020**, *378*, Art.N. 15. doi:10.1007/s41061-019-0278-8.

9.   Wang, X.; Bukoreshtliev, N.; Gerdes, H.H. Developing Neurons Form Transient Nanotubes Facilitating Electrical Coupling and Calcium Signaling with Distant Astrocytes. *PLoS One* **2012**, *7*, e47429. doi:10.1371/journal.pone.0047429.

10.   Lovat, V.; Pantarotto, D.; Lagostena, L.; Cacciari, B.; Grandolfo, M.; Righi, M.; Spalluto, G.; Prato, M.; Ballerini, L. Carbon Nanotube Substrates Boost Neuronal Electrical Signaling. *Nano Lett.* **2005**, *5*, 1107–1110. doi:10.1021/nl050637m.

11. Fabbro, A.; Bosi, S.; Ballerini, L.; Prato, M. Carbon Nanotubes: Artificial Nanomaterials to Engineer Single Neurons and Neuronal Networks. *ACS Chem. Neurosci.* **2012**, *3*, 611–618. doi:10.1021/cn300048q.

12. Singh, S.; Mishra, S.; Juha, S.; Pramanik, M.; Padmanabhan, P.; Gulyás, B. Nanotechnology Facilitated Cultured Neuronal Network and Its Applications. *Int. J. Mol. Sci.* **2021**, *22*. doi:10.3390/ijms22115552.

13. Cellot, G.; Toma, F.M.; Kasap Varley, Z.; Laishram, J.; Villari, A.; Quintana, M.; Cipollone, S.; Prato, M.; Ballerini, L. Carbon Nanotube Scaffolds Tune Synaptic Strength in Cultured Neural Circuits: Novel Frontiers in Nanomaterial–Tissue Interactions. *J. Neurosci.* **2011**, *31*, 12945–12953. doi:10.1523/JNEUROSCI.1332-11.2011.

14. Pampaloni, N.P.; Scaini, D.; Perissinotto, F.; Bosi, S.; Prato, M.; Ballerini, L. Sculpting neurotransmission during synaptic development by 2D nanostructured interfaces. *Nanomedicine* **2018**, *14*, 2521–2532. doi:10.1016/j.nano.2017.01.020.

15. Massobrio, P.; Massobrio, G.; Martinoia, S. Interfacing Cultured Neurons to Microtransducers Arrays: A Review of the Neuro-Electronic Junction Models. *Front. Neurosci.* **2016**, *10*, 282. doi:10.3389/fnins.2016.00282.

16. Tang, C.; Xie, S.; Wang, M.; Feng, J.; Han, Z.; Wu, X.; Wang, L.; Chen, C.; Wang, J.; Jiang, L.; Chen, P.; Sun, X.; Peng, H. A fiber-shaped neural probe with alterable elastic moduli for direct implantation and stable electronic–brain interfaces. *J. Mater. Chem. B* **2020**, *8*, 4387–4394. doi:10.1039/D0TB00508H.

17. Sangwan, V.; Hersam, M. Neuromorphic nanoelectronic materials. *Nat. Nanotechnol.* **2020**, *15*, 517–528. doi:10.1038/s41565-020-0647-z.

18. Jacobs, C.B.; Vickrey, T.L.; Venton, B.J. Functional groups modulate the sensitivity and electron transfer kinetics of neurochemicals at carbon nanotube modified microelectrodes. *Analyst* **2011**, *136*, 3557–3565. doi:10.1039/C0AN00854K.

19. Sanghavi, B.J.; Wolfbeis, O.S.; Hirsch, T.; Swami, N.S. Nanomaterial-based electrochemical sensing of neurological drugs and neurotransmitters. *Microchi. Acta* **2015**, *182*, 1–41. doi:10.1007/s00604-014-1308-4.

20. Bala, K.; Sharma, D.; Gupta, N. Carbon-Nanotube-Based Materials for Electrochemical Sensing of the Neurotransmitter Dopamine. *ChemElectroChem* **2019**, *6*, 274–288. doi:10.1002/celc.201801319.

21. Zhang, A.; Lieber, C.M. Nano-Bioelectronics. *Chem. Rev.* **2016**, *116*, 215–257. doi:10.1021/acs.chemrev.5b00608.

22. Gupta, S.; Murthy, C.; Prabha, C.R. Recent advances in carbon nanotube based electrochemical biosensors. *Int. J. Biol. Macromol.* **2018**, *108*, 687 – 703. doi:10.1016/j.ijbiomac.2017.12.038.

23. Oh, J.W.; Yoon, Y.W.; Heo, J.; Yu, J.; Kim, H.; Kim, T.H. Electrochemical detection of nanomolar dopamine in the presence of neurophysiological concentration of ascorbic acid and uric acid using charge-coated carbon nanotubes via facile and green preparation. *Talanta* **2016**, *147*, 453 – 459. doi:10.1016/j.talanta.2015.10.020.

24. Sun, Y.; He, K.; Zhang, Z.; Zhou, A.; Duan, H. Real-time electrochemical detection of hydrogen peroxide secretion in live cells by Pt nanoparticles decorated graphene–carbon nanotube hybrid paper electrode. *Biosens. Bioelectron.* **2015**, *68*, 358 – 364. doi:10.1016/j.bios.2015.01.017.

25. Ensafi, A.A.; Karimi-Maleh, H. Modified multiwall carbon nanotubes paste electrode as a sensor for simultaneous determination of 6-thioguanine and folic acid using ferrocenedicarboxylic acid as a mediator. *J. Electronal. Chem.* **2010**, *640*, 75 – 83. doi:10.1016/j.jelechem.2010.01.010.

26. Yang, C.; Trikantzopoulos, E.; Jacobs, C.B.; Venton, B.J. Evaluation of carbon nanotube fiber microelectrodes for neurotransmitter detection: Correlation of electrochemical performance and surface properties. *Anal. Chim. Acta* **2017**, *965*, 1 – 8. doi:10.1016/j.aca.2017.01.039.

27. Cho, Y.; Borgens, R. The effect of an electrically conductive carbon nanotube/collagen composite on neurite outgrowth of PC12 cells. *J. Biomed. Mater. Res. A* **2010**, *95*, 510–7. doi:10.1002/jbm.a.32841.

28. Barsan, M.M.; Ghica, M.E.; Brett, C.M. Electrochemical sensors and biosensors based on redox polymer/carbon nanotube modified electrodes: A review. *Anal. Chim. Acta* **2015**, *881*, 1 – 23. doi:10.1016/j.aca.2015.02.059.

29. Liu, S.; Zhao, Y.; Hao, W.; Zhang, X.D.; Ming, D. Micro- and nanotechnology for neural electrode-tissue interfaces. *Biosens. Bioelectron.* **2020**, *170*, 112645. doi:10.1016/j.bios.2020.112645.

30. Yeh, S.R.; Chen, Y.C.; Su, H.C.; Yew, T.R.; Kao, H.H.; Lee, Y.T.; Liu, T.A.; Chen, H.; Chang, Y.C.; Chang, P.; Chen, H. Interfacing Neurons both Extracellularly and Intracellularly Using CarbonNanotube Probes with Long-Term Endurance. *Langmuir* **2009**, *25*, 7718–7724. doi:10.1021/la900264x.

31.   Abidian, M.R.; Corey, J.M.; Kipke, D.R.; Martin, D.C. Conducting-Polymer Nanotubes Improve Electrical Properties, Mechanical Adhesion, Neural Attachment, and Neurite Outgrowth of Neural Electrodes. *Small* **2010**, *6*, 421–429. doi:10.1002/smll.200901868.

32.   Luo, X.; Weaver, C.L.; Zhou, D.D.; Greenberg, R.; Cui, X.T. Highly stable carbon nanotube doped poly(3,4-ethylenedioxythiophene) for chronic neural stimulation. *Biomaterials* **2011**, *32*, 5551 – 5557. doi:10.1016/j.biomaterials.2011.04.051.

33.   Malvindi, M.A.; Carbone, L.; Quarta, A.; Tino, A.; Manna, L.; Pellegrino, T.; Tortiglione, C. Rod-Shaped Nanocrystals Elicit Neuronal Activity In Vivo. *Small* **2008**, *4*, 1747–1755. doi:10.1002/smll.200800413.

34.   Ciofani, G.; Danti, S.; D'Alessandro, D.; Ricotti, L.; Moscato, S.; Bertoni, G.; Falqui, A.; Berrettini, S.; Petrini, M.; Mattoli, V.; Menciassi, A. Enhancement of Neurite Outgrowth in Neuronal-Like Cells following Boron Nitride Nanotube-Mediated Stimulation. *ACS Nano* **2010**, *4*, 6267–6277. doi:10.1021/nn101985a.

35.   Ciofani, G.; Raffa, V.; Vittorio, O.; Cuschieri, A.; Pizzorusso, T.; Costa, M.; Bardi, G. In Vitro and In Vivo Biocompatibility Testing of Functionalized Carbon Nanotubes. *Method. Mol. Biol.* **2010**, *625*, 67–83. doi:10.1007/978-1-60761-579-8-7.

36.   Vankoningsloo, S.; Piret, J.P.; Saout, C.; Noel, F.; Mejia, J.; Zouboulis, C.; Delhalle, J.; Lucas, S.; Toussaint, O. Cytotoxicity of multi-walled carbon nanotubes in three skin cellular models: Effects of sonication, dispersive agents and corneous layer of reconstructed epidermis. *Nanotoxicology* **2010**, *4*, 84–97. doi:10.3109/17435390903428869.

37.   Haniu, H.; Saito, N.; Matsuda, Y.; Kim, Y.A.; Park, K.; Tsukahara, T.; Usui, Y.; Aoki, K.; Shimizu, M.; Ogihara, N.; Hara, K.; Takanashi, S.; Okamoto, M.; Ishigaki, N.; Nakamura, K.; Kato, H. Effect of dispersants of multi-walled carbon nanotubes on cellular uptake and biological responses. *Int. J. Nanomed.* **2011**, *6*, 3295–307. doi:10.2147/IJN.S26573.

38.   Kim, J.; Sung, J.; Song, K.; Lee, J.H.; Kim, S.; Lee, G.; Ahn, K.H.; Lee, J.; Shin, J.; Park, J.; Yu, I.J. Persistent DNA Damage Measured by Comet Assay of Sprague Dawley Rat Lung Cells after Five Days of Inhalation Exposure and 1 Month Post-Exposure to Dispersed Multi-Wall Carbon Nanotubes (MWCNTs) Generated by New MWCNT Aerosol Generation System. *Toxicol. Sci.* **2012**, *128*, 439–48. doi:10.1093/toxsci/kfs161.

39.   Zhang, Y.; Xu, Y.; li, Z.; Chen, T.; Burks, S.; Howard, P.; Paule, M.; Slikker, W.; Watanabe, F.; Mustafa, T.; Biris, A.; Ali, S. Mechanistic Toxicity Evaluation of Uncoated and PEGylated Single-Walled Carbon Nanotubes in Neuronal PC12 Cells. *ACS Nano* **2011**, *5*, 7020–33. doi:10.1021/nn2016259.

40.   Chen, L.; Hu, P.; Zhang, L.; Huang, S.; Luo, L.; Huang, C. Toxicity of graphene oxide and multi-walled carbon nanotubes against human cells and zebrafish. *Sci. China Chem.* **2012**, *55*, 2209–2216. doi:10.1007/s11426-012-4620-z.

41.   Fujita, K.; Fukuda, M.; Endoh, S.; Kato, H.; Maru, J.; Nakamura, A.; Uchino, K.; Shinohara, N.; Obara, S.; Nagano, R.; Horie, M.; Kinugasa, S.; Hashimoto, H.; Kishimoto, A. Physical properties of single-wall carbon nanotubes in cell culture and their dispersal due to alveolar epithelial cell response. *Toxicol. Mech. Method.* **2013**, *23*, 598–609. doi:10.3109/15376516.2013.811568.

42.   Chen, T.; Yang, J.; Ren, G.; Yang, Z.; Zhang, T. Multi-walled carbon nanotube increases the excitability of hippocampal CA1 neurons through inhibition of potassium channels in rat's brain slices. *Toxicol. Lett.* **2013**, *217*, 121 – 128. doi:10.1016/j.toxlet.2012.12.013.

43.   Hernández-Ferrer, J.; Pérez-Bruzón, R.N.; Azanza, M.J.; González, M.; Del Moral, R.; Ansón-Casaos, A.; de la Fuente, J.M.; Marijuan, P.C.; Martínez, M.T. Study of neuron survival on polypyrrole-embedded single-walled carbon nanotube substrates for long-term growth conditions. *J. Biomed. Mater. Res. A* **2014**, *102*, 4443–4454. doi:10.1002/jbm.a.35110.

44.   Vicentini, N.; Gatti, T.; Salice, P.; Scapin, G.; Marega, C.; Filippini, F.; Menna, E. Covalent functionalization enables good dispersion and anisotropic orientation of multi-walled carbon nanotubes in a poly(l-lactic acid) electrospun nanofibrous matrix boosting neuronal differentiation. *Carbon* **2015**, *95*, 725 – 730. doi:10.1016/j.carbon.2015.08.094.

45.   Komane, P.; Kumar, P.; Choonara, Y.; Pillay, V. Functionalized, Vertically Super-Aligned Multiwalled Carbon Nanotubes for Potential Biomedical Applications. *Int. J. Mol. Sci.* **2020**, *21*, 2276. doi:10.3390/ijms21072276.

46.   Yang, D.; Shen, J.; Fan, J.; Chen, Y.; Guo, X. Paracellular permeability changes induced by multi-walled carbon nanotubes in brain endothelial cells and associated roles of hemichannels. *Toxicology* **2020**, *440*, 152491. doi:10.1016/j.tox.2020.152491.

47. Chio, L.; Pinals, R.L.; Murali, A.; Goh, N.S.; Landry, M.P. Covalent Surface Modification Effects on Single-Walled Carbon Nanotubes for Targeted Sensing and Optical Imaging. *Adv. Funct. Mater.* **2020**, *30*, 1910556. doi:10.1002/adfm.201910556.

48. Yen, S.J.; Hsu, W.L.; Chen, Y.C.; Su, H.C.; Chang, Y.C.; Chen, H.; Yeh, S.R.; Yew, T.R. The enhancement of neural growth by amino-functionalization on carbon nanotubes as a neural electrode. *Biosens. Bioelectron.* **2011**, *26*, 4124 – 4132. doi:10.1016/j.bios.2011.04.003.

49. Bosi, S.; Rauti, R.; Laishram, J.; Turco, A.; Lonardoni, D.; Nieus, T.; Prato, M.; Scaini, D.; Ballerini, L. From 2D to 3D: Novel nanostructured scaffolds to investigate signalling in reconstructed neuronal networks. *Sci. Rep.* **2015**, *5*, 9562. doi:10.1038/srep09562.

50. Koppes, A.; Keating, K.; McGregor, A.; Koppes, R.; Kearns, K.; Ziemba, A.; McKay, C.; Zuidema, J.; Rivet, C.; Gilbert, R.; Thompson, D. Robust neurite extension following exogenous electrical stimulation within single walled carbon nanotube-composite hydrogels. *Acta Biomater.* **2016**, *39*, 34 – 43. doi:10.1016/j.actbio.2016.05.014.

51. Singh, N.; Chen, J.; Koziol, K.K.; Hallam, K.R.; Janas, D.; Patil, A.J.; Strachan, A.; G. Hanley, J.; Rahatekar, S.S. Chitin and carbon nanotube composites as biocompatible scaffolds for neuron growth. *Nanoscale* **2016**, *8*, 8288–8299. doi:10.1039/C5NR06595J.

52. Shrestha, S.; Shrestha, B.K.; Lee, J.; Joong, O.K.; Kim, B.S.; Park, C.H.; Kim, C.S. A conducting neural interface of polyurethane/silk-functionalized multiwall carbon nanotubes with enhanced mechanical strength for neuroregeneration. *Mater. Sci. Eng. C* **2019**, *102*, 511 – 523. doi:10.1016/j.msec.2019.04.053.

53. Steel, E.M.; Azar, J.Y.; Sundararaghavan, H.G. Electrospun hyaluronic acid-carbon nanotube nanofibers for neural engineering. *Materialia* **2020**, *9*, 100581. doi:10.1016/j.mtla.2019.100581.

54. Fabbro, A.; Sucapane, A.; Toma, F.; Calura, E.; Rizzetto, L.; Carrieri, C.; Roncaglia, P.; Martinelli, V.; Scaini, D.; Masten, L.; Turco, A.; Gustincich, S.; Prato, M.; Ballerini, L. Adhesion to Carbon Nanotube Conductive Scaffolds Forces Action-Potential Appearance in Immature Rat Spinal Neurons. *PLoS One* **2013**, *8*, e73621. doi:10.1371/journal.pone.0073621.

55. Kim, Y.G.; Kim, J.W.; Pyeon, H.J.; Hyun, J.K.; Hwang, J.Y.; Choi, S.J.; Lee, J.Y.; Deák, F.; Kim, H.W.; Lee, Y.I. Differential stimulation of neurotrophin release by the biocompatible nano-material (carbon nanotube) in primary cultured neurons. *J. Biomater. Appl.* **2014**, *28*, 790–797. doi:10.1177/0885328213481637.

56. Shin, J.; Choi, E.J.; Cho, J.H.; Cho, A.N.; Jin, Y.; Yang, K.; Song, C.; Cho, S.W. Three-Dimensional Electroconductive Hyaluronic Acid Hydrogels Incorporated with Carbon Nanotubes and Polypyrrole by Catechol-Mediated Dispersion Enhance Neurogenesis of Human Neural Stem Cells. *Biomacromolecules* **2017**, *18*, 3060–3072. doi:10.1021/acs.biomac.7b00568.

57. Simonovic, J.; Toljic, B.; Nikolic, N.; Peric, M.; Vujin, J.; Panajotovic, R.; Gajic, R.; Bekyarova, E.; Cataldi, A.; Parpura, V.; Milasin, J. Differentiation of stem cells from apical papilla into neural lineage using graphene dispersion and single walled carbon nanotubes. *J. Biomed. Mater. Res. A* **2018**, *106*, 2653–2661. doi:10.1002/jbm.a.36461.

58. Pouladzadeh, F.; Katbab, A.A.; Haghighipour, N.; Kashi, E. Carbon nanotube loaded electrospun scaffolds based on thermoplastic urethane (TPU) with enhanced proliferation and neural differentiation of rat mesenchymal stem cells: The role of state of electrical conductivity. *Eur. Polym. J.* **2018**, *105*, 286 – 296. doi:10.1016/j.eurpolymj.2018.05.011.

59. Tonellato, M.; Piccione, M.; Gasparotto, M.; Bellet, P.; Tibaudo, L.; Vicentini, N.; Bergantino, E.; Menna, E.; Vitiello, L.; Di Liddo, R.; Filippini, F. Commitment of Autologous Human Multipotent Stem Cells on Biomimetic Poly-L-lactic Acid-Based Scaffolds Is Strongly Influenced by Structure and Concentration of Carbon Nanomaterial. *Nanomaterials* **2020**, *10*, 415. doi:10.3390/nano10030415.

60. Hirata, E.; Akasaka, T.; Uo, M.; Takita, H.; Watari, F.; Yokoyama, A. Carbon nanotube-coating accelerated cell adhesion and proliferation on poly (L-lactide). *Appl. Surf. Sci.* **2012**, *262*, 24–27. doi:10.1016/j.apsusc.2012.01.012.

61. Holt, B.; Shams, H.; Horst, T.; Basu, S.; Rape, A.; Wang, Y.L.; Rohde, G.; Mofrad, M.; Islam, M.; Dahl, K. Altered Cell Mechanics from the Inside: Dispersed Single Wall Carbon Nanotubes Integrate with and Restructure Actin. *J. Funct. Biomater.* **2012**, *3*, 398. doi:10.3390/jfb3020398.

62. Liedtke, W.; Yeo, M.; Zhang, H.; Wang, Y.; Gignac, M.; Miller, S.; Berglund, K.; Liu, J. Highly Conductive Carbon Nanotube Matrix Accelerates Developmental Chloride Extrusion in Central Nervous

System Neurons by Increased Expression of Chloride Transporter KCC2. *Small* **2013**, *9*, 1066–1075. doi:10.1002/smll.201201994.

63. Xiang, C.; Zhang, Y.; Guo, W.; Liang, X.J. Biomimetic carbon nanotubes for neurological disease therapeutics as inherent medication. *Acta Pharm. Sin. B* **2020**, *10*, 239 – 248. doi:10.1016/j.apsb.2019.11.003.

64. Sun, T.; Han, D.; Rhemann, K.; Chi, L.; Fuchs, H. Stereospecific Interaction between Immune Cells and Chiral Surfaces. *J. Am. Chem. Soc.* **2007**, *129*, 1496–1497. doi:10.1021/ja0686155.

65. Hazen, R.; Sholl, D. Chiral selection on inorganic crystalline surfaces. *Nat. Mater.* **2003**, *2*, 367–74. doi:10.1038/nmat879.

66. Skandani, A.A.; Zeineldin, R.; Al-Haik, M. Effect of Chirality and Length on the Penetrability of Single-Walled Carbon Nanotubes into Lipid Bilayer Cell Membranes. *Langmuir* **2012**, *28*, 7872–7879. doi:10.1021/la3011162.

67. Al-Jamal, K.T.; Nerl, H.; Müller, K.H.; Ali-Boucetta, H.; Li, S.; Haynes, P.D.; Jinschek, J.R.; Prato, M.; Bianco, A.; Kostarelos, K.; Porter, A.E. Cellular uptake mechanisms of functionalised multi-walled carbon nanotubes by 3D electron tomography imaging. *Nanoscale* **2011**, *3*, 2627–2635. doi:10.1039/C1NR10080G.

68. Dionigi, C.; Bianchi, M.; D'Angelo, P.; Chelli, B.; Greco, P.; Shehu, A.; Tonazzini, I.; Lazar, A.N.; Biscarini, F. Control of neuronal cell adhesion on single-walled carbon nanotube 3D patterns. *J. Mater. Chem.* **2010**, *20*, 2213–2218. doi:10.1039/B918543G.

69. Abdolmaleki, A.; Mallakpour, S.; Borandeh, S. Amino acid-functionalized multi-walled carbon nanotubes for improving compatibility with chiral poly(amide-ester-imide) containing l-phenylalanine and l-tyrosine linkages. *Appl. Surf. Sci.* **2013**, *287*, 117 – 123. doi:10.1016/j.apsusc.2013.09.088.

70. Strano, M. Carbon nanotubes: Sorting out left from right. *Nat. Nanotechnol.* **2007**, *2*, 340–1. doi:10.1038/nnano.2007.157.

71. Kane, C.L.; Mele, E.J. Size, Shape, and Low Energy Electronic Structure of Carbon Nanotubes. *Phys. Rev. Lett.* **1997**, *78*, 1932–1935. doi:10.1103/PhysRevLett.78.1932.

72. Komatsu, N. Separation of nanocarbons by molecular recognition. *J. Incl. Phenom. Macro.* **2008**, *61*, 195–216. doi:10.1007/s10847-008-9418-4.

73. Pierre-Louis, O. Adhesion of membranes and filaments on rippled surfaces. *Phys. Rev. E* **2008**, *78*, 021603. doi:10.1103/PhysRevE.78.021603.

74. Roberts, M.J.; Leach, M.K.; Bedewy, M.; Meshot, E.R.; Copic, D.; Corey, J.M.; Hart, A.J. Growth of primary motor neurons on horizontally aligned carbon nanotube thin films and striped patterns. *J. Neural Eng.* **2014**, *11*, 036013. doi:10.1088/1741-2560/11/3/036013.

75. Schneider, J.J. Vertically Aligned Carbon Nanotubes as Platform for Biomimetically Inspired Mechanical Sensing, Bioactive Surfaces, and Electrical Cell Interfacing. *Adv. Biosyst.* **2017**, *1*, 1700101. doi:10.1002/adbi.201700101.

76. Sten-Knudsen, O. *Biological Membranes*; Cambridge University Press, 2002; p. Ch. 4.

77. Naundorf, B.; Wolf, F.; Volgushev, M. Unique features of action potential initiation in cortical neurons. *Nature* **2006**, *440*, 1060–3. doi:10.1038/nature04610.

78. Zykov, V. *Simulation of Wave Processes in Excitable Media*; Manchester University Press, 1987; pp. Ch. 5,6,7.

79. Lin, Z.; Xie, C.; Osakada, Y.; Cui, Y.; Cui, B. Iridium Oxide Nanotube Electrodes for Highly Sensitive and Prolonged Intracellular Measurement of Action Potentials. *Nat. Commun.* **2014**, *5*, 3206. doi:10.1038/ncomms4206.

80. Comtois, P.; Vinet, A. Curvature effects on activation speed and repolarization in an ionic model of cardiac myocytes. *Phys. Rev. E* **1999**, *60*, 4619–4628. doi:10.1103/PhysRevE.60.4619.

81. Kiran, M.S.R.N.; Ramamurty, U.; Misra, A. Mechanical and electrical contact resistance characteristics of a cellular assembly of carbon nanotubes. *Nanotechnology* **2012**, *24*, 015707. doi:10.1088/0957-4484/24/1/015707.

82. Guharay, F.; Sachs, F. Stretch-activated single ion channel currents in tissue-cultured embryonic chick skeletal muscle. *J. Physiol.* **1984**, *352*, 685–701. doi:10.1113/jphysiol.1984.sp015317.

83. Das, P.; Schwarz, W.H. Solitons in cell membranes. *Phys. Rev. E* **1995**, *51*, 3588–3612. doi:10.1103/PhysRevE.51.3588.

84. Stolyarova, E.; Rim, K.T.; Ryu, S.; Maultzsch, J.; Kim, P.; Brus, L.E.; Heinz, T.F.; Hybertsen, M.S.; Flynn, G.W. High-resolution scanning tunneling microscopy imaging of mesoscopic graphene sheets on an insulating surface. *Proc. Natl. Acad. Sci.* **2007**, *104*, 9209–9212. doi:10.1073/pnas.0703337104.

85. Wang, X.; Veruki, M.L.; Bukoreshtliev, N.V.; Hartveit, E.; Gerdes, H.H. Animal cells connected by nanotubes can be electrically coupled through interposed gap-junction channels. *Proc. Natl. Acad. Sci.* **2010**, *107*, 17194–17199. doi:10.1073/pnas.1006785107.

86. Safinya, C.R.; Raviv, U.; Needleman, D.J.; Zidovska, A.; Choi, M.C.; Ojeda-Lopez, M.A.; Ewert, K.K.; Li, Y.; Miller, H.P.; Quispe, J.; Carragher, B.; Potter, C.S.; Kim, M.W.; Feinstein, S.C.; Wilson, L. Nanoscale Assembly in Biological Systems: From Neuronal Cytoskeletal Proteins to Curvature Stabilizing Lipids. *Adv. Mater.* **2011**, *23*, 2260–2270. doi:10.1002/adma.201004647.

87. Marzo, L.; Gousset, K.; Zurzolo, C. Multifaceted Roles of Tunneling Nanotubes in Intercellular Communication. *Front. Physiol.* **2012**, *3*, 72. doi:10.3389/fphys.2012.00072.

88. Gerdes, H.H.; Rustom, A.; Wang, X. Tunneling nanotubes, an emerging intercellular communication route in development. *Mech. Dev.* **2013**, *130*, 381 – 387. doi:10.1016/j.mod.2012.11.006.

89. Nawaz, M.; Fatima, F. Extracellular Vesicles, Tunneling Nanotubes, and Cellular Interplay: Synergies and Missing Links. *Front. Mol. Biosci.* **2017**, *4*, 50. doi:10.3389/fmolb.2017.00050.

90. De Volder, M.F.L.; Tawfick, S.H.; Baughman, R.H.; Hart, A.J. Carbon Nanotubes: Present and Future Commercial Applications. *Science* **2013**, *339*, 535–539. doi:10.1126/science.1222453.

91. Tombler, T.; Zhou, C.; Alexseyev, L.; Kong, J.; Dai, H.; Liu, L.; Jayanthi, C.; Tang, M.; Wu, S.Y. Reversible Electromechanical Characteristics of Carbon Nanotubes Under Local-Probe Manipulation. *Nature* **2000**, *405*, 769–72. doi:10.1038/35015519.

92. Nardelli, M.B.; Bernholc, J. Mechanical deformations and coherent transport in carbon nanotubes. *Phys. Rev. B* **1999**, *60*, R16338–R16341. doi:10.1103/PhysRevB.60.R16338.

93. Baughman, R.H.; Cui, C.; Zakhidov, A.A.; Iqbal, Z.; Barisci, J.N.; Spinks, G.M.; Wallace, G.G.; Mazzoldi, A.; De Rossi, D.; Rinzler, A.G.; Jaschinski, O.; Roth, S.; Kertesz, M. Carbon Nanotube Actuators. *Science* **1999**, *284*, 1340–1344. doi:10.1126/science.284.5418.1340.

94. Li, C.; Thostenson, E.T.; Chou, T.W. Sensor. Actuat. based on carbon nanotubes and their composites: A review. *Compos. Sci. Technol.* **2008**, *68*, 1227 – 1249. doi:10.1016/j.compscitech.2008.01.006.

95. Pollack, G. *Cells, gels and the engines of life. (A new, unifying approach to cell function)*; Ebner & Sons, Seattle WA, US, 2001; chapter III, IV, V.

96. Heimburg, T.; Jackson, A.D. On soliton propagation in biomembranes and nerves. *Proc. Natl. Acad. Sci.* **2005**, *102*, 9790–9795. doi:10.1073/pnas.0503823102.

97. Tasaki, I.; Watanabe, A.; Sandlin, R.; Carnay, L. Changes in fluorescence, turbidity, and birefringence associated with nerve excitation. *Proc. Natl. Acad. Sci.* **1968**, *61*, 883–888. doi:10.1073/pnas.61.3.883.

98. Shneider, M.N.; Pekker, M. Non-thermal mechanism of weak microwave fields influence on neurons. *J. Appl. Phys.* **2013**, *114*, 104701. doi:10.1063/1.4821027.

99. Pekker, M.; Shneider, M.N. Comment on "Non-thermal mechanism of weak microwave fields influence on neurons" [J. Appl. Phys. 114, 104701 (2013)]. *J. Appl. Phys.* **2016**, *119*, 086101. doi:10.1063/1.4942821.

100. Lundholm, I.V.; Rodilla, H.; Wahlgren, W.Y.; Duelli, A.; Bourenkov, G.; Vukusic, J.; Friedman, R.; Stake, J.; Schneider, T.; Katona, G. Terahertz radiation induces non-thermal structural changes associated with Fröhlich condensation in a protein crystal. *Struct. Dynam.* **2015**, *2*, 054702. doi:10.1063/1.4931825.

101. Haiss, W. Surface stress of clean and adsorbate-covered solids. *Rep. Progr. Phys.* **2001**, *64*, 591–648. doi:10.1088/0034-4885/64/5/201.

102. Journet, C.; Bernier, P. Production of Carbon Nanotubes. *Appl. Phys. A* **1998**, *67*, 1–9. doi:10.1007/s003390050731.

103. Das, T.K.; Prusty, S. Review on Conducting Polymers and Their Applications. *Polym. Plast. Technol.* **2012**, *51*, 1487–1500. doi:10.1080/03602559.2012.710697.

104. Hughes, J.M.; Aherne, D.; Bergin, S.D.; O'Neill, A.; Streich, P.V.; Hamilton, J.P.; Coleman, J.N. Using solution thermodynamics to describe the dispersion of rod-like solutes: application to dispersions of carbon nanotubes in organic solvents. *Nanotechnology* **2012**, *23*, 265604. doi:10.1088/0957-4484/23/26/265604.

105. Shaffer, M.S.P.; Windle, A.H. Analogies between Polymer Solutions and Carbon Nanotube Dispersions. *Macromolecules* **1999**, *32*, 6864–6866. doi:10.1021/ma990095t.

106. Usrey, M.L.; Chaffee, A.; Jeng, E.S.; Strano, M.S. Application of Polymer Solubility Theory to Solution Phase Dispersion of Single-Walled Carbon Nanotubes. *J. Phys. Chem. C* **2009**, *113*, 9532–9540. doi:10.1021/jp810992u.

107. Fakhri, N.; MacKintosh, F.C.; Lounis, B.; Cognet, L.; Pasquali, M. Brownian Motion of Stiff Filaments in a Crowded Environment. *Science* **2010**, *330*, 1804–1807. doi:10.1126/science.1197321.

108. Hrabetova, S.; Cognet, L.; Rusakov, D.A.; Nägerl, U.V. Unveiling the Extracellular Space of the Brain: From Super-resolved Microstructure to In Vivo Function. *J. Neurosci.* **2018**, *38*, 9355–9363. doi:10.1523/JNEUROSCI.1664-18.2018.

109. Szleifer, I.; Yerushalmi-Rozen, R. Polymers and carbon nanotubes - Dimensionality, interactions and nanotechnology. *Polymer* **2005**, *46*, 7803–7818. doi:10.1016/j.polymer.2005.05.104.

110. Lin, K.h.; Crocker, J.C.; Prasad, V.; Schofield, A.; Weitz, D.A.; Lubensky, T.C.; Yodh, A.G. Entropically Driven Colloidal Crystallization on Patterned Surfaces. *Phys. Rev. Lett.* **2000**, *85*, 1770–1773. doi:10.1103/PhysRevLett.85.1770.

111. Schilling, T.; Jungblut, S.; Miller, M.A. Depletion-Induced Percolation in Networks of Nanorods. *Phys. Rev. Lett.* **2007**, *98*, 108303. doi:10.1103/PhysRevLett.98.108303.

112. Wang, X.; Xia, T.; Addo Ntim, S.; Ji, Z.; George, S.; Meng, H.; Zhang, H.; Castranova, V.; Mitra, S.; Nel, A. Quantitative Techniques for Assessing and Controlling the Dispersion and Biological Effects of Multiwalled Carbon Nanotubes in Mammalian Tissue Culture Cells. *ACS Nano* **2010**, *4*, 7241–52. doi:10.1021/nn102112b.

113. Georgakilas, V.; Kordatos, K.; Prato, M.; Guldi, D.M.; Holzinger, M.; Hirsch, A. Organic Functionalization of Carbon Nanotubes. *J. Am. Chem. Soc.* **2002**, *124*, 760–761. doi:10.1021/ja016954m.

114. Hobbie, E.K.; Fry, D.J. Rheology of concentrated carbon nanotube suspensions. *J. Chem. Phys.* **2007**, *126*, 124907. doi:10.1063/1.2711176.

115. Kayatin, M.J.; Davis, V.A. Viscoelasticity and Shear Stability of Single-Walled Carbon Nanotube/Unsaturated Polyester Resin Dispersions. *Macromolecules* **2009**, *42*, 6624–6632. doi:10.1021/ma901010d.

116. Jung de Andrade, M.; Dias Lima, M.; Skákalová, V.; Pérez Bergmann, C.; Roth, S. Electrical properties of transparent carbon nanotube networks prepared through different techniques. *Phys. Status Solidi RRL* **2007**, *1*, 178–180. doi:10.1002/pssr.200701115.

117. Incze, A.; Pasturel, A.; Peyla, P. Mechanical properties of graphite oxides: Ab initio simulations and continuum theory. *Phys. Rev. B* **2004**, *70*, 212103. doi:10.1103/PhysRevB.70.212103.

118. Horie, M.; Stowe, M.; Tabei, M.; Kato, H.; Nakamura, A.; Endoh, S.; Morimoto, Y.; Fujita, K. Dispersant affects the cellular influences of single-wall carbon nanotube: The role of CNT as carrier of dispersants. *Toxicol. Mech. Method.* **2013**, *23*, 315–322. doi:10.3109/15376516.2012.755595.

119. Maier, J. Thermodynamics of Nanosystems with a Special View to Charge Carriers. *Adv. Mater.* **2009**, *21*, 2571–2585. doi:10.1002/adma.200900598.

120. Linford, R. *Solid State Surface Science II*; Dekker, New York, US, 1973.

121. Gaillard, C.; Cellot, G.; Li, S.; Toma, F.M.; Dumortier, H.; Spalluto, G.; Cacciari, B.; Prato, M.; Ballerini, L.; Bianco, A. Carbon Nanotubes Carrying Cell-Adhesion Peptides do not Interfere with Neuronal Functionality. *Adv. Mater.* **2009**, *21*, 2903–2908. doi:10.1002/adma.200900050.

122. Giugliano, M.; Prato, M.; Ballerini, L. Nanomaterial/neuronal hybrid system for functional recovery of the CNS. *Drug Discov. Today* **2008**, *5*, 37 – 43. doi:10.1016/j.ddmod.2008.07.004.

123. Mazzatenta, A.; Giugliano, M.; Campidelli, S.; Gambazzi, L.; Businaro, L.; Markram, H.; Prato, M.; Ballerini, L. Interfacing Neurons with Carbon Nanotubes: Electrical Signal Transfer and Synaptic Stimulation in Cultured Brain Circuits. *J. Neurosci.* **2007**, *27*, 6931–6936. doi:10.1523/JNEUROSCI.1051-07.2007.

124. Sucapane, A.; Cellot, G.; Prato, M.; Giugliano, M.; Parpura, V.; Ballerini, L. Interactions Between Cultured Neurons and Carbon Nanotubes: A Nanoneuroscience Vignette. *J. Nanoneurosci.* **2009**, *1*, 10–16. doi:10.1166/jns.2009.002.

125. D. Stauffer, A.A. *Introduction to Percolation Theory*; Taylor & Francis, London, UK, 1985; chapter Ch. 1,2.

126. Bollobás, B.; Riordan, O. *Percolation.*; Cambridge University Press, 2006; pp. I–X, 1–323.

127. Saberi, A.A. Recent advances in percolation theory and its applications. *Phys. Rep.* **2015**, *578*, 1 – 32. doi:10.1016/j.physrep.2015.03.003.

128. Nan, C.; Shen, Y.; Ma, J. Physical Properties of Composites Near Percolation. *Annu. Rev. Mater. Res.* **2010**, *40*, 131–151. doi:10.1146/annurev-matsci-070909-104529.

129. Kim, Y.; Zhu, J.; Yeom, B.; Prima, M.; Su, X.; Kim, J.G.; Yoo, S.J.; Uher, C.; Kotov, N. Stretchable nanoparticle conductors with self-organized conductive pathways. *Nature* **2013**, *500*, 59–63. doi:10.1038/nature12401.

130. Roman, H.E.; Yussouff, M. Particle-size effect on the conductivity of dispersed ionic conductors. *Phys. Rev. B* **1987**, *36*, 7285–7288. doi:10.1103/PhysRevB.36.7285.

131. Kota, A.K.; Cipriano, B.H.; Duesterberg, M.K.; Gershon, A.L.; Powell, D.; Raghavan, S.R.; Bruck, H.A. Electrical and Rheological Percolation in Polystyrene/MWCNT Nanocomposites. *Macromolecules* **2007**, *40*, 7400–7406. doi:10.1021/ma0711792.

132. Arbabi, S.; Sahimi, M. Critical properties of viscoelasticity of gels and elastic percolation networks. *Phys. Rev. Lett.* **1990**, *65*, 725–728. doi:10.1103/PhysRevLett.65.725.

133. Bauhofer, W.; Kovacs, J.Z. A review and analysis of electrical percolation in carbon nanotube polymer composites. *Compos. Sci. Technol.* **2009**, *69*, 1486 – 1498. doi:10.1016/j.compscitech.2008.06.018.

134. Kang, B.; cai Yu, D.; quan Chang, S.; Chen, D.; dong Dai, Y.; Ding, Y. Intracellular uptake, trafficking and subcellular distribution of folate conjugated single walled carbon nanotubes within living cells. *Nanotechnology* **2008**, *19*, 375103. doi:10.1088/0957-4484/19/37/375103.

135. Larkum, M.E.; Kaiser, K.M.M.; Sakmann, B. Calcium electrogenesis in distal apical dendrites of layer 5 pyramidal cells at a critical frequency of back-propagating action potentials. *Proc. Natl. Acad. Sci.* **1999**, *96*, 14600–14604. doi:10.1073/pnas.96.25.14600.

136. Diba, K.; Koch, C.; Segev, I. Spike propagation in dendrites with stochastic ion channels. *J. Comp. Neurosci.* **2006**, *20*, 77–84. doi:10.1007/s10870-006-4770-0.

137. Johnston, D.; Christie, B.; Frick, A.; Gray, R.; Hoffman, D.; Schexnayder, L.; Watanabe, S.; Yuan, L.L. Active dendrites, potassium channels and synaptic plasticity. *Phil. Trans. Roy. Soc. B* **2003**, *358*, 667–74. doi:10.1098/rstb.2002.1248.

138. Fattahi, P.; Yang, G.; Kim, G.; Abidian, M.R. A Review of Organic and Inorganic Biomaterials for Neural Interfaces. *Adv. Mater.* **2014**, *26*, 1846–1885. doi:10.1002/adma.201304496.

139. Parshani, R.; Buldyrev, S.V.; Havlin, S. Interdependent Networks: Reducing the Coupling Strength Leads to a Change from a First to Second Order Percolation Transition. *Phys. Rev. Lett.* **2010**, *105*, 048701. doi:10.1103/PhysRevLett.105.048701.

140. Kittel, C. *Introduction to Solid State Physics*; John Wiley & Sons, New York, US, 1986; chapter Ch. 6.

141. La Camera, G.; Rauch, A.; Thurbon, D.; Lüscher, H.R.; Senn, W.; Fusi, S. Multiple Time Scales of Temporal Response in Pyramidal and Fast Spiking Cortical Neurons. *J. Neurophysiol.* **2006**, *96*, 3448–3464. doi:10.1152/jn.00453.2006.

142. Buchholtz, F.; Schinor, N.; Schneider, F.W. Stochastic Nonlinear Dynamics: How Many Ion Channels are in a Single Neuron? *J. Phys. Chem. B* **2002**, *106*, 5086–5090. doi:10.1021/jp0120662.

143. Hanein, Y.; Bareket-Keren, L. Carbon nanotube-based multi electrode arrays for neuronal interfacing: progress and prospects. *Front. Neural Circuits* **2013**, *6*, 122. doi:10.3389/fncir.2012.00122.

144. Basser, P.J.; Roth, B.J. New Currents in Electrical Stimulation of Excitable Tissues. *Annu. Rev. Biomed. Eng.* **2000**, *2*, 377–397. doi:10.1146/annurev.bioeng.2.1.377.

145. Obukhov, S.P. First Order Rigidity Transition in Random Rod Networks. *Phys. Rev. Lett.* **1995**, *74*, 4472–4475. doi:10.1103/PhysRevLett.74.4472.

146. Sahini, M.; Sahimi, M. *Applications Of Percolation Theory*; London: CRC Press, UK, 1994; chapter Ch. 12, 13.

147. Coniglio, A.; Angelis, U.; Forlani, A. Pair connectedness and cluster size. *J. Phys. A* **2001**, *10*, 1123. doi:10.1088/0305-4470/10/7/011.

148. Bug, A.L.R.; Safran, S.A.; Webman, I. Continuum percolation of permeable objects. *Phys. Rev. B* **1986**, *33*, 4716–4724. doi:10.1103/PhysRevB.33.4716.

149. Bug, A.L.R.; Safran, S.A.; Webman, I. Continuum Percolation of Rods. *Phys. Rev. Lett.* **1985**, *54*, 1412–1415. doi:10.1103/PhysRevLett.54.1412.

150. Grossiord, N.; Loos, J.; Regev, O.; Koning, C.E. Toolbox for Dispersing Carbon Nanotubes into Polymers To Get Conductive Nanocomposites. *Chem. Mater.* **2006**, *18*, 1089–1099. doi:10.1021/cm051881h.

151. Munson-McGee, S.H. Estimation of the critical concentration in an anisotropic percolation network. *Phys. Rev. B* **1991**, *43*, 3331–3336. doi:10.1103/PhysRevB.43.3331.

152. Zakri, C.; Poulin, P. Phase behavior of nanotube suspensions: from attraction induced percolation to liquid crystalline phases. *J. Mater. Chem.* **2006**, *16*, 4095–4098. doi:10.1039/B607378F.

153. Bug, A.L.R.; Safran, S.A.; Grest, G.S.; Webman, I. Do Interactions Raise or Lower a Percolation Threshold? *Phys. Rev. Lett.* **1985**, *55*, 1896–1899. doi:10.1103/PhysRevLett.55.1896.

154. Berhan, L.; Sastry, A.M. Modeling percolation in high-aspect-ratio fiber systems. I. Soft-core versus hard-core models. *Phys. Rev. E* **2007**, *75*, 041120. doi:10.1103/PhysRevE.75.041120.

155. Berhan, L.; Sastry, A.M. Modeling percolation in high-aspect-ratio fiber systems. II. The effect of waviness on the percolation onset. *Phys. Rev. E* **2007**, *75*, 041121. doi:10.1103/PhysRevE.75.041121.

156. Kyrylyuk, A.V.; van der Schoot, P. Continuum percolation of carbon nanotubes in polymeric and colloidal media. *Proc. Natl. Acad. Sci.* **2008**, *105*, 8221–8226. doi:10.1073/pnas.0711449105.

157. Lee, P.; Lee, J.; Lee, H.; Yeo, J.; Hong, S.; Nam, K.H.; Lee, D.; Lee, S.S.; Ko, S.H. Highly Stretchable and Highly Conductive Metal Electrode by Very Long Metal Nanowire Percolation Network. *Adv. Mater.* **2012**, *24*, 3326–3332. doi:10.1002/adma.201200359.

158. Blouwolff, J.; Fraden, S. The coordination number of granular cylinders. *Europhys. Lett.* **2006**, *76*, 1095–1101. doi:10.1209/epl/i2006-10376-1.

159. Li, C.; Chou, T.W. A direct electrifying algorithm for backbone identification. *J. Phys. A* **2007**, *40*, 14679–14686. doi:10.1088/1751-8113/40/49/004.

160. Stenull, O.; Janssen, H.K.; Oerding, K. Effects of surfaces on resistor percolation. *Phys. Rev. E* **2001**, *63*, 056128. doi:10.1103/PhysRevE.63.056128.

161. Lv, L.; Liu, Y.; Zhang, P.; Zhang, X.; Liu, J.; Chen, T.; Su, P.; Li, H.; Zhou, Y. The nanoscale geometry of TiO2 nanotubes influences the osteogenic differentiation of human adipose-derived stem cells by modulating H3K4 trimethylation. *Biomaterials* **2015**, *39*, 193 – 205. doi:10.1016/j.biomaterials.2014.11.002.

162. Kinnear, C.; Moore, T.L.; Rodriguez-Lorenzo, L.; Rothen-Rutishauser, B.; Petri-Fink, A. Form Follows Function: Nanoparticle Shape and Its Implications for Nanomedicine. *Chem. Rev.* **2017**, *117*, 11476–11521. doi:10.1021/acs.chemrev.7b00194.

163. Bolz, A.; Fröhlich, R.; Schmidt, K.; Schaldach, M. Effect of smooth, porous and fractal surface structure on the properties of an interface. *J. Mater. Sci. Mater. Med.* **1995**, *6*, 844–848. doi:10.1007/BF00134329.

164. Soriano, J.; Rodríguez Martínez, M.; Tlusty, T.; Moses, E. Development of input connections in neural cultures. *Proc. Natl. Acad. Sci.* **2008**, *105*, 13758–13763. doi:10.1073/pnas.0707492105.

165. da F. Costa, L.; Coelho, R. Growth-driven percolations: The dynamics of connectivity in neuronal systems. *Eur. Phys. J. B* **2005**, *47*, 571–581. doi:10.1140/epjb/e2005-00354-5.

166. Rubinstein, M.; Colby, R. *Polymer Physics*; Oxford University Press, 2003; p. Ch.6.

167. Plaksin, M.; Shapira, E.; Kimmel, E.; Shoham, S. Thermal Transients Excite Neurons through Universal Intramembrane Mechanoelectrical Effects. *Phys. Rev. X* **2018**, *8*, 011043. doi:10.1103/PhysRevX.8.011043.

168. Qiu, L.; Zhu, N.; Feng, Y.; Michaelides, E.E.; Żyła, G.; Jing, D.; Zhang, X.; Norris, P.M.; Markides, C.N.; Mahian, O. A review of recent advances in thermophysical properties at the nanoscale: From solid state to colloids. *Phys. Rep.* **2020**, *843*, 1 – 81. doi:10.1016/j.physrep.2019.12.001.

169. Mingo, N.; Broido, D.A. Carbon Nanotube Ballistic Thermal Conductance and Its Limits. *Phys. Rev. Lett.* **2005**, *95*, 096105. doi:10.1103/PhysRevLett.95.096105.

170. Yao, Z.; Wang, J.S.; Li, B.; Liu, G.R. Thermal conduction of carbon nanotubes using molecular dynamics. *Phys. Rev. B* **2005**, *71*, 085417. doi:10.1103/PhysRevB.71.085417.

171. Fraczek-Szczypta, A. Carbon nanomaterials for nerve tissue stimulation and regeneration. *Mater. Sci. Eng. C* **2014**, *34*, 35–49. doi:10.1016/j.msec.2013.09.038.

172. Charlier, J.C.; Blase, X.; Roche, S. Electronic and transport properties of nanotubes. *Rev. Mod. Phys.* **2007**, *79*, 677–732. doi:10.1103/RevModPhys.79.677.

173. Prasher, R. Thermal conductance of single-walled carbon nanotube embedded in an elastic half-space. *Appl. Phys. Lett.* **2007**, *90*, 143110. doi:10.1063/1.2719240.

174. Kumar, S.; Alam, M.A.; Murthy, J.Y. Effect of percolation on thermal transport in nanotube composites. *Appl. Phys. Lett.* **2007**, *90*, 104105. doi:10.1063/1.2712428.

175. Small, J.P.; Perez, K.M.; Kim, P. Modulation of Thermoelectric Power of Individual Carbon Nanotubes. *Phys. Rev. Lett.* **2003**, *91*, 256801. doi:10.1103/PhysRevLett.91.256801.

176. D'Agosta, R.; Ventra, M.D. Local electron and ionic heating effects on the conductance of nanostructures. *J. Phys.: Condens. Matter* **2008**, *20*, 374102. doi:10.1088/0953-8984/20/37/374102.

177. Mahan, G. *Thermoelectric Power of Carbon Nanotubes, in* Thermoelectrics Handbook: Macro to Nano, *Ed. D.M. Rowe*; Taylor & Francis, New York, US, 2006; p. Ch. 17.

178.   Sarria, I.; Ling, J.; Gu, J.G.   Thermal sensitivity of voltage-gated Na+ channels and A-type K+ channels contributes to somatosensory neuron excitability at cooling temperatures. *J. Neurochem.* **2012**, *122*, 1145–1154. doi:10.1111/j.1471-4159.2012.07839.x.

179.   Andersen, S.; Jackson, A.; Heimburg, T. Towards a thermodynamic theory of nerve pulse propagation. *Progr. Neurobiol.* **2009**, *88*, 104–13. doi:10.1016/j.pneurobio.2009.03.002.

180.   Tkačik, G.; Mora, T.; Marre, O.; Amodei, D.; Palmer, S.E.; Berry, M.J.; Bialek, W. Thermodynamics and signatures of criticality in a network of neurons. *Proc. Natl. Acad. Sci. USA* **2015**, *112*, 11508–11513. doi:10.1073/pnas.1514188112.

181.   Masson, j.b.; Gallot, G. A model for thermal exchange in axons during action potential propagation. *Eur. Biophys. J.* **2008**, *37*, 1001–6. doi:10.1007/s00249-008-0329-5.

182.   Garrido, J. Observable Quantities for Electrodiffusion Processes in Membranes. *J. Phys. Chem. B* **2008**, *112*, 3013–3018. doi:10.1021/jp071578z.

183.   Demirel, Y.; Sandler, S. Thermodynamics and bioenergetics. *Biophys. Chem.* **2002**, *97*, 87 – 111. doi:10.1016/S0301-4622(02)00069-8.

184.   Waters, J.; Schaefer, A.; Sakmann, B. Backpropagating action potentials in neurones: measurement, mechanisms and potential functions. *Progr. Biophys. Mol. Biol.* **2005**, *87*, 145 – 170. doi:10.1016/j.pbiomolbio.2004.06.009.

185.   Stuart, G.; Hausser, M. Dendritic coincidence detection of EPSPs and action potentials. *Nat. Neurosci.* **2001**, *4*, 63–71. doi:10.1038/82910.

186.   Aqrawe, Z.; Montgomery, J.; Travas-Sejdic, J.; Svirskis, D. Conducting polymers for neuronal microelectrode array recording and stimulation. *Sensor. Actuat. B* **2018**, *257*, 753 – 765. doi:10.1016/j.snb.2017.11.023.

187.   Robinson, J.; Jorgolli, M.; Shalek, A.; Yoon, M.H.; Gertner, R.; Park, H. Vertical nanowire electrode arrays as a scalable platform for intracellular interfacing to neuronal circuits. *Nat. Nanotechnol.* **2012**, *7*, 180–4. doi:10.1038/nnano.2011.249.

188.   Wang, Y.; Li, Z.; Wang, J.; Li, J.; Lin, Y. Graphene and graphene oxide: biofunctionalization and applications in biotechnology. *Trends Biotechnol.* **2011**, *29*, 205 – 212. doi:10.1016/j.tibtech.2011.01.008.

189.   Novoselov, K.; Falko, V.; Colombo, L.; Gellert, P.; Schwab, M.; Kim, K. A Roadmap for graphene. *Nature* **2012**, *490*, 192–200. doi:10.1038/nature11458.

190.   Hamada, N.; Sawada, S.i.; Oshiyama, A. New one-dimensional conductors: Graphitic microtubules. *Phys. Rev. Lett.* **1992**, *68*, 1579–1581. doi:10.1103/PhysRevLett.68.1579.

191.   Bandaru, P.R. Electrical Properties and Applications of Carbon Nanotube Structures. *J. Nanosci. Nanotechnol.* **2007**, *7*, 1239–1267. doi:10.1166/jnn.2007.307.

192.   Haldane, F.D.M. 'Luttinger liquid theory' of one-dimensional quantum fluids. I. Properties of the Luttinger model and their extension to the general 1D interacting spinless Fermi gas. *J. Phys. C* **1981**, *14*, 2585–2609. doi:10.1088/0022-3719/14/19/010.

193.   Delaney, P.; Choi, H.; Ihm, J.; Louie, S.; Cohen, M. Broken symmetry and pseudogaps in ropes of carbon nanotubes. *Nature* **1998**, *391*, 466–468. doi:10.1038/35099.

194.   Kim, Y.H.; Chang, K.J. Subband mixing rules in circumferentially perturbed carbon nanotubes: Effects of transverse electric fields. *Phys. Rev. B* **2001**, *64*, 153404. doi:10.1103/PhysRevB.64.153404.

195.   Li, Y.; Rotkin, S.V.; Ravaioli, U. Electronic Response and Bandstructure Modulation of Carbon Nanotubes in a Transverse Electrical Field. *Nano Lett.* **2003**, *3*, 183–187. doi:10.1021/nl0259030.

196.   Lai, P.; Chen, S.; Lin, M. Electronic properties of single-walled carbon nanotubes under electric and magnetic fields. *Physica E* **2008**, *40*, 2056–2058. doi:10.1016/j.physe.2007.09.099.

197.   Lee, C.; Su, W.; Chen, R.; Lin, M. Low-energy electronic properties of finite double-walled carbon nanotubes under external fields. *Physica E* **2009**, *41*, 1226 – 1231. doi:10.1016/j.physe.2009.02.005.

198.   Ding, J.; Kan, B.; Yuan, N.; Wang, J.; Chen, Z.; Chen, X. The effect of external electric fields on the electronic structure of (5,5)/(10,0) metal–semiconductor single wall carbon nanotube intramolecule junction. *Physica E* **2010**, *42*, 1590 – 1596. doi:10.1016/j.physe.2010.01.003.

199.   E.R. Kandel, J.H. Schwartz, T.J. *Essentials of Neural Science and Behavior*; Appleton & Lange, Stamford Connecticut, US, 1995; pp. Ch. II,III,IV.

200.   Weiss, T. *Cellular Biophysics*; MIT Press, Cambridge MA, US, 1995; pp. Vol. 1,2.

201.   Ajayan, P.M. Nanotubes from Carbon. *Chem. Rev.* **1999**, *99*, 1787–1800. doi:10.1021/cr970102g.

202. Forró, L.; Schönenberger, C., Physical Properties of Multi-wall Nanotubes. In *Carbon Nanotubes: Synthesis, Structure, Properties, and Applications*; Dresselhaus, M.S.; Dresselhaus, G.; Avouris, P., Eds.; Springer Berlin Heidelberg: Berlin, Heidelberg, 2001; pp. 329–391. doi:10.1007/3-540-39947-X-13.

203. Hashimoto, A.; Suenaga, K.; Urita, K.; Shimada, T.; Sugai, T.; Bandow, S.; Shinohara, H.; Iijima, S. Atomic Correlation Between Adjacent Graphene Layers in Double-Wall Carbon Nanotubes. *Phys. Rev. Lett.* **2005**, *94*, 045504. doi:10.1103/PhysRevLett.94.045504.

204. Kiang, C.H.; Endo, M.; Ajayan, P.M.; Dresselhaus, G.; Dresselhaus, M.S. Size Effects in Carbon Nanotubes. *Phys. Rev. Lett.* **1998**, *81*, 1869–1872. doi:10.1103/PhysRevLett.81.1869.

205. Tison, Y.; Giusca, C.; Stolojan, V.; Hayashi, Y.; Silva, S. The inner shell influence on the electronic structure of double-walled carbon nanotubes. *Adv. Mater.* **2008**, *20*, 189–194. doi:10.1002/adma.200700399.

206. Moradian, R.; Azadi, S.; Refii-tabar, H. When double-wall carbon nanotubes can become metallic or semiconducting. *J. Phys.: Condens. Matter* **2007**, *19*, 176209. doi:10.1088/0953-8984/19/17/176209.

207. Lim, S.C.; Jo, C.S.; Jeong, H.J.; Shin, Y.M.; Lee, Y.H.; Samayoa, I.A.; Choi, J. Effect of Oxidation on Electronic and Geometric Properties of Carbon Nanotubes. *Jpn. J. Appl. Phys.* **2002**, *41*, 5635–5639. doi:10.1143/jjap.41.5635.

208. Girvin, S.M.; Glazman, L.I.; Jonson, M.; Penn, D.R.; Stiles, M.D. Quantum fluctuations and the single-junction Coulomb blockade. *Phys. Rev. Lett.* **1990**, *64*, 3183–3186. doi:10.1103/PhysRevLett.64.3183.

209. Egger, R.; Gogolin, A.O. Bulk and Boundary Zero-Bias Anomaly in Multiwall Carbon Nanotubes. *Phys. Rev. Lett.* **2001**, *87*, 066401. doi:10.1103/PhysRevLett.87.066401.

210. Frank, S.; Poncharal, P.; Wang, Z.L.; Heer, W.A.d. Carbon Nanotube Quantum Resistors. *Science* **1998**, *280*, 1744–1746. doi:10.1126/science.280.5370.1744.

211. Liang, W.; Bockrath, M.; Bozovic, D.; Hafner, J.; Tinkham, M.; Park, H. Fabry-Perot interference in a nanotube electron waveguide. *Nature* **2001**, *411*, 665–9. doi:10.1038/35079517.

212. Linke, H.; Omling, P.; Xu, H.; Lindelof, P.E. Electron-electron interaction in a narrow, disordered electron gas in nonequilibrium. *Phys. Rev. B* **1997**, *55*, 4061–4064. doi:10.1103/PhysRevB.55.4061.

213. Semet, V.; Binh, V.T.; Guillot, D.; Teo, K.B.K.; Chhowalla, M.; Amaratunga, G.A.J.; Milne, W.I.; Legagneux, P.; Pribat, D. Reversible electromechanical characteristics of individual multiwall carbon nanotubes. *Appl. Phys. Lett.* **2005**, *87*, 223103. doi:10.1063/1.2136229.

214. Aharonov, Y.; Bohm, D. Further Considerations on Electromagnetic Potentials in the Quantum Theory. *Phys. Rev.* **1961**, *123*, 1511–1524. doi:10.1103/PhysRev.123.1511.

215. Stetter, A.; Vancea, J.; Back, C.H. Determination of the intershell conductance in a multiwall carbon nanotube. *Appl. Phys. Lett.* **2008**, *93*, 172103. doi:10.1063/1.3006426.

216. Naeemi, A.; Meindl, J.D. Compact physical models for multiwall carbon-nanotube interconnects. *IEEE Electr. Device Lett.* **2006**, *27*, 338–340. doi:10.1109/LED.2006.873765.

217. Zeitler, R.; Fromherz, P. The Thermal Voltage Fluctuations in the Planar Core-Coat Conductor of a Neuron-Semiconductor Interface. *Langmuir* **2013**, *29*, 6084–6090. doi:10.1021/la4002169.

218. Wei, D.; Liu, Y. The Intramolecular Junctions of Carbon Nanotubes. *Adv. Mater.* **2008**, *20*, 2815–2841. doi:10.1002/adma.200800589.

219. Kim, J.; Kim, J.R.; Lee, J.O.; Park, J.W.; So, H.M.; Kim, N.; Kang, K.; Yoo, K.H.; Kim, J.J. Fano Resonance in Crossed Carbon Nanotubes. *Phys. Rev. Lett.* **2003**, *90*, 166403. doi:10.1103/PhysRevLett.90.166403.

220. Park, J.Y.; Rosenblatt, S.; Yaish, Y.; Sazonova, V.; Üstünel, H.; Braig, S.; Arias, T.A.; Brouwer, P.W.; McEuen, P.L. Electron-Phonon Scattering in Metallic Single-Walled Carbon Nanotubes. *Nano Lett.* **2004**, *4*, 517–520. doi:10.1021/nl035258c.

221. Salahuddin, S.; Lundstrom, M.; Datta, S. Transport effects on signal propagation in quantum wires. *IEEE Trans. Electron Dev.* **2005**, *52*, 1734–1742. doi:10.1109/TED.2005.852170.

222. Alicea, J.; Bena, C.; Balents, L.; Fisher, M.P.A. Charge accumulation on a Luttinger liquid. *Phys. Rev. B* **2004**, *69*, 155332. doi:10.1103/PhysRevB.69.155332.

223. Fuhrer, M.; Lim, A.; Shih, L.; Varadarajan, U.; Zettl, A.; McEuen, P. Transport through crossed nanotubes. *Physica E* **2000**, *6*, 868–871. doi:10.1016/S1386-9477(99)00228-3.

224. Beck, M.; Shylendra, A.; Sangwan, V.; Guo, S.; Rojas, W.; Yoo, H.; Bergeron, H.; Su, K.; Trivedi, A.; Hersam, M. Spiking neurons from tunable Gaussian heterojunction transistors. *Nat. Commun.* **2020**, *11*, Art.N. 1565. doi:10.1038/s41467-020-15378-7.

225. Jariwala, D.; Sangwan, V.K.; Lauhon, L.J.; Marks, T.J.; Hersam, M.C. Carbon nanomaterials for electronics, optoelectronics, photovoltaics, and sensing. *Chem. Soc. Rev.* **2013**, *42*, 2824–2860. doi:10.1039/C2CS35335K.

226. Buldum, A.; Lu, J.P. Contact resistance between carbon nanotubes. *Phys. Rev. B* **2001**, *63*, 161403. doi:10.1103/PhysRevB.63.161403.

227. Yoon, Y.G.; Mazzoni, M.S.C.; Choi, H.J.; Ihm, J.; Louie, S.G. Structural Deformation and Intertube Conductance of Crossed Carbon Nanotube Junctions. *Phys. Rev. Lett.* **2001**, *86*, 688–691. doi:10.1103/PhysRevLett.86.688.

228. Kim, D.H.; Huang, J.; Shin, H.K.; Roy, S.; Choi, W. Transport Phenomena and Conduction Mechanism of Single-Walled Carbon Nanotubes (SWNTs) at Y- and Crossed-Junctions. *Nano Lett.* **2006**, *6*, 2821–2825. doi:10.1021/nl061977q.

229. He, H.B.; Zhou, J.C.; Hu, H.F.; Li, Y.B. Numerical simulation of I–V characteristics of carbon nanotube based tunneling systems. *Diam. Relat. Mater.* **2001**, *10*, 1814 – 1817. Proceedings of the 7th International Conference on New Diamond Science and Technology(ICNDST-7), doi:10.1016/S0925-9635(01)00456-3.

230. Chen, Y.F.; Fuhrer, M.S. Tuning from Thermionic Emission to Ohmic Tunnel Contacts via Doping in Schottky-Barrier Nanotube Transistors. *Nano Lett.* **2006**, *6*, 2158–2162. doi:10.1021/nl061379b.

231. Liu, P.; Wei, Y.; Jiang, K.; Sun, Q.; Zhang, X.; Fan, S.; Zhang, S.; Ning, C.; Deng, J. Thermionic emission and work function of multiwalled carbon nanotube yarns. *Phys. Rev. B* **2006**, *73*, 235412. doi:10.1103/PhysRevB.73.235412.

232. Appenzeller, J.; Radosavljević, M.; Knoch, J.; Avouris, P. Tunneling Versus Thermionic Emission in One-Dimensional Semiconductors. *Phys. Rev. Lett.* **2004**, *92*, 048301. doi:10.1103/PhysRevLett.92.048301.

233. Gao, B.; Komnik, A.; Egger, R.; Glattli, D.C.; Bachtold, A. Evidence for Luttinger-Liquid Behavior in Crossed Metallic Single-Wall Nanotubes. *Phys. Rev. Lett.* **2004**, *92*, 216804. doi:10.1103/PhysRevLett.92.216804.

234. Wakaya, F.; Katayama, K.; Gamo, K. Contact resistance of multiwall carbon nanotubes. *Microelectron. Eng.* **2003**, *67-68*, 853 – 857. Proceedings of the 28th International Conference on Micro- and Nano-Engineering, doi:10.1016/S0167-9317(03)00147-3.

235. Meunier, V.; Nardelli, M.B.; Bernholc, J.; Zacharia, T.; Charlier, J.C. Intrinsic electron transport properties of carbon nanotube Y-junctions. *Appl. Phys. Lett.* **2002**, *81*, 5234–5236. doi:10.1063/1.1533842.

236. Smith, P.R.; Carey, J.D.; Cox, D.C.; Forrest, R.D.; Silva, S.R.P. On the importance of the electrostatic environment for the transport properties of freestanding multiwall carbon nanotubes. *Nanotechnology* **2009**, *20*, 145202. doi:10.1088/0957-4484/20/14/145202.

237. Bachtold, A.; de Jonge, M.; Grove-Rasmussen, K.; McEuen, P.L.; Buitelaar, M.; Schönenberger, C. Suppression of Tunneling into Multiwall Carbon Nanotubes. *Phys. Rev. Lett.* **2001**, *87*, 166801. doi:10.1103/PhysRevLett.87.166801.

238. Hunger, T.; Lengeler, B.; Appenzeller, J. Transport in ropes of carbon nanotubes: Contact barriers and Luttinger liquid theory. *Phys. Rev. B* **2004**, *69*, 195406. doi:10.1103/PhysRevB.69.195406.

239. Basu, R.; Iannacchione, G. Dielectric response of multiwalled carbon nanotubes as a function of applied ac-electric fields. *J. Appl. Phys.* **2008**, *104*, 114107. doi:10.1063/1.3035963.

240. Zhao, Y.; Wei, B.; Ajayan, P.; Ramanath, G.; Lu, T.M.; Wang, G.C.; Rubio, A.; Roche, S. Frequency-dependent electrical transport in carbon nanotubes. *Phys. Rev. B* **2001**, *64*, 2014021–2014024.

241. Meunier, V.; Nardelli, M.B.; Bernholc, J.; Zacharia, T.; Charlier, J.C. Intrinsic electron transport properties of carbon nanotube Y-junctions. *Appl. Phys. Lett.* **2002**, *81*, 5234–5236. doi:10.1063/1.1533842.

242. Zhang, W.J.; Zhang, J.Y.; Li, P.J.; Shen, X.; Zhang, Q.F.; Wu, J.L. The effects of contacts and ambipolar electrical transport in nitrogen doped multiwall carbon nanotubes. *Nanotechnology* **2008**, *19*, 085202. doi:10.1088/0957-4484/19/8/085202.

243. Collins, P.; Bradley, K.; Ishigami, M.; Zettl, A. Extreme Oxygen Sensitivity of Electronic Properties of Carbon Nanotubes. *Science* **2000**, *287*, 1801–4. doi:10.1126/science.287.5459.1801.

244. Dumitrescu, I.; Wilson, N.R.; Macpherson, J.V. Functionalizing Single-Walled Carbon Nanotube Networks: Effect on Electrical and Electrochemical Properties. *J. Phys. Chem. C* **2007**, *111*, 12944–12953. doi:10.1021/jp067256x.

245. Wang, S.; Li, Y.; Zhao, R.; Jin, T.; Zhang, L.; Li, X. Chitosan surface modified electrospun poly(-caprolactone)/carbon nanotube composite fibers with enhanced mechanical, cell proliferation and antibacterial properties. *Int. J. Biol. Macromol.* **2017**, *104*, 708—715. doi:10.1016/j.ijbiomac.2017.06.044.

246. Teo, K.; Singh, C.; Chhowalla, M.; Milne, W. Catalytic Synthesis of Carbon Nanotubes and Nanofibers. *Encyclopedia of Nanoscience and Nanotechnology* **2003**, *1*, 665.

247. Fa, W.; Chen, J.; Liu, H.; Dong, J. Structural and electronic properties of the metal-metal intramolecular junctions of single-walled carbon nanotubes. *Phys. Rev. B* **2004**, *69*, 235413. doi:10.1103/PhysRevB.69.235413.

248. Hu, W.; Peng, C.; Lv, M.; Li, X.; Zhang, Y.; Chen, N.; Fan, C.; Huang, Q. Protein Corona-Mediated Mitigation of Cytotoxicity of Graphene Oxide. *ACS Nano* **2011**, *5*, 3693–3700. doi:10.1021/nn200021j.

249. Heremans, J., Nanometer-Scale Thermoelectric Materials. In *Springer Handbook of Nanotechnology*; Bhushan, B., Ed.; Springer Berlin Heidelberg: Berlin, Heidelberg, 2007; pp. 345–374. doi:10.1007/978-3-540-29857-1-12.

250. Li, H.; Pan, L.; Zhang, Y.; Zou, L.; Sun, C.; Zhan, Y.; Sun, Z. Kinetics and thermodynamics study for electrosorption of NaCl onto carbon nanotubes and carbon nanofibers electrodes. *Chem. Phys. Lett.* **2010**, *485*, 161 – 166. doi:10.1016/j.cplett.2009.12.031.

251. Lim, S.C.; Choi, Y.C.; Jeong, H.J.; Shin, Y.M.; An, K.H.; Bae, D.J.; Lee, Y.H.; Lee, N.S.; Kim, J.M. Effect of Gas Exposure on Field Emission Properties of Carbon Nanotube Arrays. *Adv. Mater.* **2001**, *13*, 1563–1567. doi:10.1002/1521-4095(200110)13:20$<$1563$::$AID-ADMA1563$>$3.0.CO;2-H.

252. Hwang, Y.; Lee, Y.H. Adsorption of H$_2$O Molecules at the Open Ends of Singlewalled Carbon Nanotubes. *J. Korean Phys. Soc.* **2003**, pp. S267–S271.

253. Miyata, Y.; Yanagi, K.; Maniwa, Y.; Kataura, H. Highly Stabilized Conductivity of Metallic Single Wall Carbon Nanotube Thin Films. *J. Phys. Chem. C* **2008**, *112*, 3591–3596. doi:10.1021/jp077709d.

254. Fajardo, A.; Lewis, N. Rate Constants for Charge Transfer Across Semiconductor-Liquid Interfaces. *Science* **1996**, *274*, 969–72. doi:10.1126/science.274.5289.968.

255. Sebastian, K.; Doyen, G. Electrochemical scanning tunneling microscopy: does the orientational polarization of the liquid play any role? *Surf. Sci. Lett.* **1993**, *290*, L703 – L710. doi:10.1016/0167-2584(93)90928-C.

256. Rosenwaks, Y.; Thacker, B.R.; Bertness, K.; Nozik, A.J. Ideal Behavior at Illuminated Semiconductor-Liquid Junctions. *J. Phys. Chem.* **1995**, *99*, 7871–7874. doi:10.1021/j100020a007.

257. Hepel, M. Quantum conductance of monatomic Ni nanobridges. *Electrochim. Acta* **2006**, *51*, 5811–5824. doi:10.1016/j.electacta.2006.03.034.

258. de Gennes, P.G. *Scaling Concepts in Polymer Physics; Cornell University Press*; Cornell University Press, Ithaca, US, 1979; chapter 1,2,3.

259. Skákalová, V.; Kaiser, A.B.; Woo, Y.S.; Roth, S. Electronic transport in carbon nanotubes: From individual nanotubes to thin and thick networks. *Phys. Rev. B* **2006**, *74*, 085403. doi:10.1103/PhysRevB.74.085403.

260. Morigaki, K. *Physics of Amorphous Semiconductors*; Imperial College Press, London, 1999; chapter 7, pp. 1–5. doi:10.1142/9789812817556-0001.

261. Yu, L.; Shearer, C.; Shapter, J. Recent Development of Carbon Nanotube Transparent Conductive Films. *Chem. Rev.* **2016**, *116*, 13413–13453. doi:10.1021/acs.chemrev.6b00179.

262. Lipomi, D.J.; Lee, J.A.; Vosgueritchian, M.; Tee, B.C.K.; Bolander, J.A.; Bao, Z. Electronic Properties of Transparent Conductive Films of PEDOT:PSS on Stretchable Substrates. *Chem. Mater.* **2012**, *24*, 373–382. doi:10.1021/cm203216m.

263. Topinka, M.A.; Rowell, M.W.; Goldhaber-Gordon, D.; McGehee, M.D.; Hecht, D.S.; Gruner, G. Charge Transport in Interpenetrating Networks of Semiconducting and Metallic Carbon Nanotubes. *Nano Lett.* **2009**, *9*, 1866–1871. doi:10.1021/nl803849e.

264. Xu, H.; Zhang, S.; Anlage, S.M.; Hu, L.; Grüner, G. Frequency- and electric-field-dependent conductivity of single-walled carbon nanotube networks of varying density. *Phys. Rev. B* **2008**, *77*, 075418. doi:10.1103/PhysRevB.77.075418.

265. Han, J.; Zhu, Z.; Wang, Z.; Zhang, W.; Yu, L.; Sun, L.; Wang, T.; He, F.; Liao, Y. The conductivity of single walled nanotube films in Terahertz region. *Phys. Lett. A* **2003**, *310*, 457 – 459. doi:10.1016/S0375-9601(03)00382-7.

266. Dyre, J.C.; Schröder, T.B. Universality of ac conduction in disordered solids. *Rev. Mod. Phys.* **2000**, *72*, 873–892. doi:10.1103/RevModPhys.72.873.

267. Petit, P.; Jouguelet, E.; Fischer, J.E.; Rinzler, A.G.; Smalley, R.E. Electron spin resonance and microwave resistivity of single-wall carbon nanotubes. *Phys. Rev. B* **1997**, *56*, 9275–9278. doi:10.1103/PhysRevB.56.9275.

268. M. Doi, S.E. *The Theory of Polymer Dynamics*; Oxford University Press, New York, US, 1994; chapter 3,8,9,10. doi:10.1142/9789812817556-0001.

269. Mezzasalma, S.A. *Macromolecules in Solution and Brownian Relativity*; Academic Press-Elsevier, London, 2008; pp. Ch. 2,3. doi:10.1016/S1573-4285(07)00009-9.

270. Hecht, D.; Hu, L.; Grüner, G. Conductivity scaling with bundle length and diameter in single walled carbon nanotube networks. *Appl. Phys. Lett.* **2006**, *89*, 133112. doi:10.1063/1.2356999.

271. de Asis Jr, E.D.; Leung, J.; Wood, S.; Nguyen, C.V. Empirical study of unipolar and bipolar configurations using high resolution single multi-walled carbon nanotube electrodes for electrophysiological probing of electrically excitable cells. *Nanotechnology* **2010**, *21*, 125101. doi:10.1088/0957-4484/21/12/125101.

272. Graugnard, E.; de Pablo, P.J.; Walsh, B.; Ghosh, A.W.; Datta, S.; Reifenberger, R. Temperature dependence of the conductance of multiwalled carbon nanotubes. *Phys. Rev. B* **2001**, *64*, 125407. doi:10.1103/PhysRevB.64.125407.

273. Mishchenko, E.G.; Andreev, A.V.; Glazman, L.I. Zero-Bias Anomaly in Disordered Wires. *Phys. Rev. Lett.* **2001**, *87*, 246801. doi:10.1103/PhysRevLett.87.246801.

274. Astorga, H.; Mendoza, D. Electrical conductivity of multiwall carbon nanotubes thin films. *Opt. Mater.* **2005**, *27*, 1228 – 1230. Proceedings of the First Topical Meeting on Nanostructured Materials and Nanotechnology CIO 2004, doi:10.1016/j.optmat.2004.11.014.

275. Sun, Y.; Miyasato, T.; Kirimoto, K.; Kusunoki, M. Metallic–nonmetallic transition on the conductivity temperature dependence of multiwall carbon nanotubes. *Appl. Phys. Lett.* **2005**, *86*, 223108. doi:10.1063/1.1927696.

276. Nick, C.; Yadav, S.; Joshi, R.; Thielemann, C.; Schneider, J. Growth and structural discrimination of cortical neurons on randomly oriented and vertically aligned dense carbon nanotube networks. *Beilstein J. Nanotech.* **2014**, *5*, 1575–9. doi:10.3762/bjnano.5.169.

277. Vashist, S.K.; Zheng, D.; Al-Rubeaan, K.; Luong, J.H.; Sheu, F.S. Advances in carbon nanotube based electrochemical sensors for bioanalytical applications. *Biotechnol. Adv.* **2011**, *29*, 169 – 188. doi:10.1016/j.biotechadv.2010.10.002.

278. Jacobs, C.B.; Peairs, M.J.; Venton, B.J. Review: Carbon nanotube based electrochemical sensors for biomolecules. *Anal. Chim. Acta* **2010**, *662*, 105 – 127. doi:10.1016/j.aca.2010.01.009.

279. Arsiwala, A.; Desai, P.; Patravale, V. Recent Advances in Micro/Nanoscale Biomedical Implants. *J. Control. Release* **2014**, *189*, 25–45. doi:10.1016/j.jconrel.2014.06.021.

280. Laing, C.R.; Longtin, A. Periodic forcing of a model sensory neuron. *Phys. Rev. E* **2003**, *67*, 051928. doi:10.1103/PhysRevE.67.051928.

281. Masoller, C.; Torrent, M.C.; García-Ojalvo, J. Interplay of subthreshold activity, time-delayed feedback, and noise on neuronal firing patterns. *Phys. Rev. E* **2008**, *78*, 041907. doi:10.1103/PhysRevE.78.041907.

282. Kavan, L.; Dunsch, L., Electrochemistry of Carbon Nanotubes. In *Carbon Nanotubes: Advanced Topics in the Synthesis, Structure, Properties and Applications*; Jorio, A.; Dresselhaus, G.; Dresselhaus, M.S., Eds.; Springer Berlin Heidelberg: Berlin, Heidelberg, 2008; pp. 567–604. doi:10.1007/978-3-540-72865-8-18.

283. Li, C.; Chou, T.W. Electrostatic charge distribution on single-walled carbon nanotubes. *Appl. Phys. Lett.* **2006**, *89*, 063103. doi:10.1063/1.2335411.

284. Keblinski, P.; Nayak, S.K.; Zapol, P.; Ajayan, P.M. Charge Distribution and Stability of Charged Carbon Nanotubes. *Phys. Rev. Lett.* **2002**, *89*, 255503. doi:10.1103/PhysRevLett.89.255503.

285. Léonard, F.m.c.; Tersoff, J. Novel Length Scales in Nanotube Devices. *Phys. Rev. Lett.* **1999**, *83*, 5174–5177. doi:10.1103/PhysRevLett.83.5174.

286. Xue, Y.; Ratner, M.A. Scaling analysis of electron transport through metal–semiconducting carbon nanotube interfaces: Evolution from the molecular limit to the bulk limit. *Phys. Rev. B* **2004**, *70*, 205416. doi:10.1103/PhysRevB.70.205416.

287. Morrison, S. *Electrochemistry at semiconductor and oxidized metal electrodes*; Plenum Press, New York, US, 1980; chapter 3.

288. Israelachvili, J. *Intermolecular and Surface Forces*; Academic Press, London, UK, 1992; chapter 12. doi:10.1016/C2009-0-21560-1.

289.   Mezzasalma, S.; Baldovino, D. Characterization of Silicon Nitride Surface in Water and Acid Environment: A General Approach to the Colloidal Suspensions. *J. Colloid Interface Sci.* **1996**, *180*, 413 – 420. doi:10.1006/jcis.1996.0320.

290.   Lyklema, J.; Minor, M. On surface conduction and its role in electrokinetics. *Colloid. Surf. A* **1998**, *140*, 33 – 41. doi:10.1016/S0927-7757(97)00266-5.

291.   Harris, D. *Quantitative Chemical Analysis*; W.H. Freeman and Company, New York, US, 1987; chapter 19.

292.   J.O'M. Bockris, D.D. *Electro-Chemical Science*; Barnes, Noble, New York, US, 1972.

293.   Raimondi, F.; Scherer, G.G.; Kötz, R.; Wokaun, A. Nanoparticles in Energy Technology: Examples from Electrochemistry and Catalysis. *Angew. Chem. Int. Edit.* **2005**, *44*, 2190–2209. doi:10.1002/anie.200460466.

294.   Tang, T.; Jagota, A. Model for Modulation of Conductance in a Carbon Nanotube Field Effect Transistor by Electrochemical Gating. *J. Comp. Theor. Nanosci.* **2008**, *5*, 1989–1996. doi:10.1166/jctn.2008.1005.

295.   Corio, P.; Jorio, A.; Demir, N.; Dresselhaus, M.S. Spectro-electrochemical studies of single wall carbon nanotubes films. *Chem. Phys. Lett.* **2004**, *392*, 396–402. doi:10.1016/j.cplett.2004.05.050.

296.   Heller, I.; Kong, J.; Williams, K.A.; Dekker, C.; Lemay, S.G. Electrochemistry at Single-Walled Carbon Nanotubes: The Role of Band Structure and Quantum Capacitance. *J. Am. Chem. Soc.* **2006**, *128*, 7353–7359. doi:10.1021/ja061212k.

297.   Dai, J.; Li, J.; Zeng, H.; Cui, X. Measurements on quantum capacitance of individual single walled carbon nanotubes. *Appl. Phys. Lett.* **2009**, *94*, 093114. doi:10.1063/1.3093443.

298.   Uchida, K.; Okada, S.; Shiraishi, K.; Oshiyama, A. Quantum effects in a double-walled carbon nanotube capacitor. *Phys. Rev. B* **2007**, *76*, 155436. doi:10.1103/PhysRevB.76.155436.

299.   Andrews, R. Neuromodulation. *Ann. N.Y. Acad. Sci.* **2010**, *1199*, 212–20. doi:10.1111/j.1749-6632.2009.05380.x.

300.   Mezzasalma, S.A. Influence of a nanorod molecular layer on the biological activity of neuronal cells. A semiclassical model for complex solid/liquid interfaces with carbon nanotubes. *J. Coll. Interface Sci.* **2011**, *360*, 805 – 817. doi:10.1016/j.jcis.2011.05.007.

301.   Horowitz, J.; Gingrich, T. Thermodynamic uncertainty relations constrain non-equilibrium fluctuations. *Nat. Phys.* **2019**, *16*, 1–6. doi:10.1038/s41567-019-0702-6.

302.   Latessa, L.; Pecchia, A.; Di Carlo, A.; Lugli, P. Negative quantum capacitance of gated carbon nanotubes. *Phys. Rev. B* **2005**, *72*, 035455. doi:10.1103/PhysRevB.72.035455.

303.   Kavan, L.; Dunsch, L.; Kataura, H. Electrochemical tuning of electronic structure of carbon nanotubes and fullerene peapods. *Carbon* **2004**, *42*, 1011 – 1019. European Materials Research Society 2003, Symposium B: Advanced Multifunctional Nanocarbon Materials and Nanosystems, doi:10.1016/j.carbon.2003.12.024.

304.   Goldsmith, B.; Coroneus, J.; Khalap, V.; Kane, A.; Weiss, G.; Collins, P. Conductance-Controlled Point Functionalization of Single-Walled Carbon Nanotubes. *Science* **2007**, *315*, 77–81. doi:10.1126/science.1135303.

305.   Larrimore, L.M.; Nad, S.; Zhou, X.; Abruña, H.D.; McEuen, P.L. Probing electrostatic potentials in solution with carbon nanotube transistors. *Nano Lett.* **2006**, *6 7*, 1329–33.

306.   Barisci, J.N.; Wallace, G.G.; Baughman, R.H. Electrochemical Characterization of Single-Walled Carbon Nanotube Electrodes. *J. Electrochem. Soc.* **2000**, *147*, 4580. doi:10.1149/1.1394104.

307.   Barisci, J.; Wallace, G.; Chattopadhyay, D.; Baughman, R. Electrochemical Properties of Single-Wall Carbon Nanotube Electrodes. *J. Electrochem. Soc.* **2003**, *150*, E409–E415. doi:10.1149/1.1593045.

308.   Zheng, M.; Diner, B.A. Solution Redox Chemistry of Carbon Nanotubes. *J. Am. Chem. Soc.* **2004**, *126*, 15490–15494. doi:10.1021/ja0457967.

309.   Kibria, A.F.; Mo, Y.; Park, K.; Nahm, K.; Yun, M. Electrochemical hydrogen storage behaviors of CVD, AD and LA grown carbon nanotubes in KOH medium. *Int. J. Hydrog. Energy* **2001**, *26*, 823 – 829. doi:10.1016/S0360-3199(01)00007-6.

310.   Prosini, P.P.; Pozio, A.; Botti, S.; Ciardi, R. Electrochemical studies of hydrogen evolution, storage and oxidation on carbon nanotube electrodes. *J. Power Sources* **2003**, *118*, 265 – 269. doi:10.1016/S0378-7753(03)00097-1.

311.   Niessen, R.; Jonge, de, J.; Notten, P. The electrochemistry of carbon nanotubes: I. Aqueous electrolyte. *J. Electrochem. Soc.* **2006**, *153*, A1484–A1491. doi:10.1149/1.2205184.

312.   Wong, E.L.S.; Compton, R.G. Chemical Reaction of Reagents Covalently Confined to a Nanotube Surface: Nanotube-Mediated Redox Chemistry. *J. Phys. Chem. C* **2008**, *112*, 8122–8126. doi:10.1021/jp802467a.

313. Frackowiak, E.; Béguin, F. Carbon materials for the electrochemical storage of energy in capacitors. *Carbon* **2001**, *39*, 937 – 950. doi:10.1016/S0008-6223(00)00183-4.

314. Kaiser, J.P.; Wick, P.; Manser, P.; Spohn, P.; Bruinink, A. Single walled carbon nanotubes (SWCNT) affect cell physiology and cell architecture. *J. Mater. Sci. Mater. Med.* **2008**, *19*, 1523–7. doi:10.1007/s10856-007-3296-y.

315. Gupta, S.; Robertson, J. Ion transport and electrochemical tuning of Fermi level in single-wall carbon nanotube probed by in situ Raman scattering. *J. Appl. Phys.* **2006**, *100*, 083711. doi:10.1063/1.2357839.

316. Cronin, S.; Barnett, R.; Tinkham, M.; Chou, S.; Rabin, O.; Dresselhaus, M.; Swan, A.; Ünlü, M.S.; Goldberg, B. Electrochemical gating of individual single-wall carbon nanotubes observed by electron transport measurements and resonant Raman spectroscopy. *Appl. Phys. Lett.* **2004**, *84*, 2052–2054. doi:10.1063/1.1666997.

317. Madden, J.; Barisci, J.; Anquetil, P.; Spinks, G.; Wallace, G.; Baughman, R.; Hunter, I. Fast Carbon Nanotube Charging and Actuation. *Adv. Mater.* **2006**, *18*, 870–873. doi:10.1002/adma.200502136.

318. Yun, Y.; Shanov, V.; Tu, Y.; Schulz, M.J.; Yarmolenko, S.; Neralla, S.; Sankar, J.; Subramaniam, S. A Multi-Wall Carbon Nanotube Tower Electrochemical Actuator. *Nano Lett.* **2006**, *6*, 689–693. doi:10.1021/nl052435w.

319. Jagtap, P.; Gowda, P.; Das, B.; Kumar, P. Effect of electro-mechanical coupling on actuation behavior of a carbon nanotube cellular structure. *Carbon* **2013**, *60*, 169 – 174. doi:10.1016/j.carbon.2013.04.010.

320. Murakoshi, K.; ichi Okazaki, K. Electrochemical potential control of isolated single-walled carbon nanotubes on gold electrode. *Electrochim. Acta* **2005**, *50*, 3069 – 3075. doi:10.1016/j.electacta.2004.12.045.

321. Papakonstantinou, P.; Kern, R.; Robinson, L.; Murphy, H.; Irvine, J.; McAdams, E.; McLaughlin, J.; McNally, T. Fundamental Electrochemical Properties of Carbon Nanotube Electrodes. *Fuller. Nanotub. Car. Nanostr.* **2005**, *13*, 91–108. doi:10.1081/FST-200050684.

322. Liu, Z.; Xu, J.; Chen, D.; Shen, G. Flexible electronics based on inorganic nanowires. *Chem. Soc. Rev.* **2015**, *44*, 161–192. doi:10.1039/C4CS00116H.

323. Grahame, D.C. The Electrical Double Layer and the Theory of Electrocapillarity. *Chem. Rev.* **1947**, *41*, 441–501. doi:10.1021/cr60130a002.

324. Sato, N. *Electrochemistry at Metal and Semiconductor Electrodes*; Elsevier Science: Amsterdam, 1998; chapter V, pp. 119 – 199. doi:10.1016/B978-044482806-4/50005-2.

325. Gleixner, R.; Fromherz, P. The Extracellular Electrical Resistivity in Cell Adhesion. *Biophys. J.* **2006**, *90*, 2600–11. doi:10.1529/biophysj.105.072587.

326. Siddiqi, F.A.; Alvi, N.I. Transport studies with model membrane. *J. Polym. Sci. B* **1989**, *27*, 1499–1517. doi:10.1002/polb.1989.090270711.

327. Heller, I.; Kong, J.; Heering, H.A.; Williams, K.A.; Lemay, S.G.; Dekker, C. Individual Single-Walled Carbon Nanotubes as Nanoelectrodes for Electrochemistry. *Nano Lett.* **2005**, *5*, 137–142. doi:10.1021/nl048200m.

328. Campbell, J.; Sun, l.; Crooks, R. Electrochemistry Using Single Carbon Nanotubes. *J. Am. Chem. Soc.* **1999**, *121*, 3779–3780. doi:10.1021/ja990001v.

329. Nick, C.; Thielemann, C. Are Carbon Nanotube Microelectrodes Manufactured from Dispersion Stable Enough for Neural Interfaces? *Bionanoscience* **2014**, *4*, 216–225. doi:10.1007/s12668-014-0141-x.

330. Paolucci, D.; Marcaccio, M.; Bruno, C.; Paolucci, F.; Tagmatarchis, N.; Prato, M. Voltammetric quantum charging capacitance behaviour of functionalised carbon nanotubes in solution. *Electrochim. Acta* **2008**, *53*, 4059 – 4064. doi:10.1016/j.electacta.2007.10.007.

331. Keefer, E.; Botterman, B.; Romero, M.; Rossi, A.; Gross, G. Carbon nanotube coating improves neuronal recordings. *Nat. Nanotechnol.* **2008**, *3*, 434–9. doi:10.1038/nnano.2008.174.

332. Britto, P.; Santhanam, K.; Ajayan, P. Carbon nanotube electrode for oxidation of dopamine. *Bioelectroch. Bioener.* **1996**, *41*, 121–125. doi:10.1016/0302-4598(96)05078-7.

333. Wu, F.; Yu, P.; Mao, L. Self-powered electrochemical systems as neurochemical sensors: toward self-triggered in vivo analysis of brain chemistry. *Chem. Soc. Rev.* **2017**, *46*, 2692–2704. doi:10.1039/C7CS00148G.

334. Wildgoose, G.; Banks, C.; Leventis, H.; Compton, R. Chemically Modified Carbon Nanotubes for Use in Electroanalysis. *Microchim. Acta* **2005**, *152*, 187–214. doi:10.1007/s00604-005-0449-x.

335. Chmiola, J.; Yushin, G.; Dash, R.K.; Hoffman, E.N.; Fischer, J.E.; Barsoum, M.W.; Gogotsi, Y. Double-Layer Capacitance of Carbide Derived Carbons in Sulfuric Acid. *Electrochem. Solid St. Lett.* **2005**, *8*, A357. doi:10.1149/1.1921134.

336. Zhang, M.; Yudasaka, M.; Iijima, S. Dissociation of Electrolytes in a Nano-aqueous System within Single-Wall Carbon Nanotubes. *J. Phys. Chem. B* **2005**, *109*, 6037–6039. doi:10.1021/jp044372w.

337. Wenseleers, W.; Cambré, S.; Čulin, J.; Bouwen, A.; Goovaerts, E. Effect of Water Filling on the Electronic and Vibrational Resonances of Carbon Nanotubes: Characterizing Tube Opening by Raman Spectroscopy. *Adv. Mater.* **2007**, *19*, 2274–2278. doi:10.1002/adma.200790063.

338. Nikolaev, P.; Bronikowski, M.J.; Bradley, R.; Rohmund, F.; Colbert, D.T.; Smith, K.; Smalley, R.E. Gas-phase catalytic growth of single-walled carbon nanotubes from carbon monoxide. *Chem. Phys. Lett.* **1999**, *313*, 91 – 97. doi:10.1016/S0009-2614(99)01029-5.

339. Wang, B.; Král, P. Dragging of Polarizable Nanodroplets by Distantly Solvated Ions. *Phys. Rev. Lett.* **2008**, *101*, 046103. doi:10.1103/PhysRevLett.101.046103.

340. Wilson, N.R.; Guille, M.; Dumitrescu, I.; Fernandez, V.R.; Rudd, N.C.; Williams, C.G.; Unwin, P.R.; Macpherson, J.V. Assessment of the Electrochemical Behavior of Two-Dimensional Networks of Single-Walled Carbon Nanotubes. *Anal. Chem.* **2006**, *78*, 7006–7015. doi:10.1021/ac0610661.

341. Barisci, J.N.; Wallace, G.G.; Baughman, R.H. Electrochemical studies of single-wall carbon nanotubes in aqueous solutions. *J. Electroanal. Chem.* **2000**, *488*, 92 – 98. doi:10.1016/S0022-0728(00)00179-0.

342. Zhang, H.; Cao, G.; Yang, Y.; Gu, Z. Comparison Between Electrochemical Properties of Aligned Carbon Nanotube Array and Entangled Carbon Nanotube Electrodes. *J. Electrochem. Soc.* **2008**, *155*, K19. doi:10.1149/1.2811864.

343. Hu, H.; Bhowmik, P.; Zhao, B.; Hamon, M.; Itkis, M.; Haddon, R. Determination of the acidic sites of purified single-walled carbon nanotubes by acid–base titration. *Chem. Phys. Lett.* **2001**, *345*, 25 – 28. doi:10.1016/S0009-2614(01)00851-X.

344. Hiemenz, P.; Rajagopalan, R. *Principles of Colloid and Surface Chemistry, revised and expanded*; Marcel Dekker, Inc., New York, US, 1997; chapter XII.

345. Kumar, H.; Mukherjee, B.; Lin, S.T.; Dasgupta, C.; Sood, A.K.; Maiti, P.K. Thermodynamics of water entry in hydrophobic channels of carbon nanotubes. *J. Chem. Phys.* **2011**, *134*, 124105. doi:10.1063/1.3571007.

346. Godin, A.; Varela, J.; Gao, Z.; Danné, N.; Dupuis, J.; Lounis, B.; Groc, L.; Cognet, L. Single-nanotube tracking reveals the nanoscale organization of the extracellular space in the live brain. *Nat. Nanotechnol.* **2016**, *12*, 238–243. doi:10.1038/nnano.2016.248.

347. Genet, S.; Costalat, R.; Burger, J. The Influence of Plasma Membrane Electrostatic Properties on the Stability of Cell Ionic Composition. *Biophys. J.* **2001**, *81*, 2442 – 2457. doi:10.1016/S0006-3495(01)75891-2.

348. Ohki, S. Membrane potential, surface potential, and ionic permeabilities. *Physiol. Chem. Phys.* **1981**, *13*, 195—210.

349. Hoyles, M.; Kuyucak, S.; Chung, S. Energy barrier presented to ions by the vestibule of the biological membrane channel. *Biophys. J.* **1996**, *70*, 1628 – 1642. doi:10.1016/S0006-3495(96)79726-6.

350. Genet, S.; Costalat, R.; Burger, J. A Few Comments on Electrostatic Interactions in Cell Physiology. *Acta Biotheor.* **2001**, *48*, 273–87. doi:10.1023/A:1010229531210.

351. Kuyucak, S.; Hoyles, M.; Chung, S.H. Analytical Solutions of Poisson's Equation for Realistic Geometrical Shapes of Membrane Ion Channels. *Biophys. J.* **1998**, *74*, 22 – 36. doi:10.1016/S0006-3495(98)77763-X.

352. Nelson, A.; McQuarrie, D. The effect of discrete charges on the electrical properties of a membrane. I. *J. Theor. Biol.* **1975**, *55*, 13 – 27. doi:10.1016/S0022-5193(75)80106-8.

353. Ilani, S.; Donev, L.; Kindermann, M.; Mceuen, P. Measurement of the quantum capacitance of interacting electrons in carbon nanotubes. *Nat. Phys.* **2006**, *2*, 687–691. doi:10.1038/nphys412.

354. Jonscher, A.K. The physical origin of negative capacitance. *J. Chem. Soc. Faraday Trans. 2* **1986**, *82*, 75–81. doi:10.1039/F29868200075.

355. Shulman, J.; Xue, Y.Y.; Tsui, S.; Chen, F.; Chu, C.W. General mechanism for negative capacitance phenomena. *Phys. Rev. B* **2009**, *80*, 134202. doi:10.1103/PhysRevB.80.134202.

356. Mezzasalma, S.A.; Koper, G.J.M. Semiclassical approach to electrorheological fluids. Influence of solid volume fraction on the suspension yield stress. *Colloid Polym. Sci.* **2002**, *280*, 160–166.

357. Partenskii, M.; Feldman, V. Electron and molecular effects in the double layer for the metal/electrolyte solution interface. *J. Electroanal. Chem. Interface Electrochem.* **1989**, *273*, 57 – 68. doi:10.1016/0022-0728(89)87003-2.

358. Abbott, N.J.; Rönnbäck, L.; Hansson, E. Astrocyte-endothelial interactions at the blood–brain barrier. *Nat. Rev. Neurosci.* **2006**, *7*, 41–53. doi:10.1038/nrn1824.

359. Daneman, R.; Prat, A. The Blood-Brain Barrier. *Cold Spring Harb. Perspect. Biol.* **2015**, *7*, a020412. doi:10.1101/cshperspect.a020412.

360. Chen, Y.; Liu, L. Modern methods for delivery of drugs across the blood–brain barrier. *Adv. Drug Deliv. Rev.* **2012**, *64*, 640–665. Delivery of Therapeutics to the Central Nervous System, doi:10.1016/j.addr.2011.11.010.

361. Noell, S.; Mack, A.; Wolburg-Buchholz, K.; Fallier-Becker, P. Brain endothelial cells and the glio-vascular complex. *Cell Tissue Res.* **2009**, *335*, 75–96. doi:10.1007/s00441-008-0658-9.

362. Henna, T.; Raphey, V.; Sankar, R.; Ameena Shirin, V.; Gangadharappa, H.; Pramod, K. Carbon nanostructures: The drug and the delivery system for brain disorders. *Int. J. Pharm.* **2020**, *587*, 119701. doi:10.1016/j.ijpharm.2020.119701.

363. Pérez-Martínez, F.; Guerra, J.; Posadas, I.; Ceña, V. Barriers to Non-Viral Vector-Mediated Gene Delivery in the Nervous System. *Pharm. Res.* **2011**, *28*, 1843–58. doi:10.1007/s11095-010-0364-7.

364. Kagan, V.E.; Kapralov, A.A.; St. Croix, C.M.; Watkins, S.C.; Kisin, E.R.; Kotchey, G.P.; Balasubramanian, K.; Vlasova, I.I.; Yu, J.; Kim, K.; Seo, W.; Mallampalli, R.K.; Star, A.; Shvedova, A.A. Lung Macrophages "Digest" Carbon Nanotubes Using a Superoxide/Peroxynitrite Oxidative Pathway. *ACS Nano* **2014**, *8*, 5610–5621. doi:10.1021/nn406484b.

365. Masoudi Asil, S.; Ahlawat, J.; Guillama Barroso, G.; Narayan, M. Nanomaterial based drug delivery systems for the treatment of neurodegenerative diseases. *Biomater. Sci.* **2020**, *8*, 4109–4128. doi:10.1039/D0BM00809E.

366. Strazielle, N.; Ghersi-Egea, J.F. Potential Pathways for CNS Drug Delivery Across the Blood-Cerebrospinal Fluid Barrier. *Curr. Pharm. Des.* **2016**, *22*, 5463 – 5476. doi:10.2174/1381612822666160726112115.

367. Rapoport, S. Osmotic Opening of the Blood–Brain Barrier: Principles, Mechanism, and Therapeutic Applications. *Cell. Mol. Neurobiol.* **2000**, *20*, 217–30. doi:10.1023/A:1007049806660.

368. Smith, Q.R.; Rapoport, S.I. Cerebrovascular Permeability Coefficients to Sodium, Potassium, and Chloride. *J. Neurochem.* **1986**, *46*, 1732–1742. doi:10.1111/j.1471-4159.1986.tb08491.x.

369. Nagpal, K.; Singh, S.K.; Mishra, D.N. Drug targeting to brain: a systematic approach to study the factors, parameters and approaches for prediction of permeability of drugs across BBB. *Expert Opin. Drug Deliv.* **2013**, *10*, 927–955. doi:10.1517/17425247.2013.762354.

370. Orthmann, A.; Fichtner, I.; Zeisig, R. Improving the transport of chemotherapeutic drugs across the bloo„brain barrier. *Expert Rev. Clin. Pharmacol.* **2011**, *4*, 477 – 490. doi:10.1586/ecp.11.26.

371. Engelhardt, B.; Sorokin, L. The blood-brain and the blood-cerebrospinal fluid barriers: Function and dysfunction. *Semin. Immunopathol.* **2009**, *31*, 497–511. doi:10.1007/s00281-009-0177-0.

372. Brasnjevic, I.; Steinbusch, H.; Schmitz, C.; Martinez-Martinez, P. Delivery of peptide and protein drugs over the bloodbrain barrier. *Progr. Neurobiol.* **2009**, *87*, 212–251. doi:10.1016/j.pneurobio.2008.12.002.

373. Tajes, M.; Ramos-Fernández, E.; Weng-Jiang, X.; Bosch-Morató, M.; Guivernau, B.; Eraso-Pichot, A.; Salvador, B.; Fernàndez-Busquets, X.; Roquer, J.; Muñoz, F.J. The blood-brain barrier: Structure, function and therapeutic approaches to cross it. *Mol. Membr. Biol.* **2014**, *31*, 152–167. doi:10.3109/09687688.2014.937468.

374. Oberdörster, G.; Oberdörster, E.; Oberdörster, J. Nanotoxicology: An Emerging Discipline Evolving from Studies of Ultrafine Particles. *Environ. Health Perspect.* **2005**, *113*, 823–839. doi:10.1289/ehp.7339.

375. Bergen, J.M.; Pun, S.H. Analysis of the intracellular barriers encountered by nonviral gene carriers in a model of spatially controlled delivery to neurons. *J. Gene Med.* **2008**, *10*, 187–197. doi:10.1002/jgm.1137.

376. Faraji, A.; Wipf, P. Nanoparticles in cellular drug delivery. *Bioorg. Med. Chem.* **2009**, *17*, 2950–62. doi:10.1016/j.bmc.2009.02.043.

377. Misra, A.; Ganesh, S.; Shahiwala, A.; Shah, S. Drug delivery to the central nervous system: A review. *J. Pharm. Pharm. Sci.* **2002**, *6*, 252–73.

378. Nguyen, K.; Nguyet, P.; Vo, T.; Duan, W.; Tran, P.; Thao, T. Strategies of Engineering Nanoparticles for Treating Neurodegenerative Disorders. *Curr. Drug Metab.* **2017**, *18*, 786 – 797. doi:10.2174/1389200218666170125114751.

379. Zhang, M.; Mao, X.; Yu, Y.; Wang, C.X.; Yang, Y.L.; Wang, C. Nanomaterials for Reducing Amyloid Cytotoxicity. *Adv. Mater.* **2013**, *25*, 3780–3801. doi:10.1002/adma.201301210.

380. Smith, S.A.; Selby, L.I.; Johnston, A.P.R.; Such, G.K. The Endosomal Escape of Nanoparticles: Toward More Efficient Cellular Delivery. *Bioconjug. Chem.* **2019**, *30*, 263–272. doi:10.1021/acs.bioconjchem.8b00732.

381. Boussif, O.; Lezoualc'h, F.; Zanta, M.A.; Mergny, M.D.; Scherman, D.; Demeneix, B.; Behr, J.P. A versatile vector for gene and oligonucleotide transfer into cells in culture and in vivo: polyethylenimine. *Proc. Natl. Acad. Sci.* **1995**, *92*, 7297–7301. doi:10.1073/pnas.92.16.7297.

382. Pérez-Martínez, F.; Carrión, B.; Ceña, V. The Use of Nanoparticles for Gene Therapy in the Nervous System. *J. Alzheimer's Dis.* **2012**, *31*, 697–710. doi:10.3233/JAD-2012-120661.

383. Aragon, M.J.; Topper, L.; Tyler, C.R.; Sanchez, B.; Zychowski, K.; Young, T.; Herbert, G.; Hall, P.; Erdely, A.; Eye, T.; Bishop, L.; Saunders, S.A.; Muldoon, P.P.; Ottens, A.K.; Campen, M.J. Serum-borne bioactivity caused by pulmonary multiwalled carbon nanotubes induces neuroinflammation via blood–brain barrier impairment. *Proc. Natl. Acad. Sci.* **2017**, *114*, E1968–E1976. doi:10.1073/pnas.1616070114.

384. Choi, H.; Liu, W.; Misra, P.; Tanaka, E.; Zimmer, J.; Ipe, B.; Bawendi, M.; Frangioni, J. Renal clearance of quantum dots. *Nat. Biotechnol.* **2007**, *25*, 1165–70. doi:10.1038/nbt1340.

385. Redondo-Gómez, C.; Leandro-Mora, R.; Blanch-Bermúdez, D.; Bermúdez, B.; Espinoza-Araya, C.; Hidalgo-Barrantes, D.; Vega Baudrit, J.; Maio, E. Recent Advances in Carbon Nanotubes for Nervous Tissue Regeneration. *Adv. Polym. Technol.* **2020**, *2020*, Article ID 6861205, 16 pages. doi:10.1155/2020/6861205.

386. Facciolà, A.; Visalli, G.; La Maestra, S.; Ceccarelli, M.; d'Aleo, F.; Nunnari, G.; Pellicanò, G.; Di Pietro, A. Carbon nanotubes and central nervous system: Environmental risks, toxicological aspects and future perspectives. *Environ. Toxicol. Pharmacol.* **2018**, *65*, 23–30. doi:10.1016/j.etap.2018.11.006.

387. Costa, P.M.; Bourgognon, M.; Wang, J.T.W.; Al-Jamal, K.T. Functionalised carbon nanotubes: From intracellular uptake and cell-related toxicity to systemic brain delivery. *J. Control. Release* **2016**, *241*, 200–219. doi:10.1016/j.jconrel.2016.09.033.

388. Gonzalez-Carter, D.; Goode, A.E.; Kiryushko, D.; Masuda, S.; Hu, S.; Lopes-Rodrigues, R.; Dexter, D.T.; Shaffer, M.S.P.; Porter, A.E. Quantification of blood–brain barrier transport and neuronal toxicity of unlabelled multiwalled carbon nanotubes as a function of surface charge. *Nanoscale* **2019**, *11*, 22054–22069. doi:10.1039/C9NR02866H.

389. Allen, B.L.; Kichambare, P.D.; Gou, P.; Vlasova, I.I.; Kapralov, A.A.; Konduru, N.; Kagan, V.E.; Star, A. Biodegradation of Single-Walled Carbon Nanotubes through Enzymatic Catalysis. *Nano Lett.* **2008**, *8*, 3899–3903. doi:10.1021/nl802315h.

390. Zhao, Y.; Allen, B.L.; Star, A. Enzymatic Degradation of Multiwalled Carbon Nanotubes. *J. Phys. Chem. A* **2011**, *115*, 9536–9544. doi:10.1021/jp112324d.

391. Kagan, V.; Konduru, N.; Feng, W.; Allen, B.; McIntyre, J.; Volkov, Y.; Vlasova, I.; Belikova, N.; Yanamala, N.; Kapralov, A.; Tyurina, Y.; Shi, J.; Kisin, E.; Murray, A.; Franks, J.; Stolz, D.B.; Gou, P.; Klein-Seetharaman, J.; Fadeel, B.; Shvedova, A. Carbon nanotubes degraded by neutrophil myeloperoxidase induce less pulmonary inflammation. *Nat. Nanotechnol.* **2010**, *5*, 354–9. doi:10.1038/nnano.2010.44.

392. Bussy, C.; Hadad, C.; Prato, M.; Bianco, A.; Kostarelos, K. Intracellular degradation of chemically functionalized carbon nanotubes using a long-term primary microglial culture model. *Nanoscale* **2016**, *8*, 590–601. doi:10.1039/C5NR06625E.

393. Andón, F.T.; Kapralov, A.A.; Yanamala, N.; Feng, W.; Baygan, A.; Chambers, B.J.; Hultenby, K.; Ye, F.; Toprak, M.S.; Brandner, B.D.; Fornara, A.; Klein-Seetharaman, J.; Kotchey, G.P.; Star, A.; Shvedova, A.A.; Fadeel, B.; Kagan, V.E. Biodegradation of Single-Walled Carbon Nanotubes by Eosinophil Peroxidase. *Small* **2013**, *9*, 2721–2729. doi:10.1002/smll.201202508.

394. Kotchey, G.; Zhao, Y.; Kagan, V.; Star, A. Peroxidase-mediated Biodegradation of Carbon Nanotubes in vitro and in vivo. *Adv. Drug Deliv. Rev.* **2013**, *65*, 1921–1932. doi:10.1016/j.addr.2013.07.007.

395. Mu, Q.; Broughton, D.L.; Yan, B. Endosomal Leakage and Nuclear Translocation of Multiwalled Carbon Nanotubes: Developing a Model for Cell Uptake. *Nano Lett.* **2009**, *9*, 4370–4375. doi:10.1021/nl902647x.

396. Malarkey, E.B.; Reyes, R.C.; Zhao, B.; Haddon, R.C.; Parpura, V. Water Soluble Single-Walled Carbon Nanotubes Inhibit Stimulated Endocytosis in Neurons. *Nano Lett.* **2008**, *8*, 3538–3542. doi:10.1021/nl8017912.

397. Ni, Y.; Hu, H.; Malarkey, E.B.; Zhao, B.; Montana, V.; Haddon, R.C.; Parpura, V. Chemically Functionalized Water Soluble Single-Walled Carbon Nanotubes Modulate Neurite Outgrowth. *J. Nanosci. Nanotechnol.* **2005**, *5*, 1707–1712. doi:doi:10.1166/jnn.2005.189.

398. Visalli, G.; Currò, M.; Iannazzo, D.; Pistone, A.; Pruiti Ciarello, M.; Acri, G.; Testagrossa, B.; Bertuccio, M.P.; Squeri, R.; Di Pietro, A. In vitro assessment of neurotoxicity and neuroinflammation of homemade MWCNTs. *Environ. Toxicol. Pharmacol.* **2017**, *56*, 121–128. doi:10.1016/j.etap.2017.09.005.

399. GhoshMitra, S.; Diercks, D.R.; Mills, N.C.; Hynds, D.L.; Ghosh, S. Role of engineered nanocarriers for axon regeneration and guidance: Current status and future trends. *Adv. Drug Deliv. Rev.* **2012**, *64*, 110 – 125. doi:10.1016/j.addr.2011.12.013.

400. Kafa, H.; Wang, J.T.W.; Rubio, N.; Venner, K.; Anderson, G.; Pach, E.; Ballesteros, B.; Preston, J.E.; Abbott, N.J.; Al-Jamal, K.T. The interaction of carbon nanotubes with an in vitro blood-brain barrier model and mouse brain in vivo. *Biomaterials* **2015**, *53*, 437–452. doi:10.1016/j.biomaterials.2015.02.083.

401. Antonelli, A.; Serafini, S.; Menotta, M.; Sfara, C.; Pierigé, F.; Giorgi, L.; Ambrosi, G.; Rossi, L.; Magnani, M. Improved cellular uptake of functionalized single-walled carbon nanotubes. *Nanotechnology* **2010**, *21*, 425101. doi:10.1088/0957-4484/21/42/425101.

402. Kafa, H.; Wang, J.T.W.; Rubio, N.; Klippstein, R.; Costa, P.; Hassan, H.; Sosabowski, J.; Bansal, S.; Preston, J.; Abbott, N.; Al-Jamal, K. Translocation of LRP1 targeted carbon nanotubes of different diameters across the blood–brain barrier in vitro and in vivo. *J. Control. Release* **2016**, *225*, 217–229. doi:10.1016/j.jconrel.2016.01.031.

403. Kam, N.W.S.; Dai, H. Carbon Nanotubes as Intracellular Protein Transporters: Generality and Biological Functionality. *J. Am. Chem. Soc.* **2005**, *127*, 6021–6026. doi:10.1021/ja050062v.

404. Li, H.; Tan, X.; Yan, l.; Zeng, B.; Meng, J.; Xu, H.; Cao, J.M. Multi-walled carbon nanotubes act as a chemokine and recruit macrophages by activating the PLC/IP3/CRAC channel signaling pathway. *Sci. Rep.* **2017**, *7*, 226. doi:10.1038/s41598-017-00386-3.

405. You, Y.; Wang, N.; He, L.; Shi, C.; Zhang, D.; Liu, Y.; Luo, L.; Chen, T. Designing dual-functionalized carbon nanotubes with high blood–brain-barrier permeability for precise orthotopic glioma therapy. *Dalton Trans.* **2019**, *48*, 1569–1573. doi:10.1039/C8DT03948H.

406. Costa, P.; Wang, J.T.W.; Morfin, J.F.; Khanum, T.; To, W.; Sosabowski, J.; Toth, E.; Al-Jamal, K. Functionalised Carbon Nanotubes Enhance Brain Delivery of Amyloid-Targeting Pittsburgh Compound B (PiB)-Derived Ligands. *Nanotheranostics* **2018**, *2*, 168–183. doi:10.7150/ntno.23125.

407. Bardi, G.; Tognini, P.; Ciofani, G.; Raffa, V.; Costa, M.; Pizzorusso, T. Pluronic-coated carbon nanotubes do not induce degeneration of cortical neurons in vivo and in vitro. *Nanomedicine* **2009**, *5*, 96—104. doi:10.1016/j.nano.2008.06.008.

408. Shityakov, S.; Salvador, E.; Pastorin, G.; Förster, C. Blood–brain barrier transport studies, aggregation, and molecular dynamics simulation of multiwalled carbon nanotube functionalized with fluorescein isothiocyanate. *Int. J. Nanomedicine* **2015**, *10*, 1703–1713. doi:10.2147/IJN.S68429.

409. Wang, J.T.W.; Rubio, N.; Kafa, H.; Venturelli, E.; Fabbro, C.; Ménard-Moyon, C.; Da Ros, T.; Sosabowski, J.; Lawson, A.; Robinson, M.; Prato, M.; Bianco, A.; Festy, F.; Preston, J.; Kostarelos, K.; Al-Jamal, K. Kinetics of functionalised carbon nanotube distribution in mouse brain after systemic injection: Spatial to ultra-structural analyses. *J. Control. Release* **2015**, *224*, 22–32. doi:10.1016/j.jconrel.2015.12.039.

410. Pajouhesh, H.; Lenz, G. Medicinal Chemical Properties of Successful Central Nervous System Drugs. *NeuroRx* **2005**, *2*, 541–53. doi:10.1602/neurorx.2.4.541.

411. Hong, S.W.; Lee, J.; Kang, S.; Hwang, E.; Hwang, Y.S.; Lee, M.; Han, D.W.; Park, C. Enhanced Neural Cell Adhesion and Neurite Outgrowth on Graphene-Based Biomimetic Substrates. *Biomed Res. Int.* **2014**, *2014*, 212149. doi:10.1155/2014/212149.

412. Wu, D.; Pak, E.; Wingard, C.; Murashov, A. Multi-walled carbon nanotubes inhibit regenerative axon growth of dorsal root ganglia neurons of mice. *Neurosci. Lett.* **2011**, *507*, 72–7. doi:10.1016/j.neulet.2011.11.056.

413. Gladwin, K.M.; Whitby, R.L.D.; Mikhalovsky, S.V.; Tomlins, P.; Adu, J. In Vitro Biocompatibility of Multiwalled Carbon Nanotubes with Sensory Neurons. *Adv. Healthc. Mater.* **2013**, *2*, 728–735. doi:10.1002/adhm.201200233.

414. Patabendige, A.; Skinner, R.A.; Morgan, L.; Joan Abbott, N. A detailed method for preparation of a functional and flexible blood–brain barrier model using porcine brain endothelial cells. *Brain Res.* **2013**, *1521*, 16–30. doi:10.1016/j.brainres.2013.04.006.

415. Mensch, J.; Oyarzábal, J.; Mackie, C.; Augustijns, P. In vivo, in vitro and in silico methods for small molecule transfer across the BBB. *J. Pharm. Sci.* **2009**, *98 12*, 4429–68.

416. Wilhelm, I.; Krizbai, I.A. In Vitro Models of the Blood–Brain Barrier for the Study of Drug Delivery to the Brain. *Mol. Pharm.* **2014**, *11*, 1949–1963. doi:10.1021/mp500046f.

417. East, E.; de Oliveira, D.B.; Golding, J.P.; Phillips, J.B. Alignment of Astrocytes Increases Neuronal Growth in Three-Dimensional Collagen Gels and Is Maintained Following Plastic Compression to Form a Spinal Cord Repair Conduit. *Tissue Eng. Part A* **2010**, *16*, 3173–3184. doi:10.1089/ten.tea.2010.0017.

418. Lichtenstein, M.; Carretero González, N.; Pérez, E.; Pulido-Salgado, M.; Moral Vico, J.; Solà, C.; Casañ-Pastor, N.; Suñol, C. Biosafety assessment of conducting nanostructured materials by using co-cultures of neurons and astrocytes. *NeuroToxicology* **2018**, *68*, 115–125. doi:10.1016/j.neuro.2018.07.010.

419. Lee, W.; Parpura, V. Carbon nanotubes as substrates/scaffolds for neural cell growth. *Prog. Brain Res.* **2009**, *180*, 110–125. doi:10.1016/S0079-6123(08)80006-4.

420. Jafar, A.; Alshatti, Y.; Ahmad, A. Carbon nanotube toxicity: The smallest biggest debate in medical care. *Cogent Med.* **2016**, *3*, 1217970. doi:10.1080/2331205X.2016.1217970.

421. Noonan, D.; Principi, E.; Girardello, R.; Bruno, A.; Manni, I.; Gini, E.; Pagani, A.; Grimaldi, A.; Ivaldi, F.; Congiu, T.; De Stefano, D.; Piaggio, G.; Eguileor, M.; Albini, A. Systemic distribution of single-walled carbon nanotubes in a novel model: Alteration of biochemical parameters, metabolic functions, liver accumulation, and inflammation in vivo. *Int. J. Nanomedicine* **2016**, *Volume 11*, 4299–4316. doi:10.2147/IJN.S109950.

422. Yang, S.t.; Guo, W.; Lin, Y.; Deng, X.y.; Wang, H.f.; Sun, H.f.; Liu, Y.f.; Wang, X.; Wang, W.; Chen, M.; Huang, Y.p.; Sun, Y.P. Biodistribution of Pristine Single-Walled Carbon Nanotubes In Vivo. *J. Phys. Chem. C* **2007**, *111*, 17761–17764. doi:10.1021/jp070712c.

423. Cui, D.; Tian, F.; Ozkan, C.; Wang, M.; Gao, H. Effect of single wall carbon nanotubes on human HEK293 cells. *Toxicol. Lett.* **2005**, *155*, 73–85. doi:10.1016/j.toxlet.2004.08.015.

424. Zhu, L.; Chang, D.; Dai, L.; Hong, Y. DNA Damage Induced by Multiwalled Carbon Nanotubes in Mouse Embryonic Stem Cells. *Nano Lett.* **2008**, *7*, 3592–7. doi:10.1021/nl071303v.

425. Bardi, G.; Nunes, A.; Gherardini, L.; Bates, K.; Al-Jamal, K.; Gaillard, C.; Prato, M.; Bianco, A.; Pizzorusso, T.; Kostarelos, K. Functionalized Carbon Nanotubes in the Brain: Cellular Internalization and Neuroinflammatory Responses. *PLoS One* **2013**, *8*, e80964. doi:10.1371/journal.pone.0080964.

426. Mohanta, D.; Patnaik, S.; Sood, S.; Das, N. Carbon nanotubes: Evaluation of toxicity at biointerfaces. *J. Pharm. Anal.* **2019**, *9*, 293–300. doi:10.1016/j.jpha.2019.04.003.

427. Fiorito, S.; Russier, J.; Salemme, A.; Soligo, M.; Manni, L.; Krasnowska, E.; Bonnamy, S.; Flahaut, E.; Serafino, A.; Togna, G.I.; Marlier, L.N.; Togna, A.R. Switching on microglia with electro-conductive multi walled carbon nanotubes. *Carbon* **2018**, *129*, 572–584. doi:10.1016/j.carbon.2017.12.069.

428. Fiorito, S.; Monthioux, M.; Psaila, R.; Pierimarchi, P.; Zonfrillo, M.; D'Emilia, E.; Grimaldi, S.; Lisi, A.; Béguin, F.; Almairac, R.; Noé, L.; Serafino, A. Evidence for electro-chemical interactions between multi-walled carbon nanotubes and human macrophages. *Carbon* **2009**, *47*, 2789 – 2804. doi:10.1016/j.carbon.2009.06.023.

429. Bussy, C.; Al-Jamal, K.T.; Boczkowski, J.; Lanone, S.; Prato, M.; Bianco, A.; Kostarelos, K. Microglia Determine Brain Region-Specific Neurotoxic Responses to Chemically Functionalized Carbon Nanotubes. *ACS Nano* **2015**, *9*, 7815–7830. doi:10.1021/acsnano.5b02358.

430. John, A.; Subramanian, A.; Vellayappan, M.; Balaji, A.; Mohanadas, H.; Jaganathan, S. Carbon nanotubes and graphene as emerging candidates in neuroregeneration and neurodrug delivery. *Int. J. Nanomedicine* **2015**, *10*, 4267–77. doi:10.2147/IJN.S83777.

431. Rodriguez-Yañez, Y.; Muñoz, B.; Albores, A. Mechanisms of toxicity by carbon nanotubes. *Toxicol. Mech. Methods* **2013**, *23*, 178–195. doi:10.3109/15376516.2012.754534.

432. Monteiro-Riviere, N.; Nemanich, R.; Inman, A.; Wang, Y.; Riviere, J. Multi-walled carbon nanotube interactions with human epidermal keratinocytes. *Toxicol. Lett.* **2005**, *155*, 377–384. doi:10.1016/j.toxlet.2004.11.004.

433. Wang, X.; Xia, T.; Addo Ntim, S.; Ji, Z.; Lin, S.; Meng, H.; Chung, C.H.; George, S.; Zhang, H.; Wang, M.; Li, N.; Yang, Y.; Castranova, V.; Mitra, S.; Bonner, J.; Nel, A. The Dispersal State of Multi-walled Carbon Nanotubes Elicits Pro-Fibrogenic Cellular Responses that Correlate with Fibrogenesis Biomarkers and Fibrosis in the Murine Lung. *ACS Nano* **2011**, *5*, 9772–9787. doi:10.1021/nn2033055.

434. Tian, F.; Cui, D.; Schwarz, H.; Estrada, G.; Kobayashi, H. Cytotoxicity of single-wall carbon nanotubes on human fibroblasts. *Toxicol. in Vitro* **2006**, *20*, 1202–12. doi:10.1016/j.tiv.2006.03.008.

435. Ding, L.; Stilwell, J.; Zhang, T.; Elboudwarej, O.; Jiang, H.; Selegue, J.P.; Cooke, P.A.; Gray, J.W.; Chen, F.F. Molecular Characterization of the Cytotoxic Mechanism of Multiwall Carbon Nanotubes and Nano-Onions on Human Skin Fibroblast. *Nano Lett.* **2005**, *5*, 2448–2464. doi:10.1021/nl051748o.

436. Jakubek, L.; Marangoudakis, S.; Raingo, J.; Liu, X.; Lipscombe, D.; Hurt, R. The inhibition of neuronal calcium ion channels by trace levels of yttrium released from carbon nanotubes. *Biomaterials* **2009**, *30*, 6351–7. doi:10.1016/j.biomaterials.2009.08.009.

437. Polak, P.; Shefi, O. Nanometric agents in the service of neuroscience: Manipulation of neuronal growth and activity using nanoparticles. *Nanomedicine* **2015**, *11*, 1467–79. doi:10.1016/j.nano.2015.03.005.

438. Boyles, M.; Young, L.; Brown, D.; Maccalman, L.; Cowie, H.; Moisala, A.; Smail, F.; Smith, P.; Proudfoot, L.; Windle, A.; Stone, V. Multi-walled carbon nanotube induced frustrated phagocytosis, cytotoxicity and pro-inflammatory conditions in macrophages are length dependent and greater than that of asbestos. *Toxicol. in Vitro* **2015**, *29*, 1513–1528. doi:10.1016/j.tiv.2015.06.012.

439. Sato, Y.; Yokoyama, A.; Shibata, K.i.; Akimoto, Y.; Ogino, S.i.; Nodasaka, Y.; Kohgo, T.; Tamura, K.; Akasaka, T.; Uo, M.; Motomiya, K.; Jeyadevan, B.; Ishiguro, M.; Hatakeyama, R.; Watari, F.; Tohji, K. Influence of length on cytotoxicity of multi-walled carbon nanotubes against human acute monocytic leukemia cell line THP-1 in vitro and subcutaneous tissue of rats in vivo. *Mol. Biosyst.* **2005**, *1*, 176–182. doi:10.1039/B502429C.

440. Dong, L.; Witkowski, C.; Craig, M.; Greenwade, M.; KL, J. Cytotoxicity effects of different surfactant molecules conjugated to carbon nanotubes on human astrocytoma cells. *Nanoscale Res Lett.* **2009**, *4*, 1517–1523. doi:10.1007/s11671-009-9429-0.

441. Mohajeri, M.; Behnam, B.; Sahebkar, A. Biomedical applications of carbon nanomaterials: Drug and gene delivery potentials. *J. Cell. Physiol.* **2019**, *234*, 298–319. doi:10.1002/jcp.26899.

442. Podolski, I.; Podlubnaya, Z.; Godukhin, O. Fullerenes C60, antiamyloid action, the brain, and cognitive processes. *Biophysics* **2010**, *55*, 71–76. doi:10.1134/S0006350910010136.

443. Xu, H.; Bai, J.; Meng, J.; Hao, W.; Xu, H.; Cao, J.M. Multi-walled carbon nanotubes suppress potassium channel activities in PC12 cells. *Nanotechnology* **2009**, *20*, 285102. doi:10.1088/0957-4484/20/28/285102.

444. Park, K.; Chhowalla, M.; Iqbal, Z.; Sesti, F. Single-walled Carbon Nanotubes Are a New Class of Ion Channel Blockers. *J. Biol. Chem.* **2004**, *278*, 50212–6. doi:10.1074/jbc.M310216200.

445. Nunes, A.; Al-Jamal, K.; Nakajima, T.; Hariz, M.; Kostarelos, K. Application of carbon nanotubes in neurology: Clinical perspectives and toxicological risks. *Arch. Toxicol.* **2012**, *86*, 1009–20. doi:10.1007/s00204-012-0860-0.

446. Baldrighi, M.; Trusel, M.; Tonini, R.; Giordani, S. Carbon Nanomaterials Interfacing with Neurons: An In vivo Perspective. *Front. Neurosci.* **2016**, *10*, 250. doi:10.3389/fnins.2016.00250.

447. Vittorio, O.; Raffa, V.; Cuschieri, A. Influence of purity and surface oxidation on cytotoxicity of multiwalled carbon nanotubes with human neuroblastoma cells. *Nanomedicine* **2009**, *5*, 424–431. doi:10.1016/j.nano.2009.02.006.

448. Pacurari, M.; Lowe, K.; Tchounwou, P.B.; Kafoury, R. A Review on the Respiratory System Toxicity of Carbon Nanoparticles. *Int. J. Environ. Res. Public Health* **2016**, *13*. doi:10.3390/ijerph13030325.

449. Fisher, C.; Rider, A.; Han, Z.J.; Kumar, S.; Levchenko, I.; Ostrikov, K. Applications and Nanotoxicity of Carbon Nanotubes and Graphene in Biomedicine. *J. Nanomater.* **2012**, *2012*, 315185. doi:10.1155/2012/315185.

450. Raval, J.P.; Joshi, P.; Chejara, D.R. 9 - Carbon nanotube for targeted drug delivery. In *Applications of Nanocomposite Materials in Drug Delivery*; Inamuddin.; Asiri, A.M.; Mohammad, A., Eds.; Woodhead Publishing Series in Biomaterials, Woodhead Publishing, 2018; pp. 203–216. doi:10.1016/B978-0-12-813741-3.00009-1.

451. Liu, J.; Appaix, F.; Bibari, O.; Marchand, G.; Benabid, A.; Sauter-Starace, F.; Waard, M. Control of neuronal network organization by chemical surface functionalization of multi-walled carbon nanotube arrays. *Nanotechnology* **2011**, *22*, 195101. doi:10.1088/0957-4484/22/19/195101.

452. Singh, N.; Chen, J.; Koziol, K.K.; Hallam, K.R.; Janas, D.; Patil, A.J.; Strachan, A.; G. Hanley, J.; Rahatekar, S.S. Chitin and carbon nanotube composites as biocompatible scaffolds for neuron growth. *Nanoscale* **2016**, *8*, 8288–8299. doi:10.1039/C5NR06595J.

453. Watterson, W.; Moslehi, S.; Rowland, C.; Zappitelli, K.; Smith, J.; Miller, D.; Chouinard, J.; Golledge, S.; Taylor, R.; Perez, M.; Alemán, B. The Roles of an Aluminum Underlayer in the Biocompatibility and Mechanical Integrity of Vertically Aligned Carbon Nanotubes for Interfacing with Retinal Neurons. *Micromachines* **2020**, *11*, 546. doi:10.3390/mi11060546.

454. Posadas, I.; Guerra, F.J.; Ceña, V. Nonviral vectors for the delivery of small interfering RNAs to the CNS. *Nanomedicine* **2010**, *5*, 1219–1236. doi:10.2217/nnm.10.105.

455. Bekyarova, E.; Ni, Y.; Malarkey, E.; Montana, V.; Mcwilliams, J.; Haddon, R.; Parpura, V. Applications of Carbon Nanotubes in Biotechnology and Biomedicine. *J. Biomed. Nanotechnol.* **2005**, *1*, 3–17. doi:10.1166/jbn.2005.004.

456. Zheng, M.; Jagota, A.; Semke, E.; McLean, R.; Lustig, S.; Richardson, R.; Tassi, N. DNA-assisted dispersion and separation of carbon nanotubes. *Nat. Mater.* **2003**, *2*, 338–42. doi:10.1038/nmat877.

457. Jin, G.Z.; Kim, M.; Shin, U.S.; Kim, H.W. Effect of carbon nanotube coating of aligned nanofibrous polymer scaffolds on the neurite outgrowth of PC-12 cells. *Cell Biol. Int.* **2011**, *35*, 741–745. doi:10.1042/CBI20100705.

458. Chao, T.I.; Xiang, S.; Lipstate, J.F.; Wang, C.; Lu, J. Poly(methacrylic acid)-Grafted Carbon Nanotube Scaffolds Enhance Differentiation of hESCs into Neuronal Cells. *Adv. Mater.* **2010**, *22*, 3542–3547. doi:10.1002/adma.201000262.

459. Hu, H.; Ni, Y.; Montana, V.; Haddon, R.C.; Parpura, V. Chemically Functionalized Carbon Nanotubes as Substrates for Neuronal Growth. *Nano Lett.* **2004**, *4*, 507–511. doi:10.1021/nl035193d.

460. Chen, W.; Xiong, Q.; Ren, Q.; Guo, Y.; Li, G. Can amino-functionalized carbon nanotubes carry functional nerve growth factor? *Neural Regen. Res.* **2014**, *9*, 285–92. doi:10.4103/1673-5374.128225.

461. Yen, S.J.; Hsu, W.L.; Chen, Y.C.; Su, H.C.; Chang, Y.C.; Yeh, S.R.; Yew, T.R. The enhancement of neural growth by amino-functionalization on carbon nanotubes as a neural electrode. *Biosens. Bioelectron.* **2011**, *26*, 4124–32. doi:10.1016/j.bios.2011.04.003.

462. Liopo, A.; Stewart, M.; Hudson, J.; Tour, J.; Pappas, T. Biocompatibility of Native and Functionalized Single-Walled Carbon Nanotubes for Neuronal Interface. *J. Nanosci. Nanotechnol.* **2006**, *6*, 1365–74. doi:10.1166/jnn.2006.155.

463. Yoosefian, M.; Rahmanifar, E.; Etminan, N. Nanocarrier for levodopa Parkinson therapeutic drug; comprehensive benserazide analysis. *Artif. Cells Nanomed. Biotechnol.* **2018**, *46*, 434–446. doi:10.1080/21691401.2018.1430583.

464. Qin, S.; Qin, D.; Ford, W.T.; Resasco, D.E.; Herrera, J.E. Functionalization of Single-Walled Carbon Nanotubes with Polystyrene via Grafting to and Grafting from Methods. *Macromolecules* **2004**, *37*, 752–757. doi:10.1021/ma035214q.

465. Hwang, J.Y.; Shin, U.S.; Jang, W.C.; Hyun, J.K.; Wall, I.B.; Kim, H.W. Biofunctionalized carbon nanotubes in neural regeneration: a mini-review. *Nanoscale* **2013**, *5*, 487–497. doi:10.1039/C2NR31581E.

466. Hu, H.; Ni, Y.; Mandal, S.K.; Montana, V.; Zhao, B.; Haddon, R.C.; Parpura, V. Polyethyleneimine Functionalized Single-Walled Carbon Nanotubes as a Substrate for Neuronal Growth. *J. Phys. Chem. B* **2005**, *109*, 4285–4289. doi:10.1021/jp0441137.

467. Yang, S.T.; Fernando, K.; Liu, J.H.; Wang, J.; Sun, H.; Liu, Y.; Chen, M.; Huang, Y.; Wang, X.; Wang, H.; Yaping, S. Covalently PEGylated Carbon Nanotubes with Stealth Character In Vivo. *Small* **2008**, *4*, 940–4. doi:10.1002/smll.200700714.

468. Ben-Valid, S.; Dumortier, H.; Décossas, M.; Sfez, R.; Meneghetti, M.; Bianco, A.; Yitzchaik, S. Polyaniline-coated single-walled carbon nanotubes: synthesis, characterization and impact on primary immune cells. *J. Mater. Chem.* **2010**, *20*, 2408–2417. doi:10.1039/B921828A.

469. Pires, F.; Ferreira, Q.; Rodrigues, C.; Morgado, J.; Ferreira, F. Neural stem cell differentiation by electrical stimulation using a cross-linked PEDOT substrate: Expanding the use of biocompatible conjugated conductive polymers for neural tissue engineering. *Biochim. Biophys. Acta* **2015**, *1850*, 1158–68. doi:10.1016/j.bbagen.2015.01.020.

470. Luo, X.; Happe, C.; Zhou, D.; Greenberg, R.; Cui, X. Highly Stable Carbon Nanotube Doped Poly(3,4-Ethylenedioxythiophene) for Chronic Neural Stimulation. *Biomaterials* **2011**, *32*, 5551–7. doi:10.1016/j.biomaterials.2011.04.051.

471. Tadayyon, G.; Krukiewicz, K.; Britton, J.; Larrañaga, A.; Vallejo-Giraldo, C.; Fernandez-Yague, M.; Guo, Y.; Orpella-Aceret, G.; Li, L.; Poudel, A.; Biggs, M.J. In vitro analysis of a physiological strain sensor formulated from a PEDOT:PSS functionalized carbon nanotube-poly(glycerol sebacate urethane) composite. *Mater. Sci. Eng. C* **2021**, *121*, 111857. doi:10.1016/j.msec.2020.111857.

472. Liu, X.; Miller, A.L.; Park, S.; Waletzki, B.E.; Zhou, Z.; Terzic, A.; Lu, L. Functionalized Carbon Nanotube and Graphene Oxide Embedded Electrically Conductive Hydrogel Synergistically Stimulates Nerve Cell Differentiation. *ACS Appl. Mater. Interfaces* **2017**, *9*, 14677–14690. doi:10.1021/acsami.7b02072.

473. IrOx–carbon nanotube hybrids: A nanostructured material for electrodes with increased charge capacity in neural systems. *Acta Biomater.* **2014**, *10*, 4548–4558. doi:10.1016/j.actbio.2014.06.019.

474. Tan JM, Foo JB, F.S.H.M. Release behaviour and toxicity evaluation of levodopa from carboxylated single-walled carbon nanotubes. *Beilstein J. Nanotechnol.* **2015**, *6*, 243–53. doi:10.3762/bjnano.6.23.

475. Matsumoto, K.; Sato, C.; Naka, Y.; Kitazawa, A.; Whitby, R.; Shimizu, N. Neurite outgrowths of neurons with neurotrophin-coated carbon nanotubes. *J. Biosci. Bioeng.* **2007**, *103 3*, 216–20. doi:10.1263/jbb.103.216.

476. Ge, C.; Du, J.; Zhao, L.; Wang, L.; Liu, Y.; Li, D.; Yang, Y.; Zhou, R.; Zhao, Y.; Chai, Z.; Chen, C. Binding of blood proteins to carbon nanotubes reduces cytotoxicity. *Proc. Natl. Acad. Sci.* **2011**, *108*, 16968–16973. doi:10.1073/pnas.1105270108.

477. Pondman, K.; Pednekar, L.; Paudyal, B.; Tsolaki, A.; Kouser, L.; Khan, H.; Shamji, M.; Hacken, B.; Stenbeck, G.; Sim, R.; Kishore, U. Innate immune humoral factors, C1q and factor H, with differential pattern recognition properties, alter macrophage response to carbon nanotubes. *Nanomedicine* **2015**, *11*, 2109–18. doi:10.1016/j.nano.2015.06.009.

478. Matsumoto, K.; Sato, C.; Naka, Y.; Whitby, R.; Shimizu, N. Stimulation of neuronal neurite outgrowth using functionalized carbon nanotubes. *Nanotechnology* **2010**, *21*, 115101. doi:10.1088/0957-4484/21/11/115101.

479. Kim, Y.; Kim, J.W.; Pyeon, H.J.; Hyun, J.K.; Hwang, J.Y.; Choi, S.J.; Lee, J.Y.; Deák, F.; Kim, H.W.; Lee, Y. Differential stimulation of neurotrophin release by the biocompatible nano-material (carbon nanotube) in primary cultured neurons. *J. Biomater. Appl.* **2013**, *28*, 790–7. doi:10.1177/0885328213481637.

480. Kleinman, H.K.; McGarvey, M.L.; Liotta, L.A.; Robey, P.G.; Tryggvason, K.; Martin, G.R. Isolation and characterization of type IV procollagen, laminin, and heparan sulfate proteoglycan from the EHS sarcoma. *Biochemistry* **1982**, *21*, 6188–6193. doi:10.1021/bi00267a025.

481. Anastassiou, C.A.; Montgomery, S.M.; Barahona, M.; Buzsáki, G.; Koch, C. The Effect of Spatially Inhomogeneous Extracellular Electric Fields on Neurons. *J. Neurosci.* **2010**, *30*, 1925–1936. doi:10.1523/JNEUROSCI.3635-09.2010.

482. Greenbaum, A.; Anava, S.; Ayali, A.; Shein-Idelson, M.; Pur, M.; Ben-Jacob, E.; Hanein, Y. One-to-one neuron-electrode interfacing. *J. Neurosci. Methods* **2009**, *182*, 219–24. doi:10.1016/j.jneumeth.2009.06.012.

483. Poulain, F.E.; Sobel, A. The microtubule network and neuronal morphogenesis: Dynamic and coordinated orchestration through multiple players. *Mol. Cell. Neurosci.* **2010**, *43*, 15–32. doi:10.1016/j.mcn.2009.07.012.

484. Burblies, N.; Harre, J.; Schwarz, H.C.; Kranz, K.; Motz, D.; Vogt, C.; Lenarz, T.; Warnecke, A.; Behrens, P. Coatings of Different Carbon Nanotubes on Platinum Electrodes for Neuronal Devices: Preparation, Cytocompatibility and Interaction with Spiral Ganglion Cells. *PLoS One* **2016**, *11*, e0158571. doi:10.1371/journal.pone.0158571.

485. Robertson, D. The Physical Chemistry of Brain and Neural Cell Membranes: An Overview. *Neurochem. Res.* **2010**, *35*, 681–687.

486. Shein-Idelson, M.; Greenbaum, A.; Gabay, T.; Sorkin, R.; Pur, M.; Ben-Jacob, E.; Hanein, Y. Engineered neuronal circuits shaped and interfaced with carbon nanotube microelectrode arrays. *Biomed. Microdevices* **2009**, *11*, 495–501. doi:10.1007/s10544-008-9255-7.

487. Distasi, C.; Ariano, P.; Zamburlin, P.; Ferraro, M. In vitro analysis of neuron-glial cell interactions during cellular migration. *Eur. Biophys. J.* **2002**, *31*, 81–8. doi:10.1007/s00249-001-0194-y.

488. Araque, A.; Carmignoto, G.; Haydon, P.G. Dynamic Signaling Between Astrocytes and Neurons. *Annu. Rev. Physiol.* **2001**, *63*, 795–813. doi:10.1146/annurev.physiol.63.1.795.

489. Min, J.O.; Yoon, B.E. Glia and gliotransmitters on carbon nanotubes. *Nano Reviews & Experiments* **2017**, *8*, 1323853. doi:10.1080/20022727.2017.1323853.

490. Franca, E.; Jao, P.; Fang, S.P.; Alagapan, S.; Pan, L.; Yoon, J.; Yoon, Y.K.; Wheeler, B. Scale of Carbon Nanomaterials Affects Neural Outgrowth and Adhesion. *IEEE Trans. Nanobiosci.* **2016**, *15*, 1–1. doi:10.1109/TNB.2016.2519505.

491. Sorkin, R.; Greenbaum, A.; Pur, M.; Anava, S.; Ayali, A.; Ben-Jacob, E.; Hanein, Y. Process entanglement as a neuronal anchorage mechanism to rough surfaces. *Nanotechnology* **2009**, *20*, 015101. doi:10.1088/0957-4484/20/1/015101.

492. Brunetti, V.; Maiorano, G.; Rizzello, L.; Sorce, B.; Sabella, S.; Cingolani, R.; Pompa, P.P. Neurons sense nanoscale roughness with nanometer sensitivity. *Proc. Natl. Acad. Sci.* **2010**, *107*, 6264–6269. doi:10.1073/pnas.0914456107.

493. Silva, G. Neuroscience nanotechnology: Progress, opportunities and challenges. *Nat. Rev. Neurosci.* **2006**, *7*, 65–74. doi:10.1038/nrn1827.

494. Béduer, A.; Seichepine, F.; Flahaut, E.; Loubinoux, I.; Vaysse, L.; Vieu, C. Elucidation of the Role of Carbon Nanotube Patterns on the Development of Cultured Neuronal Cells. *Langmuir* **2012**, *28*, 17363–17371. doi:10.1021/la304278n.

495. Xie, J.; Chen, L.; Aatre, K.; Srivatsan, M.; Varadan, V. Somatosensory neurons grown on functionalized carbon nanotube mats. *Smart Mater. Struct.* **2006**, *15*, N85. doi:10.1088/0964-1726/15/4/N02.

496. Gupta, P.; Agrawal, A.; Murali, K.; Varshney, R.; Beniwal, S.; Manhas, S.; Roy, P.; Lahiri, D. Differential neural cell adhesion and neurite outgrowth on carbon nanotube and graphene reinforced polymeric scaffolds. *Mater. Sci. Eng. C* **2019**, *97*, 539–551. doi:10.1016/j.msec.2018.12.065.

497. Beruto, D.; Mezzasalma, S.; Oliva, P. Ion Adsorption and Agglomeration Mechanism in Si_3N_4/H_2O (l) Dispersions Compatible with Thermodynamical Stability. *J. Coll. Interface Sci.* **1997**, *186*, 318–324. doi:10.1006/jcis.1996.4623.

498. Young, B.; Pitt, W.; Cooper, S. Protein adsorption on polymeric biomaterials I. Adsorption isotherms. *J. Coll. Interface Sci.* **1988**, *124*, 28–43. doi:10.1016/0021-9797(88)90321-9.

499. Salehi, M.; Naseri-Nosar, M.; Ebrahimi-Barough, S.; Nourani, M.; Khojasteh, A.; Hamidieh, A.A.; Amani, A.; Farzamfar, S.; Ai, J. Sciatic nerve regeneration by transplantation of Schwann cells via erythropoietin controlled-releasing polylactic acid/multiwalled carbon nanotubes/gelatin nanofibrils neural guidance conduit. *J. Biomed. Mater. Res. B* **2018**, *106*, 1463–1476. doi:10.1002/jbm.b.33952.

500. Paviolo, C.; Haycock, J.; Yong, J.; Yu, A.; Stoddart, P.; Mcarthur, S. Laser exposure of gold nanorods can increase neuronal cell outgrowth. *Biotechnol. Bioeng.* **2013**, *110*, 2277–91. doi:10.1002/bit.24889.

501. Tay, C.Y.; Gu, H.; Wen Shing, L.; Yu, H.; Li, H.; Heng, B.; Tantang, H.; Loo, J.; Li, L.; Tan, L.P. Cellular behavior of human mesenchymal stem cells cultured on single-walled carbon nanotube film. *Carbon* **2010**, *48*, 1095–1104. doi:10.1016/j.carbon.2009.11.031.

502. Park, S.Y.; Namgung, S.; Kim, B.; Im, J.; Kim, J.; Sun, K.; Lee, K.; Nam, J.M.; Park, Y.; Hong, S. Carbon Nanotube Monolayer Patterns for Directed Growth of Mesenchymal Stem Cells. *Adv. Mater.* **2007**, *19*, 2530 – 2534. doi:10.1002/adma.200600875.

503. Gheith, M.; Sinani, V.; Wicksted, J.; Matts, R.; Kotov, N. Single-Walled Carbon Nanotube Polyelectrolyte Multilayers and Freestanding Films as a Biocompatible Platform for Neuroprosthetic Implants. *Adv. Mater.* **2005**, *17*, 2663–2670. doi:10.1002/adma.200500366.

504. Ghibaudo, M.; Trichet, L.; Digabel, J.; Richert, A.; Hersen, P.; Ladoux, B. Substrate Topography Induces a Crossover from 2D to 3D Behavior in Fibroblast Migration. *Biophys. J.* **2009**, *97*, 357–68. doi:10.1016/j.bpj.2009.04.024.

505. Su, W.T.; Chu, I.M.; Yang, J.Y.; Lin, C.D. The geometric pattern of a pillared substrate influences the cell-process distribution and shapes of fibroblasts. *Micron* **2006**, *37*, 699–706. doi:10.1016/j.micron.2006.03.007.

506. Guntinas-Lichius, O.; Wewetzer, K.; Tomov, T.; Azzolin, N.; Kazemi, S.; Streppel, M.; Neiss, W.; Angelov, D. Transplantation of Olfactory Mucosa Minimizes Axonal Branching and Promotes the Recovery of Vibrissae Motor Performance after Facial Nerve Repair in Rats. *J. Neurosci.* **2002**, *22*, 7121–31. doi:10.1523/JNEUROSCI.22-16-07121.2002.

507. Gupta, P.; Sharan, S.; Roy, P.; Lahiri, D. Aligned carbon nanotube reinforced polymeric scaffolds with electrical cues for neural tissue regeneration. *Carbon* **2015**, *95*, 715–724. doi:10.1016/j.carbon.2015.08.107.

508. Patel, S.; Kurpinski, K.; Quigley, R.; Gao, H.; Hsiao, B.; Poo, M.m.; Li, S. Bioactive Nanofibers: Synergistic Effects of Nanotopography and Chemical Signaling on Cell Guidance. *Nano Lett.* **2007**, *7*, 2122–8. doi:10.1021/nl071182z.

509. Xie, X.; Zhao, W.; Lee, H.R.; Liu, C.; Ye, M.; Xie, W.; Cui, B.; Criddle, C.S.; Cui, Y. Enhancing the Nanomaterial Bio-Interface by Addition of Mesoscale Secondary Features: Crinkling of Carbon Nanotube Films To Create Subcellular Ridges. *ACS Nano* **2014**, *8*, 11958–11965. doi:10.1021/nn504898p.

510. Guided neurite growth on patterned carbon nanotubes. *Sens. Actuators B Chem.* **2005**, *106*, 843–850. doi:10.1016/j.snb.2004.10.039.

511. Galvan-Garcia, P.; Keefer, E.W.; Yang, F.; Zhang, M.; Fang, S.; Zakhidov, A.A.; Baughman, R.H.; Romero, M.I. Robust cell migration and neuronal growth on pristine carbon nanotube sheets and yarns. *J. Biomater. Sci. Polym. Ed.* **2007**, *18*, 1245–1261. doi:10.1163/156856207782177891.

512. Jan, E.; Pereira, F.N.; Turner, D.L.; Kotov, N.A. In situ gene transfection and neuronal programming on electroconductive nanocomposite to reduce inflammatory response. *J. Mater. Chem.* **2011**, *21*, 1109–1114. doi:10.1039/C0JM01895C.

513. Fan, L.; Feng, C.; Zhao, W.; Qian, L.; Wang, Y.; Li, Y. Directional Neurite Outgrowth on Superaligned Carbon Nanotube Yarn Patterned Substrate. *Nano Lett.* **2012**, *12*, 3668–3673. doi:10.1021/nl301428w.

514. den Braber, E.T.; de Ruijter, J.D.; Ginsel, L.; von Recum, A.V.; Jansen, J. Orientation of ECM protein deposition, fibroblast cytoskeleton, and attachment complex components on silicone microgrooved surfaces. *J. Biomed. Mater. Res.* **1998**, *40 2*, 291–300. doi:10.1002/(SICI)1097-4636(199805)40:2<291::AID-JBM14>3.0.CO;2-P.

515. Imaninezhad, M.; Pemberton, K.; Xu, F.; Kalinowski, K.; Bera, R.; Zustiak, S.P. Directed and enhanced neurite outgrowth following exogenous electrical stimulation on carbon nanotube-hydrogel composites. *J. Neural Eng.* **2018**, *15*, 056034. doi:10.1088/1741-2552/aad65b.

516. Shrestha, S.; Shrestha, B.K.; Lee, J.; Joong, O.K.; Kim, B.S.; Park, C.H.; Kim, C.S. A conducting neural interface of polyurethane/silk-functionalized multiwall carbon nanotubes with enhanced mechanical strength for neuroregeneration. *Mater. Sci. Eng. C* **2019**, *102*, 511–523. doi:10.1016/j.msec.2019.04.053.

517. Kumar, S.; Ahlawat, W.; Kumar, R.; Dilbaghi, N. Graphene, carbon nanotubes, zinc oxide and gold as elite nanomaterials for fabrication of biosensors for healthcare. *Biosens. Bioelectron.* **2015**, *70*, 498–503. doi:10.1016/j.bios.2015.03.062.

518. Malarkey, E.B.; Fisher, K.A.; Bekyarova, E.; Liu, W.; Haddon, R.C.; Parpura, V. Conductive Single-Walled Carbon Nanotube Substrates Modulate Neuronal Growth. *Nano Lett.* **2009**, *9*, 264–268. doi:10.1021/nl802855c.

519. Kater, S.; Mattson, M.; Cohan, C.; Connor, J. Calcium regulation of the neuronal growth cone. *Trends Neurosci.* **1988**, *11*, 315–321. doi:10.1016/0166-2236(88)90094-X.

520. Ghoshmitra, S.; Diercks, D.; Mills, N.C.; Hynds, D.L.; Ghosh, S. Role of engineered nanocarriers for axon regeneration and guidance: current status and future trends. *Adv. Drug Deliv. Rev.* **2012**, *64*.

521. Zhang, H.; Patel, P.R.; Xie, Z.; Swanson, S.D.; Wang, X.; Kotov, N.A. Tissue-Compliant Neural Implants from Microfabricated Carbon Nanotube Multilayer Composite. *ACS Nano* **2013**, *7*, 7619–7629. doi:10.1021/nn402074y.

522. Tyler, W. The mechanobiology of brain function. *Nat. Rev. Neurosci.* **2012**, *13*, 867–78. doi:10.1038/nrn3383.

523. Discher, D.; Janmey, P.; Wang, Y.L. Tissue Cells Feel and Respond to the Stiffness of Their Substrate. *Science* **2005**, *310*, 1139–43. doi:10.1126/science.1116995.

524. Teixeira, A.; Ilkhanizadeh, S.; Wigenius, J.; Duckworth, J.; Inganas, O.; Hermanson, O. The promotion of neuronal maturation on soft substrates. *Biomaterials* **2009**, *30*, 4567–72. doi:10.1016/j.biomaterials.2009.05.013.

525. Koch, D.; Rosoff, W.; Jiang, J.; geller, H.; Urbach, J. Strength in the Periphery: Growth Cone Biomechanics and Substrate Rigidity Response in Peripheral and Central Nervous System Neurons. *Biophys. J.* **2012**, *102*, 452–60. doi:10.1016/j.bpj.2011.12.025.

526. Zhang, B.; Yan, W.; Zhu, Y.; Yang, W.; Le, W.; Chen, B.; Zhu, R.; Cheng, L. Nanomaterials in Neural-Stem-Cell-Mediated Regenerative Medicine: Imaging and Treatment of Neurological Diseases. *Adv. Mater.*, *30*, 1705694. doi:10.1002/adma.201705694.

527. Olenick, L.L.; Troiano, J.M.; Vartanian, A.; Melby, E.S.; Mensch, A.C.; Zhang, L.; Hong, J.; Mesele, O.; Qiu, T.; Bozich, J.; Lohse, S.; Zhang, X.; Kuech, T.R.; Millevolte, A.; Gunsolus, I.; McGeachy, A.C.; Dogangün, M.; Li, T.; Hu, D.; Walter, S.R.; Mohaimani, A.; Schmoldt, A.; Torelli, M.D.; Hurley, K.R.; Dalluge, J.; Chong, G.; Feng, Z.V.; Haynes, C.L.; Hamers, R.J.; Pedersen, J.A.; Cui, Q.; Hernandez, R.; Klaper, R.; Orr, G.; Murphy, C.J.; Geiger, F.M. Lipid Corona Formation from Nanoparticle Interactions with Bilayers. *Chem* **2018**, *4*, 2709–2723. doi:10.1016/j.chempr.2018.09.018.

528. Krol, S.; Macrez, R.; Docagne, F.; Defer, G.L.; Laurent, S.; Rahman, M.; Hajipour, M.; Kehoe, P.; Mahmoudi, M. Therapeutic Benefits from Nanoparticles: The Potential Significance of Nanoscience in Diseases with Compromise to the Blood Brain Barrier. *Chem. Rev.* **2012**, *113*, 1877–1903. doi:10.1021/cr200472g.

529. Payne, C.K. A protein corona primer for physical chemists. *J. Chem. Phys.* **2019**, *151*, 130901. doi:10.1063/1.5120178.

530. Brambilla, D.; Le Droumaguet, B.; Nicolas, J.; Hashemi, S.H.; Wu, L.P.; Moghimi, S.M.; Couvreur, P.; Andrieux, K. Nanotechnologies for Alzheimer's disease: diagnosis, therapy, and safety issues. *Nanomedicine* **2011**, *7*, 521–540. doi:10.1016/j.nano.2011.03.008.

531. Owens, D.E.; Peppas, N.A. Opsonization, biodistribution, and pharmacokinetics of polymeric nanoparticles. *Int. J. Pharm.* **2006**, *307*, 93–102. doi:10.1016/j.ijpharm.2005.10.010.

532. Tenzer, S.; Docter, D.; Kuharev, J.; Musyanovych, A.; Fetz, V.; Hecht, R.; Schlenk, F.; Fischer, D.; Kiouptsi, K.; Reinhardt, C.; Landfester, K.; Schild, H.; Maskos, M.; Knauer, S.K.; Stauber, R.H. Rapid formation of plasma protein corona critically affects nanoparticle pathophysiology. *Nat. Nanotechnol.* **2013**, *8*, 772—781. doi:10.1038/nnano.2013.181.

533. Li, H.; Luo, Y.; Wei, G. Carbon Nanotube Inhibits the Formation of -Sheet-Rich Oligomers of the Alzheimer's Amyloid-(16-22) Peptide. *Biophys. J.* **2011**, *101*, 2267–76. doi:10.1016/j.bpj.2011.09.046.

534. Fu, Z.; Luo, Y.; Derreumaux, P.; Wei, G. Induced -Barrel Formation of the Alzheimer's A25–35 Oligomers on Carbon Nanotube Surfaces: Implication for Amyloid Fibril Inhibition. *Biophys. J.* **2009**, *97*, 1795–1803. doi:10.1016/j.bpj.2009.07.014.

535. Jana, A.K.; Sengupta, N. Adsorption mechanism and collapse propensities of the full-length, monomeric Aβ(1-42) on the surface of a single-walled carbon nanotube: a molecular dynamics simulation study. *Biophys. J.* **2012**, *102*, 1889–96. doi:10.1016/j.bpj.2012.03.036.

536. Jana, A.K.; Jose, J.C.; Sengupta, N. Critical roles of key domains in complete adsorption of A peptide on single-walled carbon nanotubes: insights with point mutations and MD simulations. *Phys. Chem. Chem. Phys.* **2013**, *15*, 837–844. doi:10.1039/C2CP42933K.

537. Song, M.; Zhu, Y.; Wei, G.; Li, H. Carbon nanotube prevents the secondary structure formation of amyloid- trimers: an all-atom molecular dynamics study. *Mol. Simulat.* **2017**, *43*, 1189–1195. doi:10.1080/08927022.2017.1321757.

538. Laing, C.; Lord, G. *Stochastic Methods in Neuroscience*; Oxford University Press, Oxford, 2010.

539. McComb, W.D. *Renormalization Methods: A Guide For Beginners*; Number 9780199236527 in OUP Catalogue, Oxford University Press, Oxford, 2007.

540. Gabathuler, R. Approaches to transport therapeutic drugs across the blood–brain barrier to treat brain diseases. *Neurobiol. Dis.* **2010**, *37*, 48–57. Special Issue: Blood Brain Barrier, doi:10.1016/j.nbd.2009.07.028.

541. Johnston, H.J.; Hutchison, G.R.; Christensen, F.M.; Peters, S.; Hankin, S.; Aschberger, K.; Stone, V. A critical review of the biological mechanisms underlying the in vivo and in vitro toxicity of carbon nanotubes: The contribution of physico-chemical characteristics. *Nanotoxicology* **2010**, *4*, 207–246. doi:10.3109/17435390903569639.

542. Zhang, Y.; Liu, C., The Pharmacological and Toxicological Profiles of Carbon Nanotubes as Drug Carriers Toward Central Nervous System. In *Nanomedicine and the Nervous System*; 2012; pp. 367–387. doi:10.1201/b11835-22.

543. Malarkey, E.B.; Parpura, V. Applications of Carbon Nanotubes in Neurobiology. *Neurodegener. Dis.* **2007**, *4*, 292 – 299. doi:10.1159/000101885.

544. Wong, B.S.; Yoong, S.L.; Jagusiak, A.; Panczyk, T.; Ho, H.K.; Ang, W.H.; Pastorin, G. Carbon nanotubes for delivery of small molecule drugs. *Adv. Drug Deliv. Rev.* **2013**, *65*, 1964–2015. Carbon Nanotubes in Medicine and Biology: Therapy and Diagnostics Safety and Toxicology, doi:10.1016/j.addr.2013.08.005.

545. Baby, N.; Patnala, R.; Ling, E.A.; ThameemDheen, S. Nanomedicine and its Application in Treatment of Microglia-Mediated Neuroinflammation. *Curr. Med. Chem.* **2014**, *21*, 4215–4226. doi:10.2174/0929867321666140716101258.

546. Wei, L.; Jing, L.; Tianfu, W.; Peng, H. Photo-triggered Drug Delivery Systems for Neuron-related Applications. *Curr. Med. Chem.* **2019**, *26*, 1406–1422. doi:10.2174/0929867325666180622121801.

547. Jan, E.; Kotov, N.A. Successful Differentiation of Mouse Neural Stem Cells on Layer-by-Layer Assembled Single-Walled Carbon Nanotube Composite. *Nano Lett.* **2007**, *7*, 1123–1128. doi:10.1021/nl0620132.

548. Bianco, A.; Kostarelos, K.; Prato, M. Applications of carbon nanotubes in drug delivery. *Curr. Opin. Chem. Biol.* **2005**, *9*, 674 – 679. doi:10.1016/j.cbpa.2005.10.005.

549. Liu, Z.; Yushan, M.; Alike, Y.; Liu, Y.; Wu, S.; Ma, C.; Yusufu, A. Preparation of Multiwall Carbon Nanotubes Embedded Electroconductive Multi-Microchannel Scaffolds for Neuron Growth under Electrical Stimulation. *Biomed. Res. Int.* **2020**, *2020*, 1–14. doi:10.1155/2020/4794982.

550. Yazda, K.; Tahir, S.; Michel, T.; Loubet, B.; Manghi, M.; Bentin, J.; Picaud, F.; Palmeri, J.; Henn, F.; Jourdain, V. Voltage-activated transport of ions through single-walled carbon nanotubes. *Nanoscale* **2017**, *9*, 11976–11986. doi:10.1039/C7NR02976D.

551. Jahromi, H.K.; Farzin, A.; Hasanzadeh, E.; Barough, S.E.; Mahmoodi, N.; Najafabadi, M.R.H.; Farahani, M.S.; Mansoori, K.; Shirian, S.; Ai, J. Enhanced sciatic nerve regeneration by poly-L-lactic acid/multi-wall carbon nanotube neural guidance conduit containing Schwann cells and curcumin encapsulated chitosan nanoparticles in rat. *Mater. Sci. Eng. C* **2020**, *109*, 110564. doi:10.1016/j.msec.2019.110564.

552. Cho, Y.; Ben Borgens, R. Electrically controlled release of the nerve growth factor from a collagen–carbon nanotube composite for supporting neuronal growth. *J. Mater. Chem. B* **2013**, *1*, 4166–4170. doi:10.1039/C3TB20505C.

553. Abrami, M.; Chiarappa, G.; Farra, R.; Grassi, G.; Marizza, P.; Grassi, M. Use of low-field NMR for the characterization of gels and biological tissues. *ADMET & DMPK* **2018**, *6*, 34. doi:10.5599/admet.6.1.430.

554. Guo, J.H.; Liu, Y.; Lv, Z.J.; Wei, W.J.; Guan, X.; Guan, Q.L.; Leng, Z.Q.; Zhao, J.Y.; Miao, H.; Liu, J. Potential Neurogenesis of Human Adipose-Derived Stem Cells on Electrospun Catalpol-Loaded Composite Nanofibrous Scaffolds. *Ann. Biomed. Eng.* **2015**, *43*, 2597–2608. doi:10.1007/s10439-015-1311-x.

555. Suttee, A.; Mishra, V.; Singh, M.; Nayak, P.; Sriram, P. Carbon Nanotubes as Emerging Nanocarriers in Drug Delivery: An Overview. *Int. J. Pharm. Qual. Assur.* **2020**, *11*, 373–378. doi:10.25258/ijpqa.11.3.11.

556. Zhao, Y.; Xing, G.; Chai, Z. Nanotoxicology: Are carbon nanotubes safe? *Nat. Nanotechnol.* **2008**, *3*, 191–2. doi:10.1038/nnano.2008.77.

557. Guo, Q.; Shen, X.T.; Li, Y.Y.; Xu, S.Q. Carbon nanotubes-based drug delivery to cancer and brain. *J. Huazhong Univ. Sci. Tech., Med. Sci.* **2017**, *37*, 635–641. doi:10.1007/s11596-017-1783-z.

558. Kofoed Andersen, C.; Khatri, S.; Hansen, J.; Slott, S.; Pavan Parvathaneni, R.; Mendes, A.C.; Chronakis, I.S.; Hung, S.C.; Rajasekaran, N.; Ma, Z.; Zhu, S.; Dai, H.; Mellins, E.D.; Astakhova, K. Carbon Nanotubes—Potent Carriers for Targeted Drug Delivery in Rheumatoid Arthritis. *Pharmaceutics* **2021**, *13*. doi:10.3390/pharmaceutics13040453.

559. Ketabi, S.; Rahmani, L. Carbon nanotube as a carrier in drug delivery system for carnosine dipeptide: A computer simulation study. *Mat. Sci. Eng. C* **2017**, *73*, 173–181. doi:10.1016/j.msec.2016.12.058.

560. Divekar, S. Carbon nanotubes and advanced drug delivery system - a review. *J. Huazhong Univ. Sci. Tech., Med. Sci.* **2020**, *11*, 3636–3644. doi:10.13040/IJPSR.0975-8232.11(8).3636-44.

561. Alshehri, R.; Ilyas, A.M.; Hasan, A.; Arnaout, A.; Ahmed, F.; Memic, A. Carbon Nanotubes in Biomedical Applications: Factors, Mechanisms, and Remedies of Toxicity. *J. Med. Chem.* **2016**, *59*, 8149–8167. doi:10.1021/acs.jmedchem.5b01770.

562. Jha, R.; Singh, A.; Sharma, P.; Fuloria, N.K. Smart carbon nanotubes for drug delivery system: A comprehensive study. *J. Drug Deliv. Sci. Technol.* **2020**, *58*, 101811. doi:10.1016/j.jddst.2020.101811.

563. Ravi Kiran, A.; Kusuma Kumari, G.; Krishnamurthy, P.T. Carbon nanotubes in drug delivery: Focus on anticancer therapies. *J. Drug Deliv. Sci. Technol.* **2020**, *59*, 101892. doi:10.1016/j.jddst.2020.101892.

564. Divekar, S. Carbon Nanotubes: Smart Drug/Gene Delivery Carriers. *Int. J. Nanomedicine* **2021**, *16*, 1681–1706. doi:10.2147/IJN.S299448.